

Prabath Priyadarshana Hewagama

**NTNU**  
Norwegian University of  
Science and Technology  
Faculty of Engineering  
Department of Ocean Operations and Civil Engineering

Prabath Priyadarshana Hewagama

# Design Optimization of Exhaust Gas Economizer Using CFD Simulations for Medium Speed Marine Diesel Engines Combine with Exhaust After Treatment

June 2021





Norwegian University of  
Science and Technology

Design Optimization of Exhaust Gas  
Economizer Using CFD Simulations for  
Medium Speed Marine Diesel Engines  
Combine with Exhaust After Treatment  
**Prabath Priyadarshana Hewagama**

Master's in Product and System Design

Submission date: June 2021

Supervisor: Vilmar Æsøy and Henry Peter Piehl

Co-supervisor: Lars Erik Helland

Norwegian University of Science and Technology  
Department of Ocean Operations and Civil Engineering



---

## Abstract

This thesis presents the optimization of exhaust gas economizer unit of a waste heat recovery system for a medium speed marine diesel engine with using CFD simulations and combined system concept development with combining exhaust after treatment for the engine exhaust. The concept developments of new economizer units are also studied using simulation results to improve the efficiency of the unit through increasing the effective heat transfer surface area.

Marine emissions are harmful for both environment and human health which is regulated by setting up rules and regulation for decades. The existing fleet of vessels will be in service for several decades in the future and these vessels needs to retrofit systems to control the emissions to comply with the regulations. The heat recovery from the exhaust helps to improve the fuel efficiency of the vessel which leads to reduce the fuel consumption. The low fuel consumption causes for the lower emissions and exhaust after treatment helps to further removal of the harmful emissions from the exhaust. Improving the efficiency of the waste heat recovery system is based on the economizer unit optimization and developing new design concepts. The exhaust after treatment system mainly focused on the Nitrogen Oxide reduction and particulate matter control of the diesel exhaust.

This study mainly based on the CFD thermal simulations to evaluate and optimize an existing economizer unit through heat transfer improvements. Existing products and previous research studies are referred for the combined system development process. The CFD simulation results for the existing economizer unit is compared with the measurements results to build up the main CFD case set up. The optimization of the economizer is conducted based on the flow pattern changes using baffles and flow direction control. The new design concepts are developed based on the heat transfer surface area improvement with referring to the theory of the convection heat transfer improvements of heat exchangers.

According to the CFD simulation results, the heat transfer efficiency of the economizer unit can be increased by introducing diesel particular filter and oxidation catalyst into the exhaust treatment system which prevents the soot generation inside the economizer unit. Also, the simulations results show that, implementing baffles into the economizer unit with a optimized number of baffles and baffle cut percentage can used to improve the efficiency of the unit. The new design concepts are introduced with fins and tube arrangements with different flow patterns and gradually increasing heat transfer area simulated using CFD software. The relationship of the heat transfer area and overall heat transfer coefficient is analyzed from the simulation results to evaluate the performance. Generated back pressure with the economizer unit in new developments and total combined system is also discussed in this study to keep a stable engine performance.

For the economizer unit which is used in this study has an efficiency improvement of 18% - 20% with 3 baffles in the water region with a baffle cut percentage of 20% according to the simulations results of the optimization process. Using diesel particular filter reduce the soot build up and increase the efficiency by 7% - 9% based on the simulations which are presented in this study. It is important to combine the economizer unit with the after treatment system with considering the Nitrogen Oxides and particulate matter reduction and the economizer unit need to combine into the system after the treatment units to maintain the required temperature levels discussed in this study. This combine system is mainly focused on the retrofitting purpose for the existing vessels.

Experimental set up for validations of the CFD simulation results which are discussed in this study is required in the future phase of the research. Also, it is important to conduct a CFD study to analyze the flow behavior inside the units included in the exhaust after treatment system. The acoustic performance of the units in this combined system needs to evaluate in the future phase to identify the noise levels and requirements of the noise reduction implementations.

---

## Preface

This report is the result of my master's thesis at Norwegian University of Science and Technology in Ålesund. I would like to thank my main supervisors, Vilmar Æsøy and Henry Peter Piehl who has guided me to successfully complete this study. They helped me to finish the study in the limited time line with a continuous follow up. Also, thanks to my co-supervisor, Lars Erik Helland from Ulmatec Pyro, who has provided the required data for this study. Specially thanks for the Henry Peter Piehl, Karl Henning Halse and Marko Mikulec for the supporting in CFD related issues and providing workstation and software licenses. Thanks to all the staff at the Department of Ocean Operations and Civil Engineering at NTNU.

This work would not have been possible without the great help and motivation from my parents, my wife and friends. I would like to specially thanks my loving wife Waruni who is taking care of our son during these two years of study period. Finally, I want to thank my colleagues and everyone for outstanding moral support during this challenging time.

---

## Nomenclature

### Abbreviations

<b>CFD</b>	Computational Fluid Dynamics
<b>CHT</b>	Conjugate Heat Transfer
<b>CRT</b>	Continuous Regeneration Trap
<b>DOC</b>	Diesel Oxidation Catalyst
<b>DPF</b>	Diesel Particular Filter
<b>EAT</b>	Exhaust After Treatment
<b>ECA</b>	Emission Control Area
<b>EGE</b>	Exhaust Gas Economizer
<b>FVM</b>	Finite Volume Method
<b>HVAC</b>	Heating Ventilation and Air Conditioning
<b>IMO</b>	International Marine Organization
<b>ORC</b>	Organic Rankine Cycle
<b>RANS</b>	Reynolds Averaged Navier-Stokes
<b>SCR</b>	Selective Catalytic Reduction
<b>WHRS</b>	Waste Heat Recovery System
<b>WHR</b>	Waste Heat Recovery

### List of Symbols

$\dot{m}$	Mass flow rate [ $kg s^{-1}$ ]
$\dot{q}$	Heat transfer rate [ $W$ ]
$\Delta T$	Temperature difference [ $^{\circ}C$ ]
$\delta$	Thickness [ $m$ ]
$\eta$	Efficiency
$\rho$	Density [ $kg m^{-3}$ ]
$A$	Area [ $m^2$ ]
$b$	Width [ $m$ ]
$c_p$	Specific heat capacity [ $J kg^{-1} K^{-1}$ ]
$d$	Diameter [ $m$ ]
$h$	Convective heat transfer coefficient [ $W m^{-2} K^{-1}$ ]
$k$	Thermal conductivity [ $W m^{-1} K^{-1}$ ]
$L$	Length [ $m$ ]
$m$	Mass [ $kg$ ]

---

$P$	Perimeter [ $m$ ]
$Q$	Flow rate [ $m^3s^{-1}$ ]
$q$	Amount of heat [ $J$ ]
$R$	Thermal resistance [ $KW^{-1}$ ]
$Re$	Reynolds number
$T$	Temperature [ $^{\circ}C$ ], [ $K$ ]
$t$	Thickness [ $m$ ]
$U$	Overall heat transfer coefficient [ $Wm^{-2}K^{-1}$ ]
$V$	Velocity [ $ms^{-1}$ ]
$z$	Height [ $m$ ]

**Subscripts**

1	hot fluid
2	cold fluid
$f$	fin
$i$	inner
$lm$	log mean
$o$	outer
$s$	surface
$w$	wall



---

# Table of Contents

<b>List of Figures</b>	<b>vii</b>
<b>List of Tables</b>	<b>x</b>
<b>1 Introduction</b>	<b>1</b>
1.1 Problem and Motivation . . . . .	1
1.2 Scope of the Research . . . . .	4
1.3 Objectives and Research Question . . . . .	5
1.4 Assumptions and Limitation . . . . .	6
1.5 Structure of the Thesis . . . . .	7
<b>2 State of the Art</b>	<b>8</b>
2.1 Waste Heat Recovery Unit . . . . .	8
2.1.1 Exhaust Gas Economizer . . . . .	8
2.1.2 Existing Waste Heat Recovery Systems . . . . .	9
2.2 Exhaust After Treatment Unit . . . . .	11
2.2.1 Diesel Oxidation Catalyst - DOC . . . . .	11
2.2.2 Diesel Particular Filter - DPF . . . . .	12
2.2.3 Selective Catalytic Reduction - SCR . . . . .	12
2.2.4 Existing Exhaust After Treatment Units for Diesel Engines . . . . .	13
2.3 Waste Heat Recovery and Exhaust After Treatment Combined Unit . . . . .	14
2.3.1 Existing Combined Units . . . . .	16
2.4 Vessels with Medium Speed Diesel Engines . . . . .	17
2.4.1 Engine Performance Data . . . . .	18
2.4.2 Properties of Diesel Exhaust . . . . .	19
2.4.3 Engine Exhaust Back Pressure . . . . .	20
<b>3 Methodology and Applied Theory</b>	<b>21</b>
3.1 Research Process . . . . .	21
3.2 Thermal Efficiency of Waste Heat Recovery System . . . . .	23
3.2.1 Heat Exchanger Fundamentals . . . . .	23
3.2.2 Overall Heat Transfer Coefficient . . . . .	26
3.2.3 Fouling Resistances . . . . .	27
3.2.4 Thermal Efficiency Improvement Methods in Heat Exchangers . . . . .	28
3.3 Thermal Simulation for the Waste Heat Recovery Performance Analysis . . . . .	31

---

3.3.1	Conjugate Heat Transfer - CHT . . . . .	31
3.3.2	CFD Modeling of Heat Exchanger . . . . .	31
<b>4</b>	<b>Case Studies</b>	<b>35</b>
4.1	Proposed Cases . . . . .	35
4.2	Case 1 - CFD Model Setup . . . . .	35
4.2.1	Performance Analysis of DN500 Economizer . . . . .	38
4.3	Case 2 - Economizer Optimization to Increase the Efficiency . . . . .	43
4.3.1	Performance Analysis of DN700 Economizer . . . . .	43
4.3.2	Using Baffles . . . . .	44
4.3.3	Using Exhaust Inlet Flow Directional Controlling . . . . .	48
4.4	Case 3 -New Economizer Design Concepts . . . . .	51
4.4.1	Design 1 - Spiral Water Pipe with Fins . . . . .	52
4.4.2	Design 2 - Rectangular Water Pipe with Fins . . . . .	54
4.4.3	Design 3 - Cuboid Water Pipe Bundle with Fins . . . . .	56
4.4.4	Design 4 - Cylindrical Water Pipe Bundle with Fins . . . . .	58
<b>5</b>	<b>Results and Discussion</b>	<b>61</b>
5.1	Comparison of Measured Data with the CFD Results . . . . .	61
5.2	Effects of Using Baffles . . . . .	63
5.2.1	Number of Baffles . . . . .	63
5.2.2	Baffle Cut Percentage . . . . .	64
5.3	Effects of Using Inlet Flow Directional Controlling . . . . .	65
5.4	Performance of the New Economizer Design Concepts . . . . .	66
5.5	Combined System of Exhaust Gas Economizer and Exhaust After Treatment unit	67
5.5.1	System Arrangement . . . . .	68
5.5.2	Combined System for Retrofitting . . . . .	69
<b>6</b>	<b>Conclusions</b>	<b>71</b>
<b>7</b>	<b>Future Work</b>	<b>73</b>
	<b>Bibliography</b>	<b>74</b>
	<b>Appendix</b>	<b>77</b>
	<b>A DN500 Economizer Performance Data Sheet</b>	<b>77</b>
	<b>B Fouling Factors of Gases and Water</b>	<b>78</b>

---

---

## List of Figures

1	Emissions from a vessel [13] . . . . .	1
2	Heat balance diagram for MAN 12K98ME/MC marine diesel engine operating at 100 SMCR under ISO conditions [23] . . . . .	2
3	MARPOL Annex VI NOx emission limits [5] . . . . .	3
4	MARPOL Annex VI SOx emission limits [5] . . . . .	3
5	Scope of the research . . . . .	4
6	Schematic diagram of marine engine with economizer system [29] . . . . .	9
7	ORCAN Efficiency Pack system arrangement and working principle [16] . . . . .	9
8	Waste heat recovery concept of Ulmatec Pyro WHR systems [18] . . . . .	10
9	Ulmatec Pyro WHRS arrangement inside a vessel (left) and exhaust gas economizer (right) [18] . . . . .	10
10	After treatment system arrangement for diesel engine with CRT [37] . . . . .	11
11	Ceramic honeycomb structure of DOC (a) Ceramic structure of wall-flow type DPF (b) [37] . . . . .	12
12	Schematic drawing of Daihatsu selective catalytic reduction system in vertical (a) and horizontal (b) installations [28] . . . . .	13
13	(a) VOLVO Penta EAT unit [21], (b) CUMMINS modular EAT unit [4] and (c) MAN modular EAT unit [12] . . . . .	14
14	Section view of theorized DPFHX based on shell-and-tube heat exchanger [43] . . . . .	15
15	Proposed system arrangement of WHR and EAT in exhaust system in project "No Waste" [15] . . . . .	15
16	GESAB Catemiser working principle [8] . . . . .	16
17	MAHLE WHR and EAT in a combined system [11] . . . . .	17
18	MOU Island Wellserver vessel [14] . . . . .	17
19	Exhaust system arrangement with 4 diesel engines inside the vessel [2] . . . . .	18
20	Wärtsilä 7L32 diesel engine (a) [22], Bergen W32 40L8A Engine (b) [1] . . . . .	18
21	Wärtsilä 7L32 diesel engine exhaust data [22] . . . . .	19
22	Research approach . . . . .	21
23	WHR unit and EAT unit development procedure for a combined system . . . . .	22
24	Typical heat exchangers, (a) double-pipe heat exchanger, (b) shell-and-tube heat exchanger, (c) brazed plate heat exchanger, (d) circular finned-tube heat exchanger, and (e) plate-fin heat exchanger [3] . . . . .	23
25	(a) Schematic for counter-flow channels, (b) the temperature distributions for the counter-flow arrangement [3] . . . . .	25
26	(a) Schematic for parallel-flow channels, (b) the temperature distributions for the parallel-flow [3] . . . . .	25
27	Thermal resistance and thermal circuit for a heat exchanger [3] . . . . .	26

---

28	Thermal circuit with fouling for a heat exchanger [3] . . . . .	27
29	Different types of baffle arrangements and flow across the baffles [35] . . . . .	28
30	Flow behavior based on baffle cut ratio and baffle spacing [35] . . . . .	29
31	Schematic of the tube-fin heat exchanger [34] . . . . .	29
32	Extended fins types, plate-fin (rectangular fin) (a), circular finned-tube (b), and longitudinal finned-tube (c) [3] . . . . .	30
33	DN500 EGE unit, main dimensions (a), simplified model for CFD analysis (b), finite volume mesh for the CFD simulations (c) . . . . .	35
34	DN500, Detailed view of the generated finite volume cells for CFD simulation . . .	38
35	Water region temperature distribution plot of DN500 for 350°C exhaust flow . . .	39
36	Water and exhaust flow temperature convergence plot from the CFD simulation . .	39
37	Water and exhaust flow pressure convergence plot from the CFD simulation . . .	40
38	Water and exhaust region heat transfer rate convergence plot from the CFD simulation	40
39	Water region temperature distribution plot of DN500 for 365°C exhaust flow . . .	41
40	Water region temperature distribution plot of DN500 for 395°C exhaust flow . . .	42
41	DN700 EGE unit, main dimensions (a), simplified model for CFD analysis (b), generated mesh for the CFD simulations (c) . . . . .	43
42	Temperature distribution of the water and exhaust region of DN700 . . . . .	44
43	DN700 EGE unit 3D model with 3 baffles . . . . .	45
44	Water flow streamlines of DN700, without baffles (a), 1 baffle (b), 3 baffles (c) and 5 baffles (d) . . . . .	45
45	Water flow velocity distribution through the vertical mid section of DN700, without baffles (a), 1 baffle (b), 3 baffles (c) and 5 baffles (d) . . . . .	46
46	Water flow temperature distribution through the vertical mid section of DN700, without baffles (a), 1 baffle (b), 3 baffles (c) and 5 baffles (d) . . . . .	46
47	Water flow streamlines of DN700 with reducing the baffle cut by 10% for the 3 baffle arrangement . . . . .	47
48	Water flow velocity distribution through the vertical mid section of DN700 with reducing the baffle cut percentage by 10% for the 3 baffle arrangement . . . . .	47
49	Water flow temperature distribution through the vertical mid section of DN700 with reducing the baffle cut percentage by 10% for the 3 baffle arrangement . . . . .	48
50	Exhaust flow velocity streamlines of the DN700 . . . . .	48
51	Exhaust flow direction control of DN700 using, cone shape (a) and angular blades (b) 3D models for CFD analysis . . . . .	49
52	Exhaust flow velocity distribution through the vertical mid section of DN700 with exhaust flow direction controlling (without flow controlling and increasing cone shape angle) . . . . .	50
53	Exhaust flow velocity distribution through the vertical mid section of DN700 with exhaust flow direction controlling (increasing cone shape angle and swirl flow using angular blades) . . . . .	50

---

---

54	Design 1; water volume (a), pipe and fin arrangement (b) and model for the CFD simulation (c) . . . . .	53
55	Design 1; water flow temperature distribution of outer surface of the volume (a) and through the vertical cross section (b) . . . . .	53
56	Temperature distribution through the vertical section of the EGE unit (left) and temperature distribution of the outer surface of the fins and pipe assembly (right) of Design 1 . . . . .	54
57	Design 2; water volume (a), pipe and fin arrangement (b) and model for the CFD simulation (c) . . . . .	55
58	Design 2; water flow temperature distribution of outer surface of the volume . . . . .	55
59	Temperature distribution through the vertical section of the EGE unit (left) and temperature distribution of the outer surface of the fins and pipe assembly (right) of Design 2 . . . . .	56
60	Design 3; water volume (a), pipe and fin arrangement (b) and model for the CFD simulation (c) . . . . .	57
61	Design 3; water flow temperature distribution through the sections of the water volume . . . . .	57
62	Temperature distribution of the vertical section of the EGE unit (left) and temperature distribution of the outer surface of the fins and pipe assembly (right) of Design 3 . . . . .	58
63	Design 4; water volume (a), pipe and fin arrangement (b) and model for the CFD simulation (c) . . . . .	59
64	Design 4; water flow temperature distribution through the sections of the water volume . . . . .	59
65	Temperature distribution of the vertical section of the EGE unit (left) and temperature distribution of the outer surface of the fins and pipe assembly (right) of Design 4 . . . . .	60
66	DN500 measured data and CFD simulation results comparison graphs for, heat transfer rate (a) and exhaust gas pressure drop (b) . . . . .	61
67	DN500 temperature and pressure sensors positions . . . . .	62
68	DN500 CFD simulation results comparison graphs of heat transfer rate with and without exhaust fouling resistance . . . . .	62
69	DN700 CFD simulation results for increasing number of baffles, heat transfer rate (a), water outlet temperature (b) and water flow pressure drop (c) . . . . .	63
70	DN700 CFD simulation results for reducing baffle cut size, heat transfer rate (a), water outlet temperature (b) and water flow pressure drop (c) . . . . .	64
71	DN700 CFD simulation results for exhaust flow direction control, heat transfer rate (a), water outlet temperature (b) and exhaust pressure drop (c) . . . . .	65
72	DN700 existing design, DN700 with 3 baffles and new designs CFD simulation result for, heat transfer rate (a) and water outlet temperature (b) . . . . .	66
73	DN700 existing design, DN700 with 3 baffles and new designs CFD simulation result for exhaust pressure drop (a) and comparison of water and exhaust contact surface area (b) . . . . .	66

---

---

74	Main configurations of EAT system arrangement used for diesel engines combined with the EGE unit for waste heat recovery . . . . .	68
75	3D conceptual design of complete assembly of WHR and EAT unit for exhaust system	69
76	Existing exhaust system arrangement (a) and proposed combined system with EAT and EGE (b) . . . . .	70

## List of Tables

1	Physical properties of air ( $p = 101.13$ kPa) $T$ temperature; $\rho$ density; $h$ specific enthalpy; $s$ specific entropy; $C_p$ specific heat at constant pressure; $\mu$ viscosity; $k$ thermal conductivity [7] . . . . .	19
2	Approximate values of convection heat transfer coefficients [31] . . . . .	24
3	Exhaust gas inlet conditions for the DN500 with different exhaust temperatures . .	36
4	Water flow inlet properties for DN500 . . . . .	36
5	Exhaust gas properties for different flow temperatures . . . . .	36
6	CFD simulation results and the measured data for DN500 with 350°C exhaust inflow	41
7	CFD simulation results and the measured data for DN500 with 365°C exhaust inflow	41
8	CFD simulation results and the measured data for DN500 with 395°C exhaust inflow	42
9	CFD simulation results for the DN500 without exhaust fouling . . . . .	43
10	DN700 water and exhaust gas inlet conditions . . . . .	44
11	CFD simulation result of DN700 . . . . .	44
12	CFD simulation results comparison for the increased number of baffles for DN700 .	46
13	CFD simulation results comparison for the reducing the size of the baffle cut for DN700 . . . . .	48
14	CFD simulation results comparison for the exhaust flow direction control for DN700 with 3 baffles . . . . .	51
15	Water and exhaust contact surface area of DN700 without considering pipe thickness	51
16	Water and exhaust contact surface area of Design 1 . . . . .	52
17	CFD simulation results of Design 1 . . . . .	54
18	Water and exhaust contact surface area of Design 2 . . . . .	54
19	CFD simulation results of Design 2 . . . . .	56
20	Water and exhaust contact surface area of Design 3 . . . . .	56
21	CFD simulation results data of Design 3 . . . . .	58
22	Water and exhaust contact surface area of Design 4 . . . . .	58
23	CFD simulation results of Design 4 . . . . .	60

---

# 1 Introduction

## 1.1 Problem and Motivation

### Energy Wastage and Emission from Marine Engines

Maritime transportation considered as the main mode of transportation of the international logistics which has more than 95% of the world's total trade volume due to the continuous development of the shipping industry and this accounts for the 3% of total energy consumption [47]. Hence, this industry is responsible for higher percentage of emissions through power generation using heavy fuel and diesel engines. The energy wastage causes higher emissions due to the excessive requirement of the fuels. This reveals that the energy wastage and the emissions of the power generation have a direct relationship towards the environmental pollution.

The energy wastage and pollutants emitted to the environment from engines of the existing marine vessels are commonly discussed problems for decades. Also the sound pollution with the generated noise of the exhaust system in these marine engines are having a considerable impact to the environment. About 50% of the fuel energy which is supplied to the diesel engine in marine vessels are wasted in to the surrounding [41] as shown in Figure 2. This waste mainly consists with the heat dissipation from the exhaust gas and engine cooling requirements. The main contributor for this wastage is the exhaust gas which has a higher heat dissipation from the system to surrounding. This decreases the efficiency of the engine and there are several methods to harness considerable amount of this waste energy as an use full energy for on board operations such as electricity, hot water and steam. The heat dissipation due to the non-utilized energy in the form of waste heat is the main cause for the requirement of higher amount of fuel burning which is nearly twice of the requirement. This also causes for the increasing the amount of harmful emissions from the marine engines.



Figure 1: Emissions from a vessel [13]

Combustion products of the fuel and the remaining air are the main composition of the exhaust gas generated by the marine engines. The main component of the combustion products that can cause pollution to the atmospheric environment and cause harm to the human health is Carbon monoxide (CO), Nitrogen oxides (NO<sub>x</sub>), Hydrocarbons (HC), Sulfur oxides (SO<sub>x</sub>) and particulate matter (PM). When it consider the amount of emissions in marine applications, it contributes 2.8% of the global Green House Gases (GHG) with an amount about 1 billion tons annually. This contains NO<sub>x</sub> and SO<sub>x</sub> in with 15% and 13% respectively [19]. The most harmful impacts from the marine emissions are the climate changes due to the greenhouse gasses, depletion of the ozone layer, lowering the air quality and the acid rains. It is clear that the emission controlling of the marine

industry is an essential task to protect both environment and human health. Hence, the advanced technological developments to achieve higher efficiencies in marine engines and emissions treatment methods are used to reduce these emissions, according to the emission control regulations.

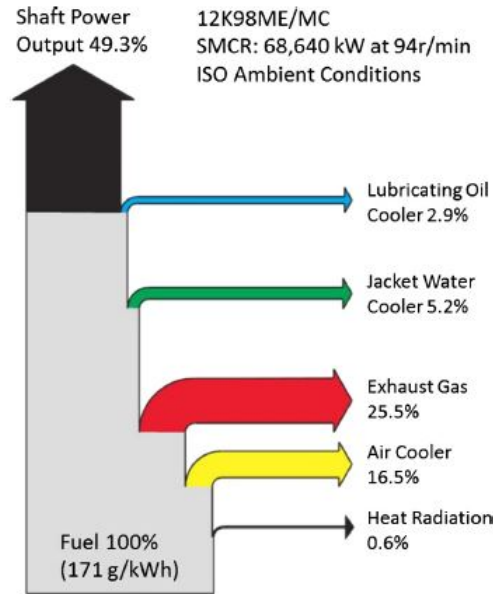


Figure 2: Heat balance diagram for MAN 12K98ME/MC marine diesel engine operating at 100 SMCR under ISO conditions [23]

### Emission Controlling in Marine Environments

Several international organizations have already taken actions to prevent the environmental impact from the marine emissions with creating regulations to emissions controlling. International Maritime Organization (IMO) has established emission standards which are commonly referred as Tier I, Tier II and Tier III. IMO ship pollution rules are contained in the “International Convention on the Prevention of Pollution from Ships”, which is known as MARPOL 73/78. The NO<sub>x</sub> emission limits of Regulation 13 of MARPOL Annex VI apply to each marine diesel engine with a power output of more than 130 kW installed on a ship [9].

NO<sub>x</sub> emission limits are set for diesel engines depending on the engine maximum operating speed, as shown in the graph in Figure 3. Tier I and Tier II limits are global, while the Tier III standards apply only in NO<sub>x</sub> Emission Control Areas (ECAs). A marine diesel engine that is installed on a ship constructed on or after the following dates and operating in the following ECAs shall comply with the Tier III NO<sub>x</sub> standard: 1 January 2016 and operating in the North American ECA and the United States Caribbean Sea ECA; or 1 January 2021 and operating in the Baltic Sea ECA or the North Sea ECA [9]. Also, Annex VI has regulations for the Sulfur content of the marine fuel as a measure to control SO<sub>x</sub> emissions. But there is no direct regulation for PM controlling. The sulfur control limits revealed by the annex VI is shown in figure 4. There are measurements which has taken to control the SO<sub>x</sub> in ECAs and globally using exhaust gas cleaning systems. Scrubbers are one of these methods currently using in ships which are using high sulfur content fuels.

This regulation has created positive impact towards the controlling harmful emissions in marine environment throughout the last decades. The SO<sub>x</sub> and NO<sub>x</sub> controlling through the developments are carried out in worldwide to achieve the targeted values. However, it is mandatory to develop the systems for the existing ships to achieve these targets. Because the existing ships will be in the service for several decades and these vessels need to be retrofitted with the emission treatment systems and fuel efficiency improvement systems such as waste heat recovery systems.



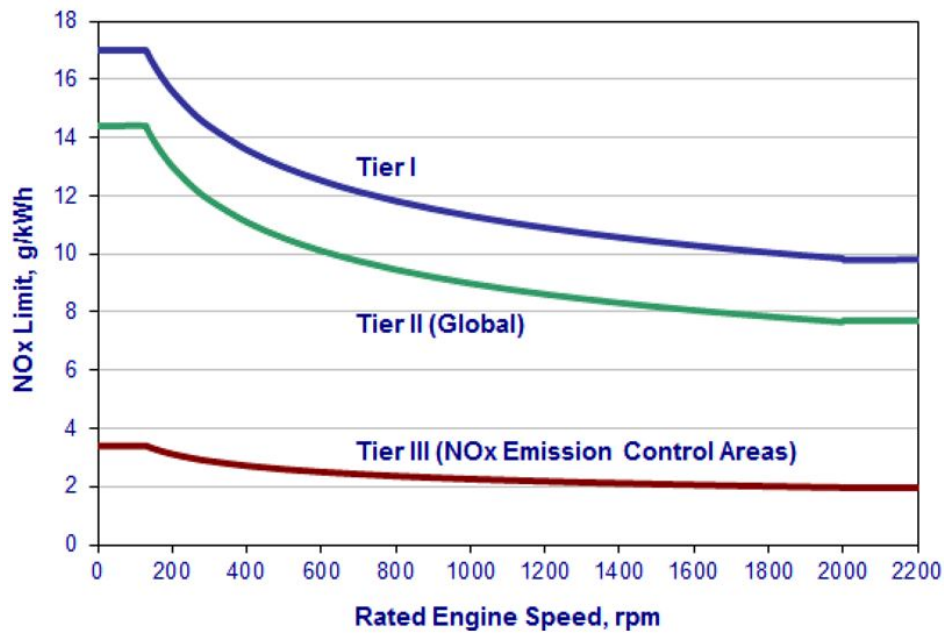


Figure 3: MARPOL Annex VI NOx emission limits [5]

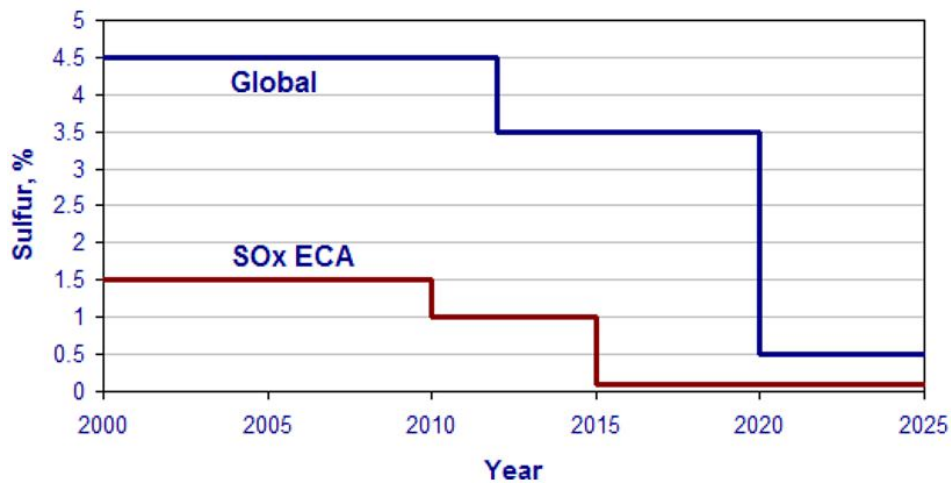


Figure 4: MARPOL Annex VI SOx emission limits [5]

### Waste Heat Recovery (WHR) and Exhaust After Treatment (EAT)

Increasing fuel efficiency and the implementing exhaust treatment methods are the main methods of the controlling emissions of the engines which are currently deployed in the ships. Waste heat recovery systems (WHRS) are used to recover the waste heat from the engines to increase the fuel efficiency. This is one of the methods to save the energy and reduce the emissions. Exhaust after treatment (EAT) systems are used to treat the exhaust gas to removing the harmful components from the exhaust to reduce the environmental impact.

The WHR systems can save the fuel around 4-16% from medium to large scale diesel engines [41]. Which is lower when the size of the engine is reduced. This depend according to the temperature of the exhaust which is limited to a range when it comes to the medium speed and slow speed engines.

In large large ships such as bulk carrier, oil tankers and container ships there are several types of waste recovery methods are currently using and also, the exhaust after treatment methods. This is a technology which has developed for decades and it is important to reduce fuel consumption needs from the current levels for the purpose of reducing the maritime emissions. This can be achieved by increasing overall power plant efficiency. It is expected that the diesel engines in the marine applications can not be replaced with alternative option in a foreseeable period of time. So, we have to deal with the reducing emissions and increasing efficiency of the diesel engines to minimize the impact. Now days, this technology has improved for the land based vehicles which has a high power generation such as heavy truck engines to low power generation passenger car engines. When it consider the existing fleet of diesel powered vessels in operation, it is more important to modify the exhaust system with EAT and WHR units to increase efficiency with reducing harmful emissions. Even these units are exists in the market, considering for the medium scale ships which need to retrofit these systems in its exhaust system, it will be a matter of system arrangement and the efficiency which depends with the size of the engine.

When it is focused on the diesel engine emissions controlling and increasing fuel efficiency, several developments has carried out for the ground vehicles such as trucks with combination of WHR and EAT. It is important to consider the marine diesel engines in the context of the emission controlling and environmental protection which is mainly focused on this study. The WHR optimization and integrating in to a one system with EAT as a concept development is mainly focused for this study with the industrial collaboration waste heat recovery systems manufacturing industry for marine engines. It is required to study the efficiency of the individual units for creating the combined system with related to the system interactions parameters which will cause for the overall system performance.

## 1.2 Scope of the Research

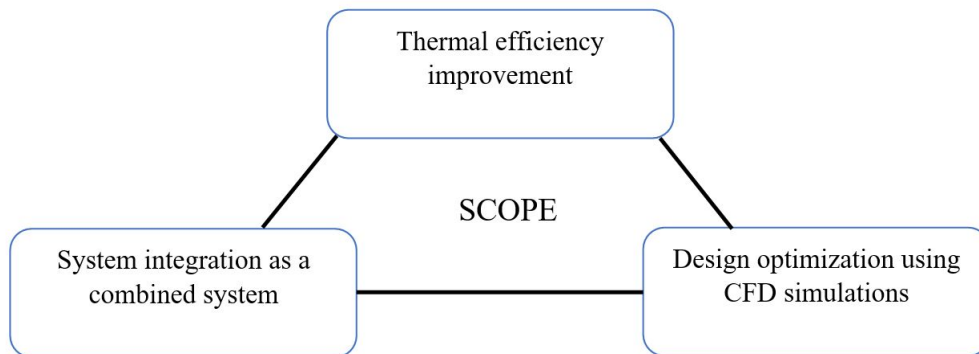


Figure 5: Scope of the research

The scope of this study is consisted with the thermal efficiency improvement of the EGE unit with design optimization based on the CFD simulations and the combined system development of the EAT and EGE with considering the system requirements as shown in Figure 5. The following section describes the scope of this study in detail.

### Thermal Efficiency Improvement

The main output parameter to evaluate the performance of the WHRS is the thermal efficiency. In this research study, the Exhaust Gas Economizer (EGE) of the WHRS is focused for the efficiency improvement and optimization which is the heat extraction unit from the exhaust gas in the WHRS. Increased thermal efficiency helps to reduce the burning of fuel in the engine which also helping the emission reduction. The EGE is mainly functioning as a heat exchanger and the thermal efficiency of the unit can be evaluated and increased by developing the initial design. The design

---

implementations required to increase the efficiency of the WHRS is mainly focused on the EGE unit with the initial geometrical shape and size of the unit. The thermal efficiency can be evaluated using simulation for the conjugate heat transfer of the EGE using Computational Fluid Dynamics (CFD) simulations. For this purpose it is required a CFD simulation tool which can model the heat transfer between two fluid regions of a heat exchanger with design improvements on both fluid regions.

### **Design Optimization Using CFD Simulations**

The design optimization of the WHR system is focused for the EGE unit with the new developments for the two flow regions of the unit with using CFD simulations. This is based on the development of the initial EGE unit design and different flow arrangement inside the unit with efficiency improvement methods according to the previous section. The CFD simulations are conducted to identify the best design modification of the unit and the new design proposals with heat transfer rate improvements between two working fluids. Study of the flow behavior of the initial design helps to find the problems of the EGE unit and the optimization process is conducted to change the flow patterns of the working fluids in the initial design to achieve a higher heat transfer rate through the design implementations. These simulations help to identify the heat transfer and the flow behavior of the EGE unit to make decisions related to the EGE performance and integrated system performance combining with the EAT unit.

### **System Integration as a Combined System**

The combined system considered in this research is consisted with the EGE unit of the WHR system and the EAT unit. These two units need to be combined into a single system for the retrofitting purposes for the existing vessels. The EGE need to be functioned to create hot water from the waste heat which can be used for the heat requirements of the vessel. The EAT unit is mainly focused on the NO<sub>x</sub> removal, and diesel particle filtration. The Sulphur removal is not considered for this study due to the using of diesel engines which are not significantly produce SO<sub>x</sub> in the exhaust compared to the heavy fuel oil engines. The combined system concept development process is based on the connection interfaces of the different units and the input and output parameters of the individual units which affects the total system performances. Also, developing these individual units in to combined unit for installing into an existing vessel included in to the scope of this study.

## **1.3 Objectives and Research Question**

The main objective of this research is optimizing a EGE for WHRS to integrate with an EAT unit as an efficient combine system which can be retrofitted into medium speed marine diesel engines selected from 1MW - 5MW engine capacity range and 400rpm - 1200rpm with considering design limitations. The optimization process is carried out with using CFD simulations for design improvement and new concept developments of EGE unit. As the starting point of this research the design refinements are conducted with the implemented methodology which is discussed in the methodology section. Hence, the efficiency of the system will vary with design according to the size of the engine and efficiency improvement method of the EGE unit. Implementations are need to be conducted with considering the output parameter of the exhaust which are temperature, flow rate and flow speed of the flow. This also consists with the new design alternatives which can be used to improve the efficiency of the system and evaluate using CFD simulations. The main objectives of this study will be based on the research questions which are mentioned bellow. The solutions for this research questions will deliver the main objective of this project which is discussed based on the case studies of this research process.

### **Research Questions**

(RQ-1) How to evaluate the key performance indicators of EGE unit?

The EGE performance need to evaluate for the process of design improvements. The heat transfer efficiency of the EGE unit causes the WHRS performance and it is required to identify key performance indicators of the unit and interaction with the heat transfer efficiency for development and system integration.

---

(RQ-2) How to optimize the EGE unit design using CFD simulations?

Initial CFD model development is required for the existing EGE unit to compare the CFD simulation results and measure values from the actual unit with different flow conditions. The optimization process is conducted based on the CFD simulation results and it requires a development process for the EGE unit with analyzing the key performance indicators of the unit. This covers the design developments and the new design proposal evaluations using CFD simulation results.

(RQ-3) What are the new design concepts for EGE with a potential gain towards the efficiency improvements?

The new concepts for the for EGE unit are developed with changing flow patterns and using efficiency improvement techniques. The potential gain is evaluated using simulations for these concepts referring to the key performance indicators for the EGE unit. The concept development process is followed a by continuous improvement method to efficiency improvement.

(RQ-4) What are the design requirements for the combined system of EGE and the EAT unit?

To evaluate the efficiency of the combined unit, the performance indicators are important for individual components of EGE and EAT. This helps to analysis the effect on performance with the changing of the units capacity and geometries. These combined units will be fitted in to the existing vessels exhaust systems. Because of this, it is essential to identify the arrangement of the compact design which can fitted in the limited space available in the vessels and connecting the combined system in to the exhaust line.

The research questions which are mentioned in this section mainly focused on the combined system of EGE and EAT implementation with improved efficiency through design optimization. The CFD model development to evaluate efficiency is mainly based on the actual unit and the result comparison is done according to the measured data. EGE design improvement mainly based on the EGEr unit and the combined unit is developed according to the current research and development data. According to the limited space available in the existing vessels, it is required that, the design should be compact and need to be designed to fit in to the existing exhaust line which will be more effective in retrofitting. For the combined system, the performance can be evaluated from the EGE efficiency and the quality of the emission. But in this project measuring the emission quality is not accounted due to the qualitative analysis. The performance of the individual units has an impact on each other and the total system performance. This also affect to the engine efficiency and the performance characteristics need to be studied with the system development stage to come up with the best possible solution. The CFD results are used to evaluate the performance levels of the developments and new designs with considering temperature and pressure variations. The combined unit development also needs to be done with considering the temperature and pressure levels which are caused by the reactions inside the EAT unit and pressure drop develop through the units. The optimization process for the EGE is done by using the CFD simulation results from the case studies based on the initial performance level improvement.

## 1.4 Assumptions and Limitation

There are several limiting factors and assumptions required for this research project. Even there are several products exist in the market similar to the combined system of EAT and WHR. The technology behind these devices are still not revealed. These developments were done for years of progressive work. The available data in the researchers are not mainly focusing a combined system development. They are focused on individual units or in some cases with interaction of two units. For analyzing these systems and EGE unit optimization, it is needed to make several assumptions on this study. This research is conducted as a qualitative research but there are comparison of the performance data through actual measurements of the initial EGE unit, based on the CFD simulation results. There is no experimental procedure carried out with this research and conclusions are made with the CFD results. The developments are implemented for a selected EGE unit with new deign concepts in the same product capacity range. Due to the multiple tasks included in to this project, the available time is another limiting factor which requires to narrow down in to the scope of the study. Hence, the study is done within the scope with required

---

simulations to evaluate and optimize the performance of EGE and concept development of the combined system for retrofitting purpose.

## 1.5 Structure of the Thesis

The thesis structure is created according to the following sequence which is briefly discussed the content of the sections in this section.

- State of the Art

In section 2, it reviews the state of art of the WHR systems, EAT systems and combined units in ground vehicle engines and marine engines. The sub sections describes the basic operations of individual units with the available information. Also the information which are extracted from the past research works which are related to the WHR and EAT is also included throughout this section according to the necessity.

- Methodology and Applied Theory

Section 3 reviews the methodology which is used for this research study with covering the sub activities in the main task. This reveals the main approach for the optimization of EGE unit with evaluating the performance and design limitations of the system. The reserch process of the methodology is developed according to the different units which are embedded to the combined system and continuous improvement requirements according to the design changes with performance evaluations. Also the basic principles with the theory of the heat transfer, heat exchanger working principles and heat transfer efficiency improvement methods are also included to this section. Then the available simulation software for CFD analysis which can be used to evaluate the system components performance is included in this section for design optimization process with the basic CFD theory used in this study.

- Case Studies

Section 4 reviews the case studies which are implemented to follow the methodology with considering the EGE optimization and new developments. This section consists the CFD model development for the thermal simulations of the EGE and new developments. Simulation results from the case studies are summarized for the data comparison in the discussion section. These case studies are important to achieve the final concept of the combined system with the different approaches to the system and EGE unit performance optimization process.

- Results and Discussion

Section 5 discusses the results from the case studies and compare them with the CFD simulation results. This includes the design modification for optimization process, new design evaluation for the EGE and the combined system concept of EGE and EAT unit which is required for the retrofitting in the vessel. CFD simulation results are evaluated with comparing the measurement data to verify the CFD model which is modeled to simulate different cases in the case studies. The results and discussion section provides a better overview of the performance of the system based on the CFD simulations to predict the performance enhancement of the system and individual units.

- Conclusion

Section 6 presents the conclusions of this research study, which is based on the results of the CFD simulations and the concept development of the combined system. It is important to note that the simulations data is required to evaluate through experimental set up which is not in the scope of this study.

- Future Work

Section 7 consists with the suggestions for the future stage of this research study based on the current study and results which are more useful for the future development of the system. This includes several steps related to the study which is not covered in this report due the time limitations. Also, it reveals the several sub projects which can be connected to this research study in the future.

---

## 2 State of the Art

### 2.1 Waste Heat Recovery Unit

EAT units and waste WHRS are generally used in most of the ships nowadays to increase operational performances levels with following the emission control regulations. These units are included to the system separately to get the required output. When it considers the engines with high power output, these systems get more expensive and complex in designs and implementation. The WHRS are used to recover thermal energy from the exhaust gas and convert into a useful electric energy, hot water or other type of heat requirements of the vessel. According to the *MAN Diesel and Turbo*, in marine engines, normally about 50% [23] of total fuel energy supply for the engine is dissipated to the environment. Even this energy amount is high, due to the low temperature of the exhaust gas, it has a low quality when it comes for an energy recovery consideration. Hence it requires an effective WHRS to harness the energy from the exhaust gas.

Types of WHRS commonly used in on-board vessels,

- **Economizer**  
Economizer used to generate steam from the fresh water using exhaust heat energy where installed in the exhaust line of the engine. This is a type of boiler and the generated steam can be used for heating requirements of the vessel.
- **Steam Turbine Generator**  
The excessive amount of steam which is generated by the economizer used to produce electrical energy using steam turbine and electrical generator. This produced electricity can be directly transfer to the electrical power requirement of the vessel.
- **Fresh Water Generator**  
The fresh water generator generate fresh water from the sea water by boiling the water at lower boiling point with the aid of reduced pressure. The required thermal energy is supplied by the waste heat of the engine.

These WHRS are capable of utilizing medium and low quality heat for power production. Also these systems are suitable for both newly building vessels and retrofitting existing vessels which is economically feasible solution. According to the *Singh and Pedersen* the WHRS mainly should have following the features [41]. Which are high efficiency utilizing waste heat, high power density to supply large power demands, adaptable to the changing vessel operational profile, easy to integrate with other power systems aboard, reliable in operation, smaller footprint due to space and weight limitations and safe in operation and handling aboard.

#### 2.1.1 Exhaust Gas Economizer

The economizer is a mechanical device which is used in WHRS in various applications such as boilers and high-power engines in ground applications and marine applications. In Figure 6 illustrates an economizer assembly in a marine engine which is used to recover the heat from the exhaust. The exhaust flow coming out from the main engine and auxiliary engine passes through the economizer. It will heat up the inlet fluid of the economizer which is working as a heat exchanger. The waste heat of the exhaust gas can be recovered through this unit which is using the fundamentals of heat and mass transfer. The exhaust side of the economizer basically consists with different types of fins to increase the heat transfer rate which results the thermal efficiency improvement of the unit. Also there are different types of economizer units using in different marine and industrial applications operating with engine exhaust and boiler exhaust which have various outer shapes and sizes.

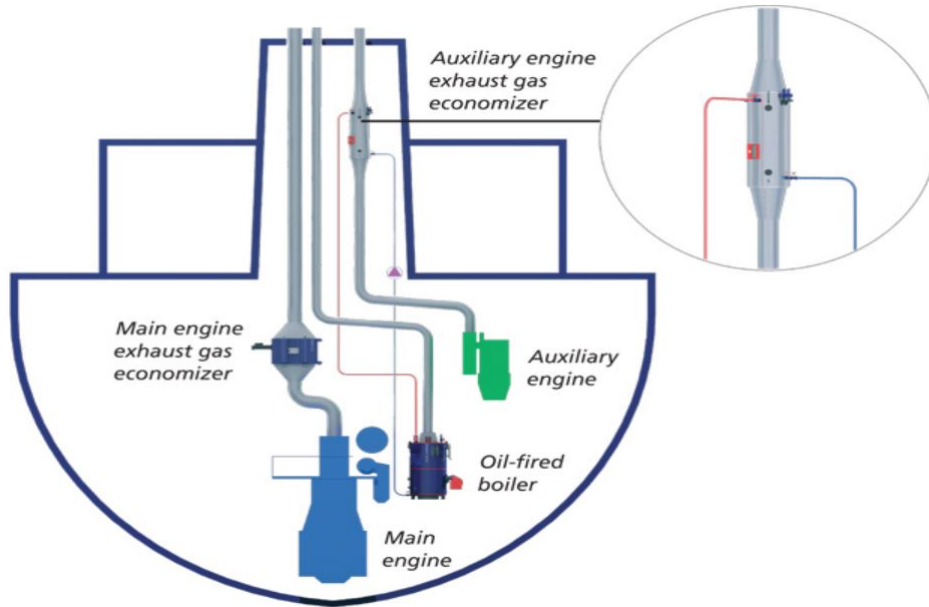


Figure 6: Schematic diagram of marine engine with economizer system [29]

### 2.1.2 Existing Waste Heat Recovery Systems

#### ORCAN Efficiency Pack

ORCAN produces different sizes of WHRS for marine engines which are ranging up to several mega watts and some of these units can be combined as modules according to the engine power. These WHR units called as *Efficiency Packs* which are mainly consist of the components of Rankine cycle (organic) which are evaporator, expander, condenser and feed pump. The separate heat exchanger is used to extract the heat from the exhaust gas as shown in Figure 7.

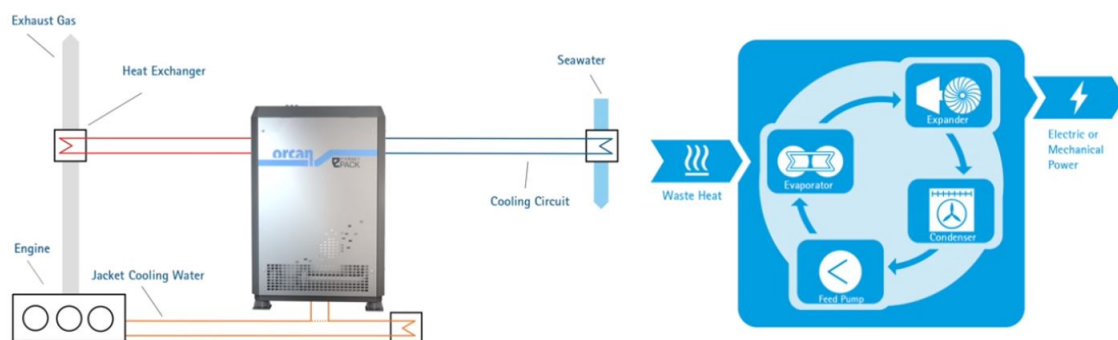


Figure 7: ORCAN Efficiency Pack system arrangement and working principle [16]

Berger Maritiem is a company which provide total solution for the EAT and WHR for medium speed marine engines with combining separate units from different manufacturers such as ORCAN

for the WHR and Fischer Abgastechnik for the diesel particulate filters and SCR units.

### Waste Heat Recovery Systems of Ulmatec Pyro

Ulmatec Pyro’s working on designing and manufacturing Waste Energy Recovery Systems to generate hot water or electrical power requirement for the onboard requirements from the waste heat of the engine. The typical system mainly consists systems to extract heat from the exhaust and cooling water, and then heating the water in the central heating system for the desired temperature level. This system enables the supply of consistence energy output with the varying exhaust gas temperature ranges.

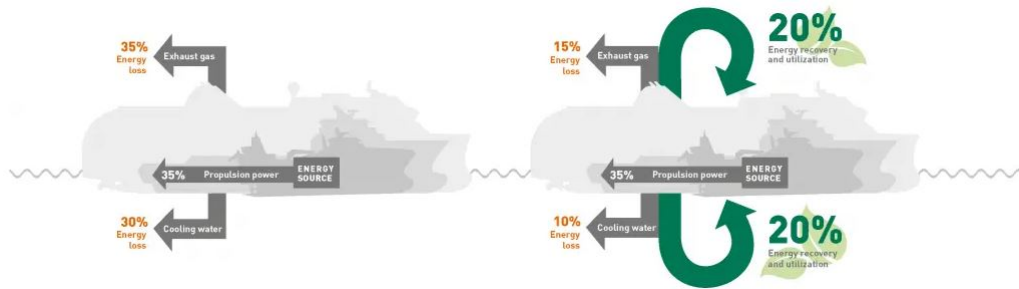


Figure 8: Waste heat recovery concept of Ulmatec Pyro WHR systems [18]

According to the product data, the system can reduce the energy loss by 35% to 15% from the engine exhaust and the 30% to 10% from the waste heat of the engine cooling water. This WHRS extracts heat and supply energy between various consumers onboard, such as the HVAC (heating ventilation and air conditioning) system, heating of bathrooms, cabins and living rooms, producing hot potable water, tank heating and heating water for the fresh-water generator and for the pool.

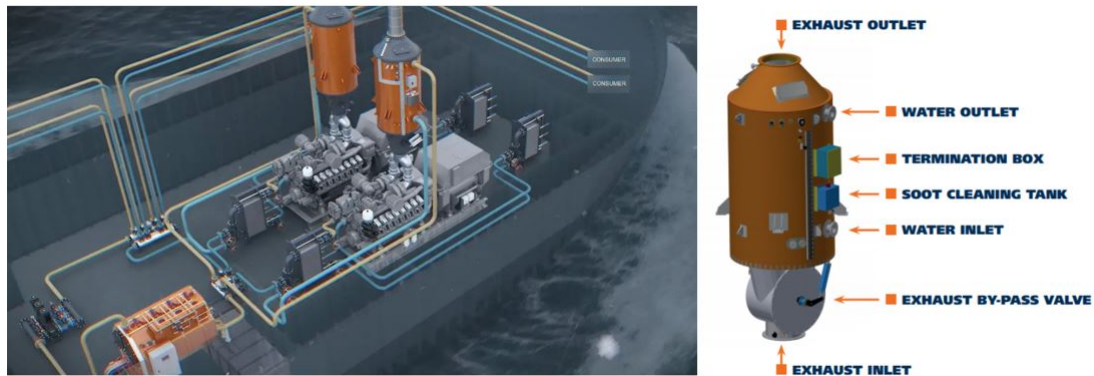


Figure 9: Ulmatec Pyro WHRS arrangement inside a vessel (left) and exhaust gas economizer (right) [18]

The exhaust gas economizer (EGE) unit in the WHRS will be considered for the improvement of WHR unit which is working as a heat exchanger to transfer exhaust heat into the supply water. This is the main heat transfer device from exhaust to usable energy. The EGE unit connects to the exhaust line between the engine and muffler unit. This device is a type of shell and tube heat exchanger which has exhaust gas runs through the tubes. This device size will vary according to the engine capacity and the range has defined according to the exhaust pipe diameter. The size



range defined as DN500 (exhaust pipe diameter 500mm), DN700, DN1200 etc. The supply flow temperature of the water ranges between 75°C and 95°C and the desired temperature out put vary according to the demand and the water supply flow rate. The water chamber is kept under pressure of ranging 6bar to 9bar to keep the water temperature up to 115°C in the output. The system does not contain EAT unit which causes the soot inside pipes of the EGE unit and the EAT unit can be installed to the system separately.

## 2.2 Exhaust After Treatment Unit

When it comes to the emissions of the marine engines, it has a considerable amounts of pollutants which are mainly Nitrogen dioxides( $\text{NO}_2$ ), Sulfur dioxides( $\text{SO}_2$ ), Hydrocarbons (HC) and particulate matter(PM) due to the burning of heavy fuel in the engine combustion process. In marine applications scrubbers are used to clean the  $\text{SO}_x$  from the exhaust and diesel particle filters used to remove the particles. For the  $\text{NO}_x$  removal of the exhaust, the catalytic cleaning process (SCR unit-selective catalytic reduction) is used which break down the  $\text{NO}_x$  to  $\text{N}_2$  by using urea a catalyst.

These systems can be seen in both land and marine applications. But the main difference is the heavy fuel oil engines which are used in ships need a scrubber to remove sulfur due to high sulfur content in the fuel. But in conventional diesel engines doe not produce considerable amount of  $\text{SO}_x$  in the exhaust.

According to *Apicella et al.* [25], after treatment devices are more effective for bringing down the emission in to acceptable level without impacting the engine performance. Sometimes there can be little impact on the engine which is considerably low.

The main parts of the after treatment devices for diesel engines consists with diesel particular filter (DPF), diesel oxidation catalyst (DOC) lean  $\text{NO}_x$  (combine unit of DOC and DPF is know as continuous regeneration trap -CRT) and selective catalytic reduction (SCR). EAT units can be combination of all these sub units or several of sub units [30].

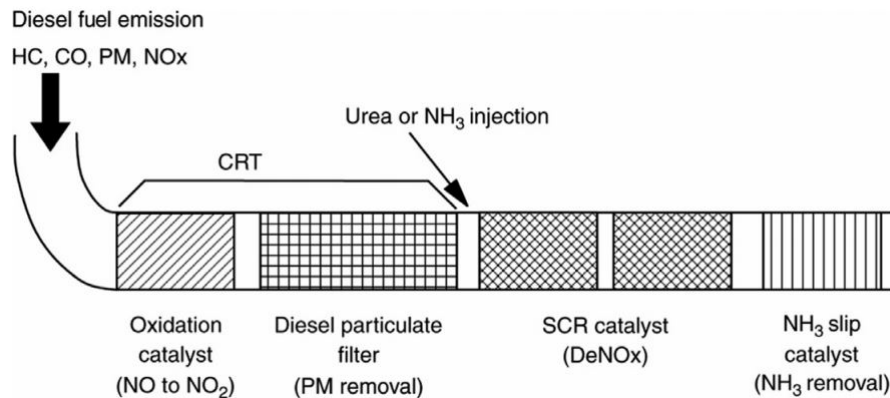


Figure 10: After treatment system arrangement for diesel engine with CRT [37]

### 2.2.1 Diesel Oxidation Catalyst - DOC

Diesel particulate filter removes particle matters of diesel with a filtering system which is commonly used in commercial vehicles for decades. DPF can be combined with DOC to oxidize CO and unburnt hydrocarbon from the exhaust. Also, DOC helps to removal process of  $\text{NO}_x$  in the SCR unit.[40] As described previously, the diesel exhaust mainly contains  $\text{NO}_x$ , CO ,HC and PM which are required to treat in the EAT unit. Typically, 90% of  $\text{NO}_x$  exists as NO in the diesel exhaust gas. Therefore, the pretreatment for the oxidation of NO to  $\text{NO}_2$  is an important process. platinum

(Pt), palladium (Pd), and ruthenium (Rh) are used as catalysts for this unit with a honeycomb structure which is made out of ceramic substrate coated with one of this material. This honeycomb structure which is shown in the Figure 11 (a) creates a pressure drop in the stream due to the large number of small holes in it. Also, HC and CO to be converted into  $\text{CO}_2$ , and  $\text{H}_2\text{O}$  due to the complex reaction process takes place inside the unit. This process creates an additional heat into the exhaust stream which is useful for the passive regeneration for the DPF unit which will be described in the next section. The actual NO conversion efficiency is 60% at  $350^\circ\text{C}$ . At higher temperatures ( $\geq 350^\circ\text{C}$ ), for instance, the actual and equilibrium NO conversion efficiencies are typically 40% and 20% at  $430^\circ\text{C}$  and  $500^\circ\text{C}$ , respectively.

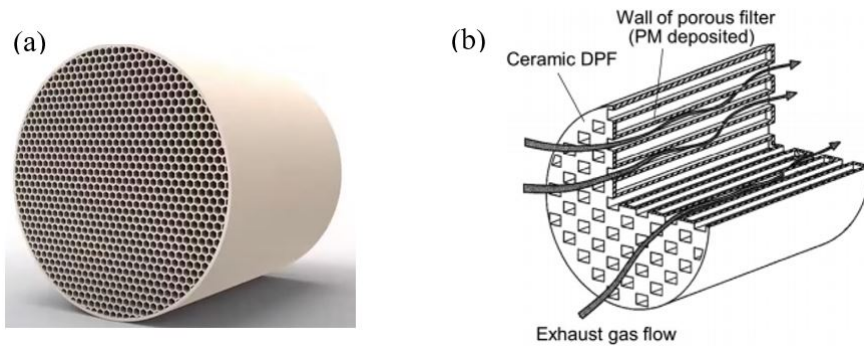


Figure 11: Ceramic honeycomb structure of DOC (a) Ceramic structure of wall-flow type DPF (b) [37]

### 2.2.2 Diesel Particular Filter - DPF

Currently, there is a lack of universally recognized international regulations concerning PM itself for exhaust gases of marine diesel engines. A reverse cleaning regeneration system using a ceramic DPF [36] is one type of a commercially available product for removing black smoke emission. Figure 11 (b) shows the structure of a ceramic wall-flow-type DPF. This type of DPF has a honeycomb structure. The flow passes through the wall of the porous filter because the plugs alternately close the passes. Exhaust gas flows into and passes through the cells of DPF as shown in the figure. PM in the exhaust gas is accumulated on the wall of the cell. Normally, the collection efficiency of DPF is more than 95% [37] for these units. Due to the particle accumulation in the filter enhance the pressure drop of the DPF which negatively affects the engine performance. So, it requires technologies for DPF cleaning or DPF regeneration to burn the accumulated soot in the filter. Soot starts to burn spontaneously in DPF by injecting fuel in front of the DPF unit into the direction of exhaust flow to create extra heat in the stream which is called as active regeneration and the passive regeneration occurs with the excessive heat generated by the DOC unit.

### 2.2.3 Selective Catalytic Reduction - SCR

SCR is a modern technological development to control the  $\text{NO}_x$  from the emissions in diesel engine with injecting catalysts which is mainly ammonia to the exhaust flow. This device normally coupled with a cleanup catalyst system (CUC) which is also known as slip catalyst to remove the remaining catalysts after the reaction process.

Diesel engines mounted in large ships, such as freighters and tankers. Generally, there are several engines of these types inside the ship. Although exhaust gases can flow together through a single stack, each engine should be fitted with its own exhaust gas treatment device. For  $\text{NO}_x$  reduction, the urea SCR method is employed for marine diesel engines. Because urea injection is safer than ammonia injection. Ammonia is dangerous gas and should be avoided in the ship loading. A

honeycomb SCR catalyst (typically  $V_2O_5$  supported on a  $TiO_2$  base material) [37] is placed inside the path of the exhaust gas from the diesel engine. An aqueous urea solution stored in the urea tank is sprayed from the urea solution nozzles placed on the exhaust upstream. The aqueous urea solution is hydrolyzed into ammonia and carbon dioxide.  $NO_x$  is cleaned via reaction with  $NH_3$  and reduced to  $N_2$ .

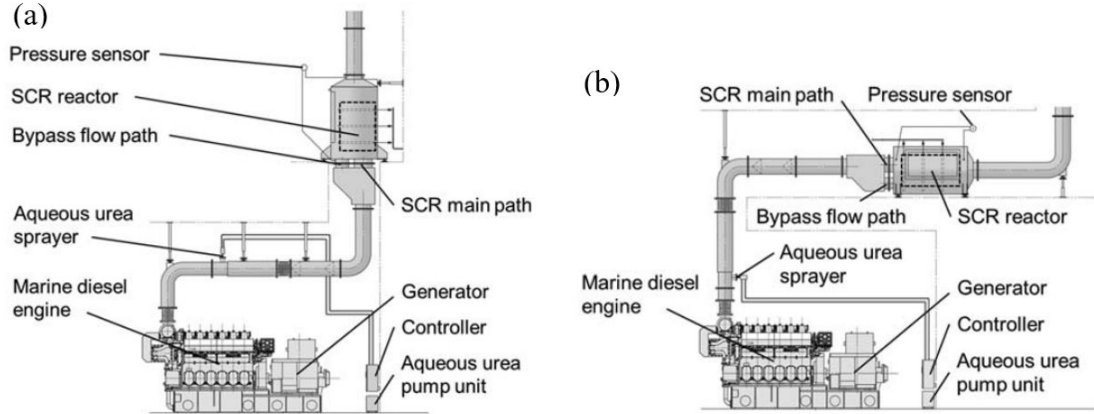


Figure 12: Schematic drawing of Daihatsu selective catalytic reduction system in vertical (a) and horizontal (b) installations [28]

$NH_3$  which is not reacted, left in the exhaust line is referred to as the  $NH_3$  slip, and its emissions must be suppressed by decomposition using an  $NH_3$  catalyst for oxidation, placed downstream of the SCR catalyst which is the ammonia slip catalyst. As an example of a performance verification test, when the exhaust gas temperature is  $350^\circ C$ , the  $NO_x$  removal efficiency more than 80% can be obtained [37]. The SCR unit can be arranged in the exhaust system of the marine diesel engines in vertical and horizontal alignments as shown in Figure 12 according to the space available for the retrofitting. Both configurations are showing the similar performance which is not dependent of the arrangement.

The impact of different configurations of EAT units for diesel engines proposed some effective configurations of the EAT units is studied by *Lao et al.* [33]. This paper reveals that the DPF and SCR units have interaction with their operational performance due to the regeneration activity of reactions.

#### 2.2.4 Existing Exhaust After Treatment Units for Diesel Engines

The EAT unit with consisting CPD,DOC and SCR for diesel engines is mainly used in ground vehicles to clean the harmful emissions. There are different units developed by several companies specially for these purposes. Figure 13 (a) shows the VOLVO Penta EAT unit which is mainly used in VOLVO heavy trucks. This EAT unit consists with several individual components which are DOC unit, DPF unit, Urea injection unit, SCR unit and ammonia slip catalyst [21]. This unit can be coupled with a separate WHR system to create combine unit to recover the waste heat and control the emissions.

Cummins has developed an EAT unit as a single unit and a modular unit to connect with diesel engines as shown in Figure 13 (b). They have a capacity range of these units for on-highway, off-highway, marine and industrial applications. The Cummins particulate filter contains the DPF which collects and oxidizes carbon to remove particulate matter (PM) and the DOC which aids in this process. After collecting the particles from the gases in the DOC and DPF, there are still  $NO$  and  $NO_2$  left in the exhaust. To reduce the  $NO_x$  levels a light mist of urea is injected into the hot exhaust stream in the decomposition reactor. The exhaust progresses from the decomposition

---

reactor into the SCR system which converts the toxic NO<sub>x</sub> and urea mixture into harmless Nitrogen gas (N<sub>2</sub>) and water vapor (H<sub>2</sub>O) [4].

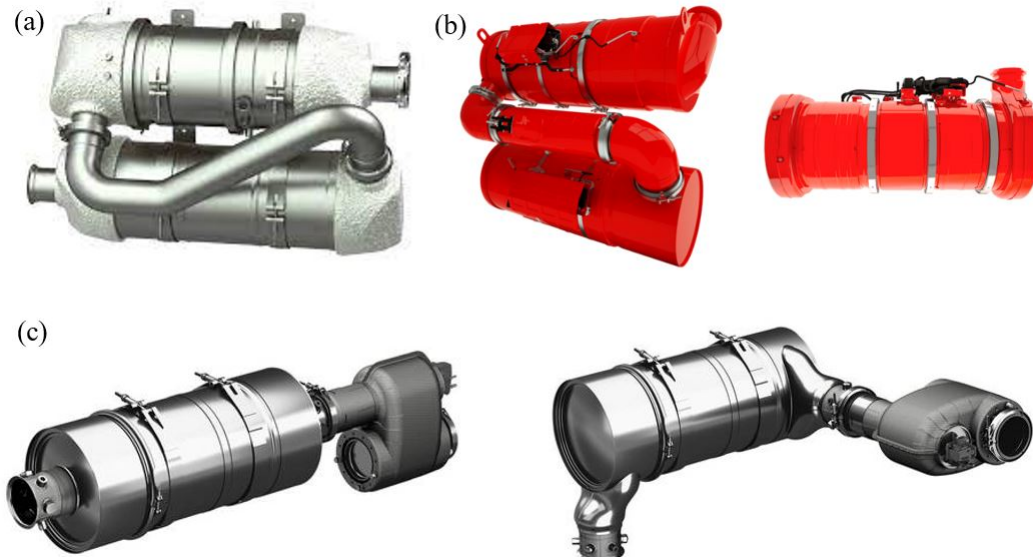


Figure 13: (a) VOLVO Penta EAT unit [21], (b) CUMMINS modular EAT unit [4] and (c) MAN modular EAT unit [12]

MAN engines has developed a modular EAT unit with DOC-DPF and SCR unit for on-road, off-road and marine applications which is shown in Figure 13 (c) with two different arrangements. Modular exhaust gas after treatment from MAN Engines excels due to its compact design and high flexibility in restricted installation spaces. It allows for a wide range of installation possibilities and system integration tailored to specific customer needs, as the individual components can be positioned differently. As like in the Cummins EAT unit injected Urea solution reacts with the nitrogen oxides and converts them into water (H<sub>2</sub>O) and harmless Nitrogen (N<sub>2</sub>). The system can either be used by itself, as SCR-only, or combined with other components such as a DOC/DPF to cover many different emission guidelines [12].

### 2.3 Waste Heat Recovery and Exhaust After Treatment Combined Unit

The EAT and WHR units are commercially available as individual units which can be integrated into a single system. Although these are separate units, their performance is affected by individual performances. Some of these units are already implemented for the ground vehicle engines and it is not common for the diesel marine engines. Diesel particulate heat exchangers (DPFH) is one of the research concepts with integrated DPF into the waste heat recovery system [43].

This research on combined DPFHX for simultaneous reduction of emissions and fuel consumption, by using the DPFHX as the evaporator in an Organic Rankine Cycle which is the concept is shown in Figure 14. The concept of DPFHX is working as a DPF and the working fluid circulates inside the DPFHX shell and over the tubes containing the DPF cores, receiving energy from the engine exhaust. Also it is possible to capture further energy from the regeneration event, where quick combustion of the particulate matter releases a significant amount of thermal energy.

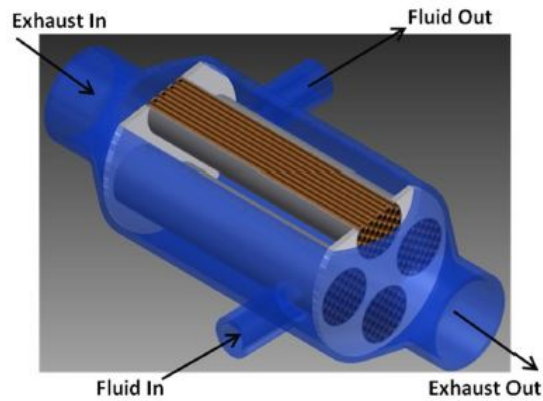


Figure 14: Section view of theorized DPFHX based on shell-and-tube heat exchanger [43]

The DPF combining with the heat exchanger helps to downsize the system which is a main factor for the retrofiting. Also, it is possible to implement noise reduction inside the SCR unit to combine and down size the unit.

The existing exhaust systems have the sub units of EAT, WHR and muffler with the arrangement as shown in Figure 15. First the exhaust enter to the EAT unit and then flows through the WHR system.

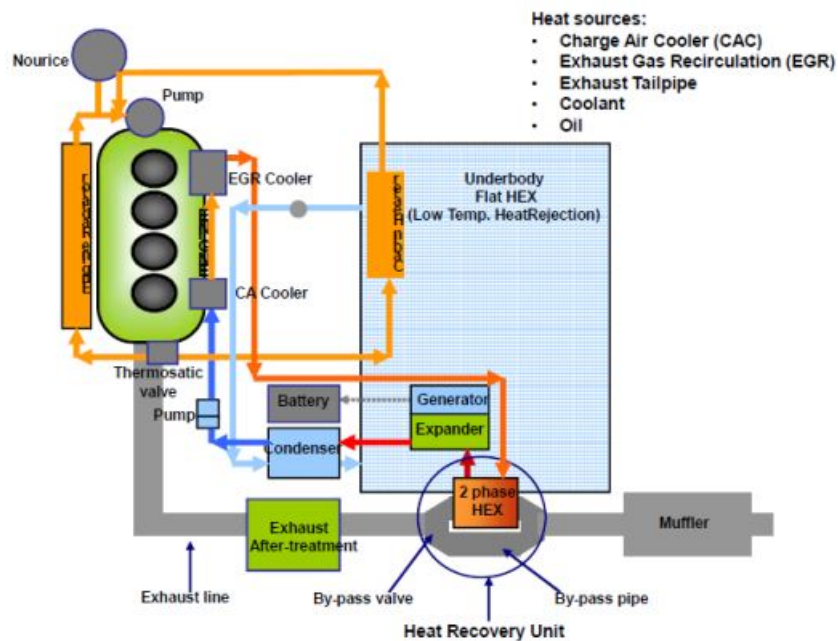


Figure 15: Proposed system arrangement of WHR and EAT in exhaust system in project "No Waste" [15]

The "No waste" project by *Federica Bettoja* has a target of more than 12% fuel saving in the diesel engines of commercial vehicles. The basic concept of implementing a Rankine cycle for the WHR unit is mainly focused for this project which is the basic cycle used in WHRS. In addition to the the EGR (exhaust gas re-circulation) system which help to provide additional heat for the intake air of the engine. It has used a hybrid system with battery to charge from the recovered heat which is converted to the useful electricity from the expander and generator system as shown

---

in the system diagram in Figure 15. The "No waste" project was conducted with collaboration of VOLVO to analyse the system performance. According to the project, first it has tested the WHRS under steady state condition with different load conditions to validate the performance of the components. The main purpose of the combined simulation was to developing the system performance characteristic measurements. The system has used a water-glycol mixture as the working fluid of the WHR unit to extract the energy with the concept of Organic Rankine Cycle (ORC). According to this project work, there were several conclusions made with regarding the integrated unit of WHR for long-haul trucks. It is considered as cheap and "plug and play" system which has a lower impact on the vehicle architecture. Because they have created this system with low weight and size which has no impact on the power-train of the truck. Also, this project demonstrated a ORC base WHR system which was able to recover 2kW energy from the exhaust and it could be improved with efficient turbine according to the conclusions [27]. This development of WHR system showed that this combined system can achieve up to 10% of cycle efficiency.

### 2.3.1 Existing Combined Units

In present, there are several companies in different part of the world are involving with development of EAT and WHR combined systems for the marine engines and ground vehicle engines such as truck engines. The recent developments can be found out from the existing products from the ongoing researches with conceptual designs which are involved with some vehicle and engine manufacturers.

#### GESAB Catemiser

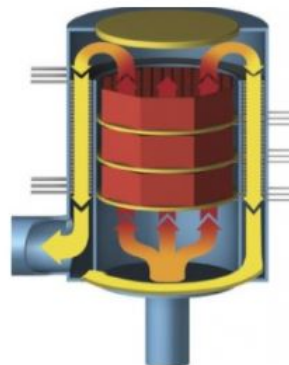


Figure 16: GESAB Catemiser working principle [8]

GESAB is a Swedish company who is manufacturing combined unit of SCR and economizer for the marine engines. The SCR unit clean the NO<sub>x</sub> in the exhaust and this unit is surrounded by spirally wound heating coils to recover the heat using the working fluid inside the coil. According to the manufacturer this unit is cost effective, low weight and less space required. These products has a range from 700kW to 6MW engine power. The working principle of the unit is not reveal by the manufacture and the systematic diagram of the unit operation is shown in Figure 16.

#### MAHLE Combined System for Commercial Vehicle Engines

The WHR unit which is produced by the German company MAHLE consists all the components in a single box shaped unit. This unit mainly focused for the low power engines of the commercial vehicles which can retrofit to the existing engines and fix to the new engines. This unit is small in size which is 55 Cm in width according to MAHLE and this is a plug and play unit for the vehicles which expands the usability of the modular design concept. This device includes WHR to convert waste heat in to electricity and DPF and SCR units to re,move the harmful emissions. The unit



---

operates over 150°C temperature of the exhaust flow.

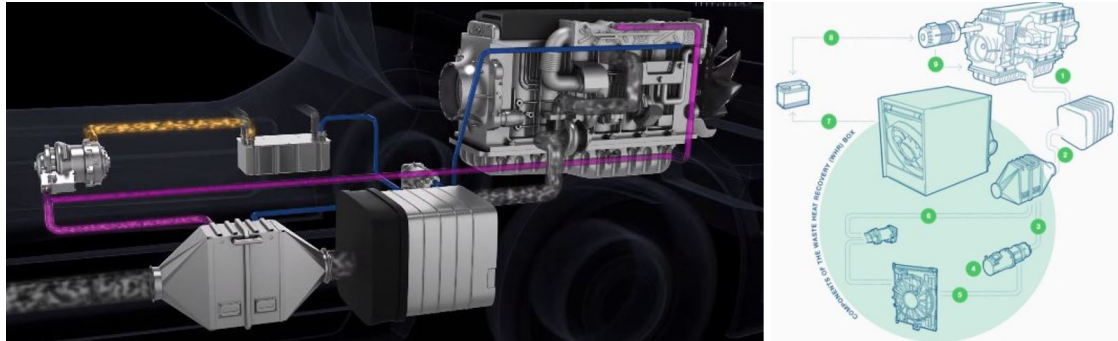


Figure 17: MAHLE WHR and EAT in a combined system [11]

## 2.4 Vessels with Medium Speed Diesel Engines

Medium speed diesel engines are ranked according to the generated power from 1MW to 10MW and speed of 400rpm to 1200rpm basically. In this study it will be focused on the 1-5MW range of diesel engines. Retrofitting a combined system of WHR and EAT will be a challenging task in these ships due to the unavailability of larger space for the installations and complicated piping arrangements inside the exhaust chamber.



Figure 18: MOU Island Wellserver vessel [14]

The exhaust system which is selected for this research is from the MOU Island Wellserver which is specially built for maintenance of oil wells with increased production and the design was developed by Rolls-Royce. The ship is 116m in length and 25m in width and operates with diesel-electric propulsion with four main generator sets and one auxiliary machinery generator set. The four diesel engines are two of type Bergen, W32: 40L8A each with an output of 3840 kW and two of W32: 40L6A each of 2880 kW.

This ship has four engines which are individually connected to a SCR unit and a muffler. The system arrangement is shown in Figure 19 for the both engine sizes. The SCR units are connected to the exhaust line vertically and there is no any special type of WHRS is used in this system. When it consider about the retrofitting needs, it is important to utilize the available space in the exhaust chamber to avoid system interactions with the other systems and piping arrangements inside the ship. This represents only the main engine exhaust arrangement and main floors has approximately 2.7m space in between.

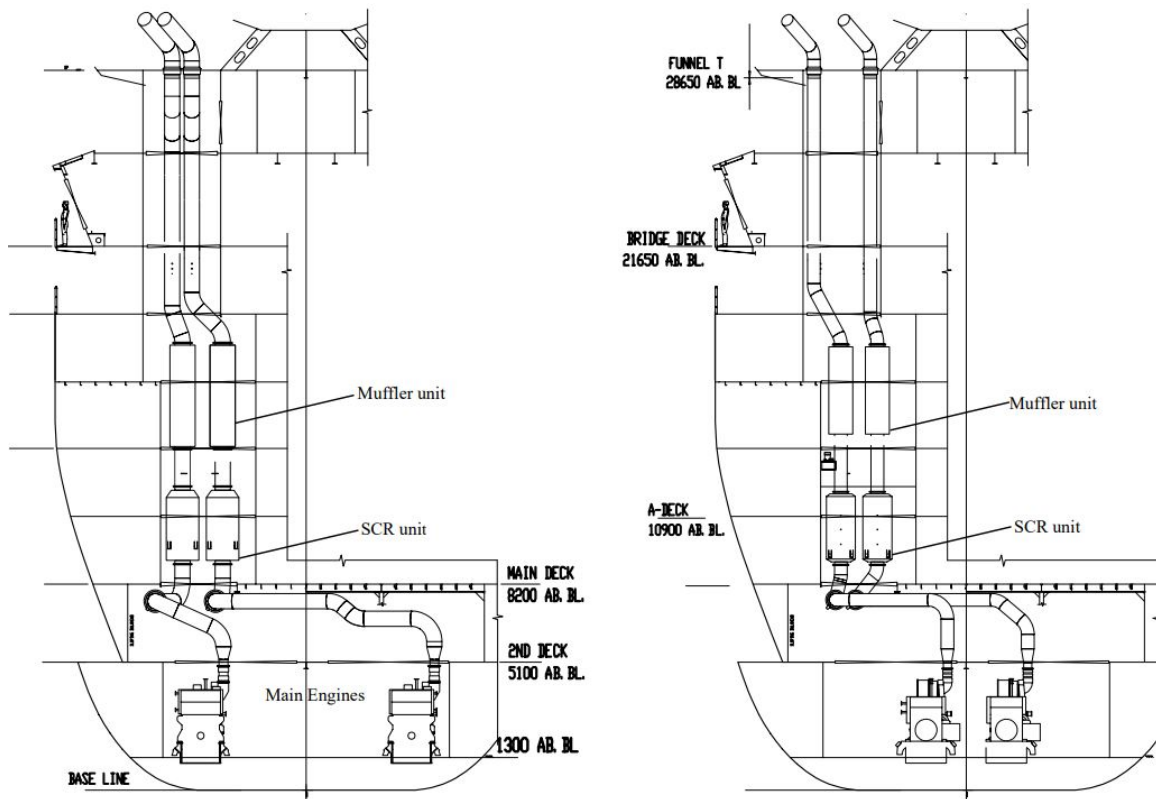


Figure 19: Exhaust system arrangement with 4 diesel engines inside the vessel [2]

#### 2.4.1 Engine Performance Data

The exhaust data of Wärtsilä 7L32 which has the similar performance of Bergen W32: 40L8A engine is used for this study due to the convenient data accessibility. The Wärtsilä 7L32 engine can supply 4060kW power in 750rpm speed according to the data sheet provide by the manufacturer.

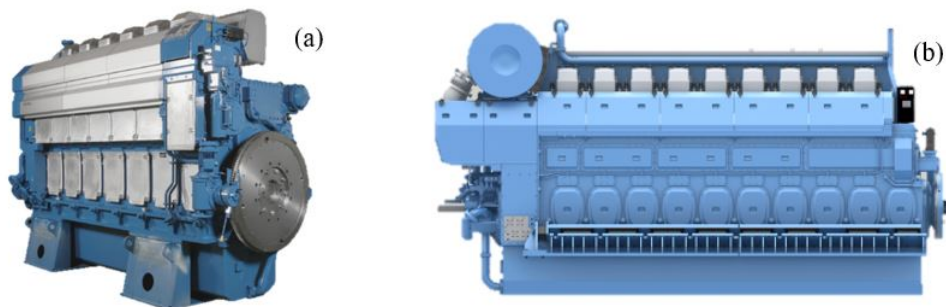


Figure 20: Wärtsilä 7L32 diesel engine (a) [22], Bergen W32 40L8A Engine (b) [1]

The exhaust data for the full engine load condition and the exhaust pipe outlet diameter of 700mm is used as shown in the table in Figure 21 which is provided by Wärtsilä. According to the data,



the exhaust has a temperature of 350°C and a flow rate of 7.63kg/s in full load condition. The other important factor is the maximum back pressure of 5kPa of the engine which is the maximum limit of affecting the performance of engine.

<b>Exhaust gas system (Note 2)</b>							
Flow at 100% load	kg/s	7.35	7.63	7.35	7.63	7.63	6.5
Flow at 85% load	kg/s	6.58	6.93	6.58	6.93	6.65	5.7
Flow at 75% load	kg/s	5.95	6.3	5.95	6.3	6.23	5.0
Flow at 50% load	kg/s	4.27	4.55	4.27	4.55	4.83	3.4
Temperature after turbocharger, 100% load (TE 517)	°C	350	350	350	350	350	350
Temperature after turbocharger, 85% load (TE 517)	°C	305	295	305	295	315	330
Temperature after turbocharger, 75% load (TE 517)	°C	305	295	305	295	315	340
Temperature after turbocharger, 50% load (TE 517)	°C	300	290	300	290	300	353
Backpressure, max.	kPa	5.0	5.0	5.0	5.0	5.0	5.0
Calculated pipe diameter for 35m/s	mm	685	698	685	698	698	644

Figure 21: Wärtsilä 7L32 diesel engine exhaust data [22]

## 2.4.2 Properties of Diesel Exhaust

Diesel exhaust gas contains more concentrations of vaporized water (H<sub>2</sub>O) and Carbon dioxide (CO<sub>2</sub>) compared to the composition of atmospheric air. H<sub>2</sub>O and CO<sub>2</sub> concentration can be varied up to 12% in diesel exhaust than the atmospheric air. The O<sub>2</sub> percentage after the combustion also decreased up to 17% in the exhaust which is normally 21% in ambient air. So, the main component of the diesel exhaust is N<sub>2</sub> same as the ambient air. When it calculates the physical properties of the exhaust, the properties of atmospheric air can be used for diesel exhaust gas calculations [38]. The error associated with neglecting the combustion products is usually no more than about 2% which is not highly affecting to the estimations.

T (K)	$\rho$ (kg/m <sup>3</sup> )	h (kJ/kg)	s (kJ/(kg·K))	C <sub>p</sub> (kJ/(kg·K))	$\mu$ (10 <sup>-4</sup> Pa·s)	k (W/(m·K))
260	1.34	260	6.727	1.006	0.165	0.0231
280	1.245	280.2	6.802	1.006	0.175	0.0247
300	1.161	300.3	6.871	1.007	0.185	0.0263
350	0.995	350.7	7.026	1.009	0.208	0.0301
400	0.871	401.2	7.161	1.014	0.23	0.0336
450	0.774	452.1	7.282	1.021	0.251	0.0371
500	0.696	503.4	7.389	1.03	0.27	0.0404
600	0.58	607.5	7.579	1.051	0.306	0.0466
800	0.435	822.5	7.888	1.099	0.37	0.0577
1000	0.348	1046.8	8.138	1.141	0.424	0.0681
1200	0.29	1278	8.349	1.175	0.473	0.0783
1400	0.249	1515	8.531	1.207	0.527	0.0927

Table 1: Physical properties of air (p = 101.13 kPa) T temperature;  $\rho$  density; h specific enthalpy; s specific entropy; C<sub>p</sub> specific heat at constant pressure;  $\mu$  viscosity; k thermal conductivity [7]

Diesel engine exhaust gases vary with speed and load of the engine. According the study carried out by Dennis P.Nolan [39], high loads and high speeds result in the highest temperatures. Generally, temperatures of 500–700°C (932–1293°F) are produced in the exhaust gases from diesel engines at 100% load to 200–300°C (392–572°F) with no load. Exhaust gases normally discharges at a temperature of around 420°C (788°F). This is a average value to get an idea about the engine exhaust.

---

The engines can be tuned on to low specific fuel consumption and high exhaust gas temperatures such as above 300°C which enables SCR unit operation in the EAT system and it can help to optimize the WHRS according to the research done by "Wärtsilä" [46]. This will have a positive impact on the system performance with related to the combining the unit in to the diesel engine, without reducing its performance due to the back pressure build up from the WHR unit.

### 2.4.3 Engine Exhaust Back Pressure

The exhaust gas pressure which is produced by the engine to overcome the flow resistance of the exhaust system in order to discharge the exhaust gases into the atmosphere is defined as engine exhaust back pressure. The exhaust back pressure is considered as the gauge pressure in the exhaust system at the outlet of the exhaust turbine in turbocharged engines or the pressure at the outlet of the exhaust manifold in other engines [6]. The engines have a desired level of maximum back pressure value for the exhaust flow and this value should not be exceeded by the sum of the pressure drops of the components such as DPF, SCR, Muffler and WHR unit along the exhaust system for a better performance of the engine. But in general, these units can cause for the increase in back pressure specially the DPF units due to the soot accumulation inside the filter substrate.

Increased exhaust pressure can cause of problems in turbocharger, increased pumping work, cylinder scavenging, combustion problems, reduced intake manifold boost pressure etc [6]. Mufflers and DPF generally result in maximum back pressures in the exhaust systems which can rise to significantly higher levels, especially if the filter is loaded with soot. Proper design with considering the pressure drops across each component of the WHR and EAT system while considering the maximum allowable back pressure value of the engine manufacturer will provide an optimum solution for the combined unit.

---

### 3 Methodology and Applied Theory

#### 3.1 Research Process

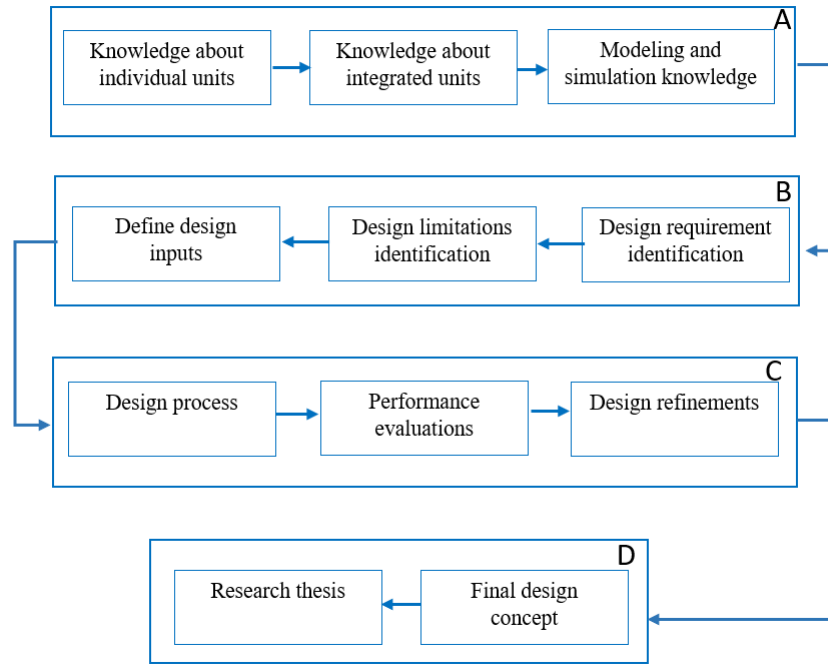


Figure 22: Research approach

The processes A represents the knowledge gathering for this research which is basically done by three steps which are for the WHR and EAT units and integrated units with the combinations of required modeling and simulation knowledge. This provides the basic literature study for the research with the current developments and products. In the process components included in B, shows the initial set up before starting the design and development of the combined system. This includes the identification of the design requirement with limitations which is important to consider for the retrofitting and the input parameters of the design. It is mainly focused on the properties of the exhaust flow for a desired engine from the selected range.

The next stage which is shown in the process components in C explains the main task of this research. This includes the design of the system and performance evaluation of the design with further refinements. The performance evaluation and refinement for the optimization is a cyclic process which is explained in detail in Figure 23. This will include the modeling and simulation of the performance of the EGE unit with regarding the interfaces. On the final stage of the research which is shown in process D, will finalized the design concept for the combined WHR and EAT system to achieve the defined objectives.

The detailed development procedure of the research process is an extended version of the research process with describing methodology in detail related to this research. The optimization procedure of this research is developing the WHR unit for a higher efficiency with using CFD analysis to evaluate the performance. The CFD model development of the EGE unit in the WHR system needs to be carried out first and comparison of the CFD result data and the measurement data can use to create proper CFD model setup.

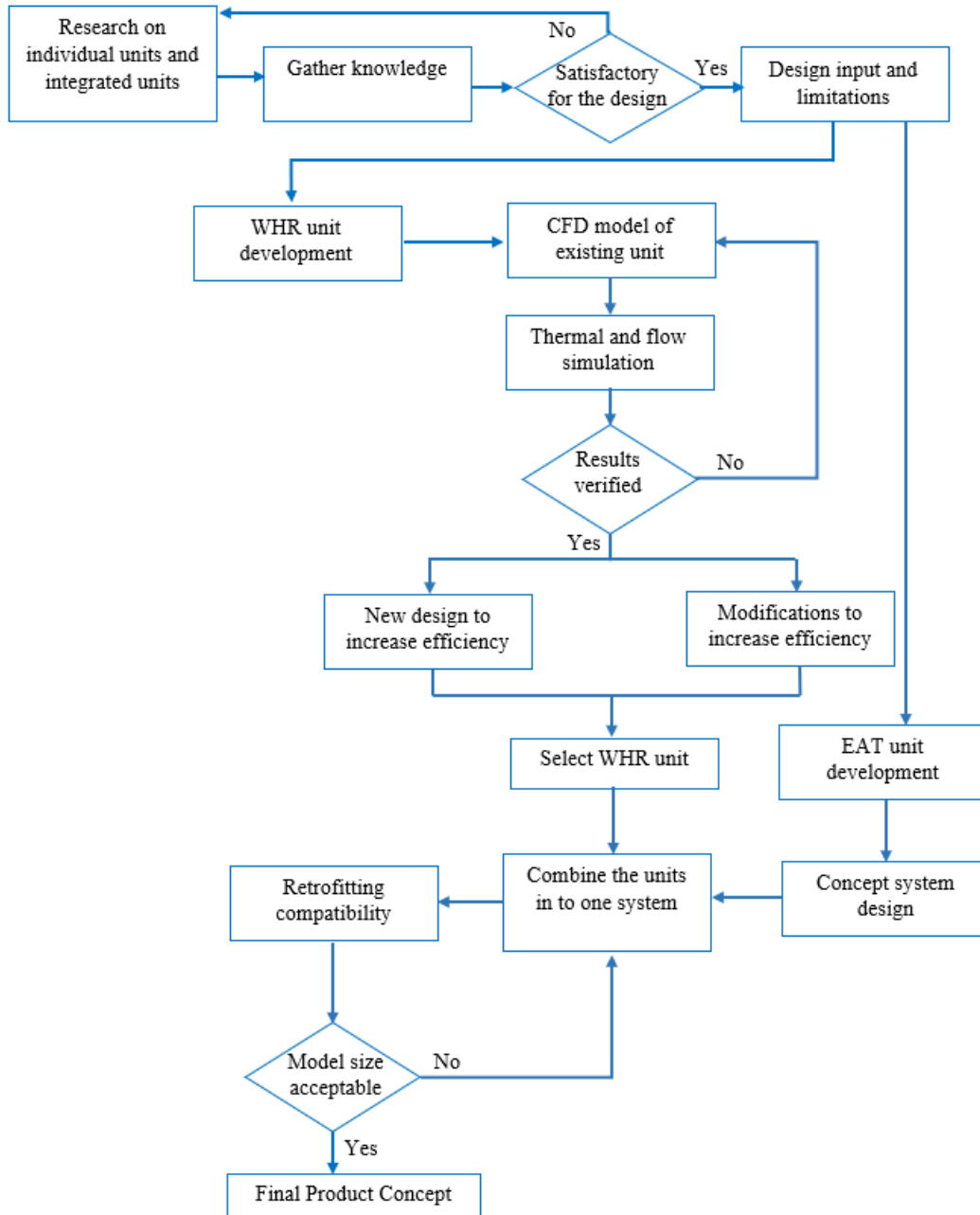


Figure 23: WHR unit and EAT unit development procedure for a combined system

Based on the CFD model development for the existing unit and the new design concepts need to be compare with their efficiency levels to identify the best possibility for a higher efficiency. EAT unit is developed as a concept, based on the available research and product data which is fitted in to the WHR as a combined system. In this case, the input parameters for both units need to be considered and a integrated concept need be developed accordingly.

---

## 3.2 Thermal Efficiency of Waste Heat Recovery System

### 3.2.1 Heat Exchanger Fundamentals

A heat exchanger is a device which is used to transfer thermal energy between two or more fluids where one fluid has a higher temperature and the other has a lower temperature. According to the flow arrangement, heat exchangers are categorized as parallel-flow arrangement where hot and cold fluids move in the same direction and counterflow arrangement where hot and cold fluids move in the opposite direction. Cross flow arrangement heat exchanger is another type where the two fluids move in cross flow perpendicular to each other. Commonly finned-tube heat exchangers and plate-fin heat exchangers have cross flow arrangement. Shell-and-tube heat exchangers, double pipe heat exchangers and plate heat exchangers normally have either parallel flow or counterflow arrangement.

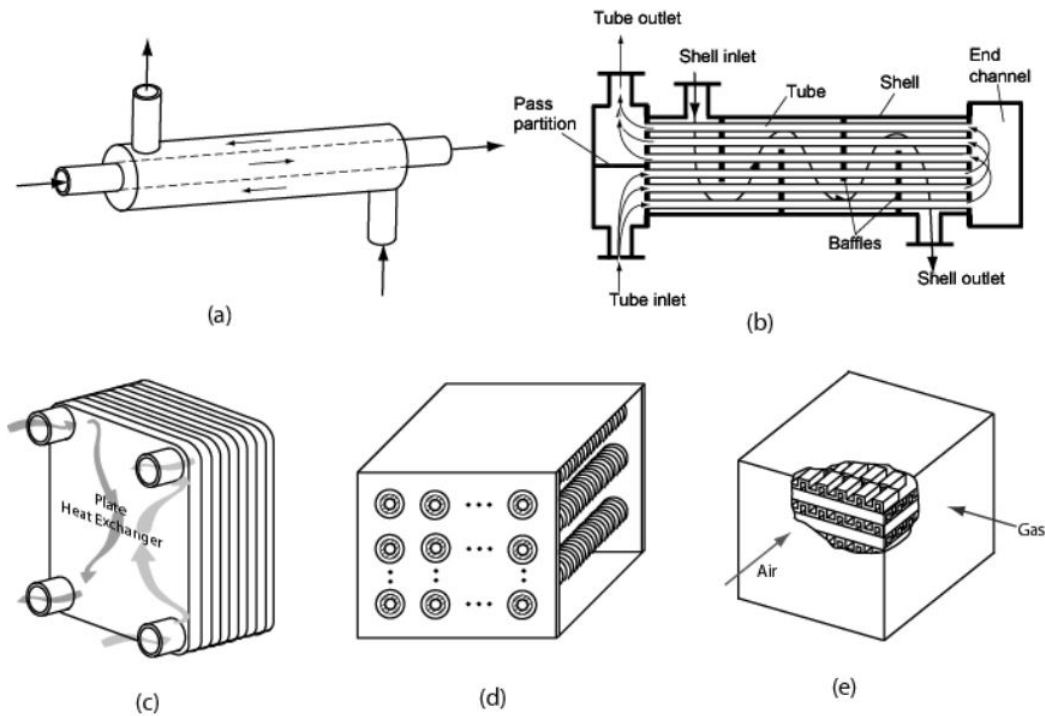


Figure 24: Typical heat exchangers, (a) double-pipe heat exchanger, (b) shell-and-tube heat exchanger, (c) brazed plate heat exchanger, (d) circular finned-tube heat exchanger, and (e) plate-fin heat exchanger [3]

Special type of heat exchangers are used to achieve a very large heat transfer area per volume which are called as compact heat exchangers. These heat exchangers have dense arrays of finned tubes or plates. These are normally used when at least one of the fluids is a gas which has a small convection heat transfer coefficient compared to the liquids. Plate heat exchangers, finned-tube heat exchangers and plate-fin heat exchangers can identify as compact heat exchangers.

The conduction and convection heat transfer effect are more dominant in heat exchanger operation. Hence, it is important to consider about these two heat transfer methods and the governing equations before study the heat transfer in a heat exchanger.

- **Conduction Heat Transfer**

Conduction heat transfer take place in solid media, when a temperature gradient exists, the heat will be transferred from higher to lower temperature region. Heat transfer rate of conduction  $q_k$  is proportional to the temperature gradient  $dT/dx$ , times the area through

---

which heat is transferred[31]. This can be defined as,

$$q_k = -kA \frac{dT}{dx} \quad (1)$$

where;  $k$  is the thermal conductivity,  $A$  is the heat transfer area,  $T$  is the temperature and  $x$  is the direction of heat flow

- **Convection Heat Transfer**

The thermal exchange process which happens when a fluid encounters a solid surface at a different temperature is called as the convection heat transfer. The movement of heated particles due to the buoyant forces causes this heat transfer and the detailed mechanism of this process is complicated. But this heat transfer is important when it analyses the heating and cooling of systems. Free convection and forced convection are the two main types of convection heat transfer.

In natural or free convection, the motive force comes from the difference of the density in the fluid, that results from its contact with a surface at a different temperature and gives rise to buoyant forces. When an outside motive force moves a fluid pass a surface at a higher or lower temperature than the fluid, the forced convection happens. More heat can be transferred at a given temperature difference in forced convection than the free convection due to the higher fluid velocity in forced convection. However, the work required to move the fluid in higher velocity in forced convection is an additional energy requirement for the system.

$$q_c = \bar{h}_c A (T_s - T_\infty) \quad (2)$$

where;  $\bar{h}_c$  is the average heat transfer coefficient,  $A$  is the surface area in contact with fluid,  $T_s$  is the surface temperature and  $T_\infty$  is the temperature of undisturbed fluid far away from heat transfer surface

Convection mode and fluid	$\bar{h}_c (W/m^2K)$
Free convection-air	5-25
Free convection-water	20-100
Forced convection-air	10-200
Forced convection-water	50-10,000
Boiling water	3,000-100,000
Condensing water vapour	5,000-100,000

Table 2: Approximate values of convection heat transfer coefficients [31]

- **Specific Heat Capacity**

To change temperature, it requires different amount of energy for different materials. The required amount of energy mainly depends on the mass of the material, specific heat capacity of the material and the desired temperature change. The energy required to raise one kilogram (kg) of the material by one degree Celsius ( $^{\circ}C$ ) is known as the specific heat capacity of the material. The amount of thermal energy stored or released as the temperature of a system changes can be calculated using the equation:

$$q = mc_p \Delta T \quad (3)$$

with; amount of heat transfer  $q$ , mass of the material  $m$ , specific heat capacity of the material  $c_p$  and temperature difference  $\Delta T$ .

Consider the two-fluids counter-flow channels across a wall in Figure 25 (a). In Figure 25 (b), it is shown flow diagram and the temperature distribution of the hot and cold fluids of a counter flow and the figure 26 (b) shows it for a parallel flow.

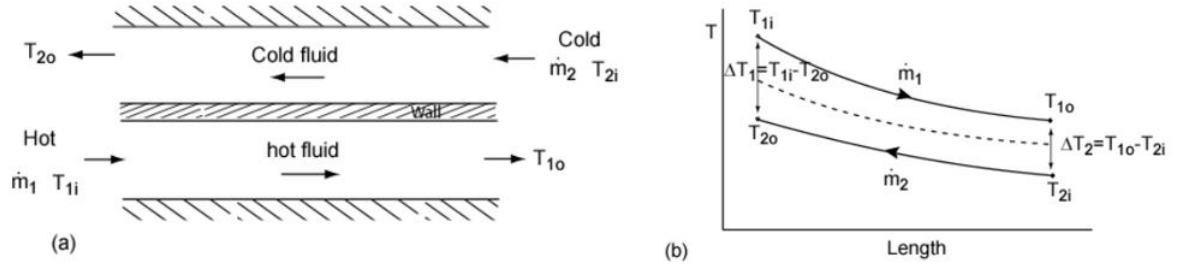


Figure 25: (a) Schematic for counter-flow channels, (b) the temperature distributions for the counter-flow arrangement [3]

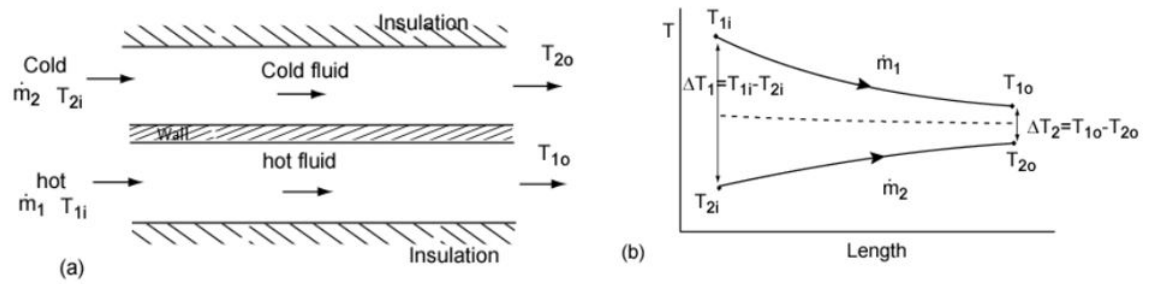


Figure 26: (a) Schematic for parallel-flow channels, (b) the temperature distributions for the parallel-flow [3]

where;  $\dot{m}_1$  is the mass flow rate hot fluid,  $\dot{m}_2$  is the mass flow rate cold fluid,  $c_{p1}$  is the specific heat of hot fluid,  $c_{p2}$  is the specific heat of cold fluid,  $T_{1i}$  is the hot fluid inlet temperature,  $T_{1o}$  is the hot fluid outlet temperature,  $T_{2i}$  is the cold fluid inlet temperature,  $T_{2o}$  is the cold fluid outlet temperature,  $\Delta T_1 = T_{1i} - T_{2i}$ ,  $\Delta T_2 = T_{1o} - T_{2o}$  for parallel-flow,  $\Delta T_1 = T_{1i} - T_{2o}$  and  $\Delta T_2 = T_{1o} - T_{2i}$  for counter-flow

The hot fluid with higher temperature  $T_{1i}$  enters the lower channel and leaves at the lower temperature  $T_{1o}$ , while the cold fluid with lower temperature  $T_{2i}$  enters the upper channel and leaves at the higher temperature  $T_{2o}$ . The temperature distributions are presented for both parallel and counter flows in Figure 25 (b) and 26 (b), where the dotted line indicates the wall temperatures along the length of the channel. The wall temperatures in parallel-flow have nearly constant compared to those changing in counter-flow. So, the counter-flow heat exchanger is usually preferable for fluid-to-fluid heat transfer. But the nearly constant wall temperature is a characteristic of the parallel flow heat exchanger where exhaust gas heat exchangers normally require a constant wall temperature to avoid corrosion [3].

Heat transfer rate of the hot fluid can be expressed as,

$$\dot{q} = \dot{m}_1 c_{p1} (T_{1i} - T_{1o}) \quad (4)$$

Heat transfer rate of the cold fluid can be expressed as,

$$\dot{q} = \dot{m}_2 c_{p2} (T_{2o} - T_{2i}) \quad (5)$$

Both these heat transfer rates are equal for the adiabatic process and it can be expressed in terms

of overall heat transfer coefficient as,

$$\dot{q} = UAF\Delta T_{lm} \quad (6)$$

with; U is the overall heat transfer coefficient, A is the heat transfer surface area at hot or cold side, F is the correction factor according to the flow arrangement (F= 1 for counter and parallel flow and  $F \leq 1$  other types) and  $T_{lm}$  is the log mean temperature difference which is defined as,

$$\Delta T_{lm} = \frac{\Delta T_1 - \Delta T_2}{\ln\left(\frac{\Delta T_1}{\Delta T_2}\right)} \quad (7)$$

### 3.2.2 Overall Heat Transfer Coefficient

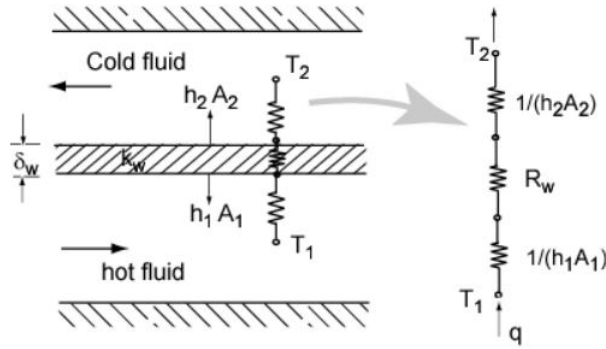


Figure 27: Thermal resistance and thermal circuit for a heat exchanger [3]

As shown in the Figure 27, the thermal circuit across the hot and cold fluids has a complex variation of temperature along the length . So, the log mean temperature is used to derive the heat transfer rate across the wall as,

$$\dot{q} = \frac{T_{(1i-1o)} - T_{(2i-2o)}}{\frac{1}{UA}} = \frac{F\Delta T_{lm}}{\frac{1}{h_1 A_1} + R_w + \frac{1}{h_2 A_2}} \quad (8)$$

where;  $h_1$  is the convective heat transfer coefficient hot fluid,  $h_2$  is the convective cold transfer coefficient hot fluid,  $A_1$  is the heat transfer area hot fluid,  $A_2$  is the heat transfer area cold fluid and  $R_w$  is the wall thermal resistance.

The thermal resistance for the wall can be expressed as,

$$R_w = \frac{\delta_w}{k_w A_w} \quad (9)$$

with;  $\delta_w$  is the wall thickness,  $k_w$  is the thermal conductivity of the material and  $A_w$  is the heat transfer area.

Thermal resistance for the walls of pipe in a tube heat exchanger,

$$R_w = \frac{\ln\left(\frac{d_o}{d_i}\right)}{2\pi k_w L} \quad (10)$$



with;  $d_o$  is the pipe outer diameter,  $d_i$  is the pipe inner diameter and  $L$  is the pipe length.

The overall heat transfer coefficient for cold fluid side with a heat transfer area  $A_2$  can be expressed as,

$$U_2 = \frac{1}{\frac{A_2}{h_1 A_1} + R_w A_2 + \frac{1}{h_2}} \quad (11)$$

For a pipe heat exchanger without considering the wall conduction due to negligible value, the overall heat transfer coefficient can be expressed as,

$$U_o = \frac{1}{\frac{d_o}{h_i d_i} + \frac{1}{h_o}} \quad (12)$$

If the pipe thickness has a negligible size, it can be further expressed as,

$$U_o = \frac{1}{\frac{1}{h_i} + \frac{1}{h_o}} \quad (13)$$

### 3.2.3 Fouling Resistances

The scale and dirt which is depositing on the surfaces of heat exchanger tubes is called as the fouling and these deposits reduce the heat transfer rate and increase the pressure drop, back pressure and pumping power. Lower flow velocities can accelerate fouling when the design is not optimized for the desired level.

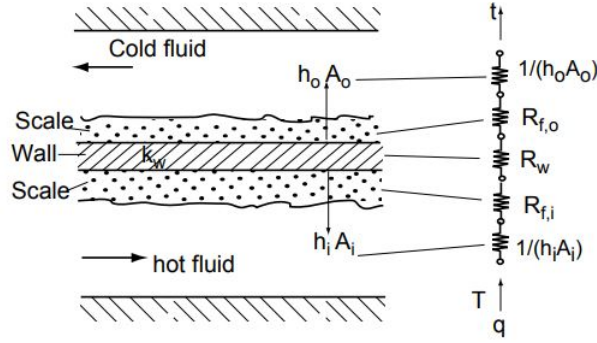


Figure 28: Thermal circuit with fouling for a heat exchanger [3]

The fouling resistance affects the overall heat transfer coefficient, which reduce the heat transfer rate. The overall heat transfer coefficient for a tube heat exchanger with inner and outer fouling effect can be expressed as,

$$U_o = \frac{1/A_o}{\frac{1}{h_i A_i} + \frac{R_{f,i}}{A_i} + R_w + \frac{R_{f,o}}{A_o} + \frac{1}{h_o A_o}} \quad (14)$$

where;  $R_{f,i}$  is the fouling resistance on inside and  $R_{f,o}$  is the fouling resistance on outside.

---

### 3.2.4 Thermal Efficiency Improvement Methods in Heat Exchangers

Heat recovery systems consists with heat exchangers to extract thermal energy from the exhaust gas. This is one of the main components where it can increase the efficiency of the WHRS. The heat exchanger design is more important which needs to supply the sufficient surface area to exchange heat from the exhaust to working fluid in an efficient manner. Also, this must be suitable for the retrofitting in to a existing system and it can not use a wide space which needs to be compact in size.

It is required to consider the pressure loss across the heat exchangers in a lower level to avoid the back pressure which will reduce the engine power and efficiency. Anyway, the heat exchanger designs for the WHRS comply with the working pressure of the fluid is essential design parameter. The exhaust of a diesel engine contains about 30% of the input energy and this energy can be recovered to produce additional power using a Rankine Cycle [26]. The Organic Rankine cycle is simple and offers a relatively better efficiency than other Rankine cycles when it considering the WHRS [44].

The total efficiency of the heat exchanger can be achieved by using the input energy and output energy of the unit which can be obtained from the simulations with a qualitative analysis. The heat exchanger design need to design with the limiting factor of the available space for retrofitting and improved surface area of heat transfer. This includes the flow arrangements of heat exchangers and their efficiencies with increased heat transfer surface area.

- **Using Baffles**

Baffles are primarily used to guide the flow of the shell side fluid and to minimize vibration effects on the tube bundle. Baffles increase the heat transfer coefficient by creating a cross flow velocity component. The baffle spacing is the distance between two adjacent baffles on the same side of the shell and is an important parameter to consider when designing a shell-and-tube heat exchanger [35].

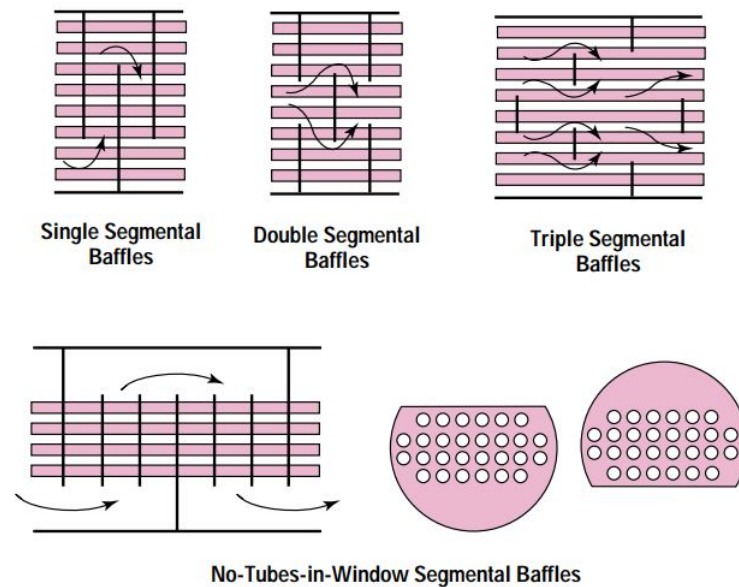


Figure 29: Different types of baffle arrangements and flow across the baffles [35]

The baffle spacing should not be less than one fifth of the inside diameter of the shell or 2 inches (50.8 mm), whichever is greater, according to the Tubular Exchanger Manufacturers Association (TEMA) guidelines [24]. Heat transfer efficiency will be low if the baffle spacing is excessively large. The pressure drop and the heat transfer coefficient usually have a positive relationship, and both are influenced by the baffle spacing. Smaller baffle spacing improves

heat transfer but increases

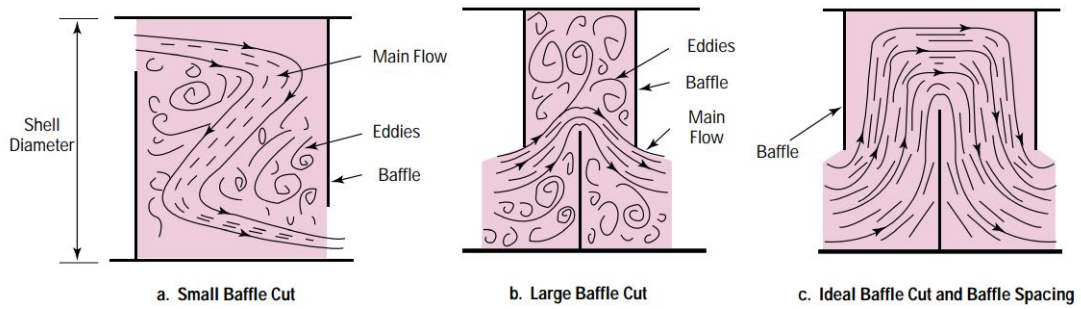


Figure 30: Flow behavior based on baffle cut ratio and baffle spacing [35]

pressure drop, requires more pumping capacity, and vice versa. The baffle cut can be between 15% and 45%, but it is suggested to use a baffle cut ratio in the range of 20–35% for optimum performance [35]. Designs with a baffle cut ratio less than 20% increase the heat transfer coefficient while the designs above 35% decrease the pressure drop.

Using calculations to evaluate the heat transfer improvement and flow resistance for a heat exchanger model with a complex arrangement with several baffles will be more complex than a numerical analysis such as using CFD analysis.

- **Using Fins**

Fins are used to improve heat transfer from surfaces in a variety of applications. The fin material has a high thermal conductivity in most cases. The fin is exposed to a moving fluid that cools or heats it, and the fin's high thermal conductivity allows more heat to be transferred from the wall to the fin. In this study EGE unit in WHRS system, it is required to use the fins to extract the maximum heat from the exhaust gas.

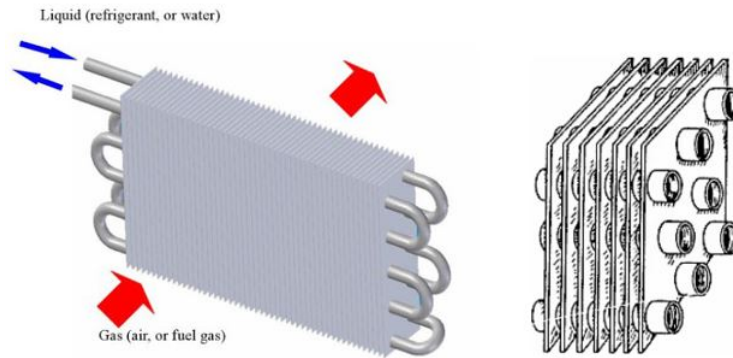


Figure 31: Schematic of the tube-fin heat exchanger [34]

To increase the heat transfer area, fins are commonly used as shown in Figure 31. The overall surface efficiency is readily expressed in terms of the single fin efficiency if the fin and primary areas are calculated. The thermal analysis is then simplified by the overall surface efficiency. Considering multiple-finned plate in both sides as shown in Figure 32 (a) overall surface efficiency is developed. Assuming the adiabatic tip as shown in Figure 32 (a) the single fin efficiency  $\eta_f$  can be developed as,

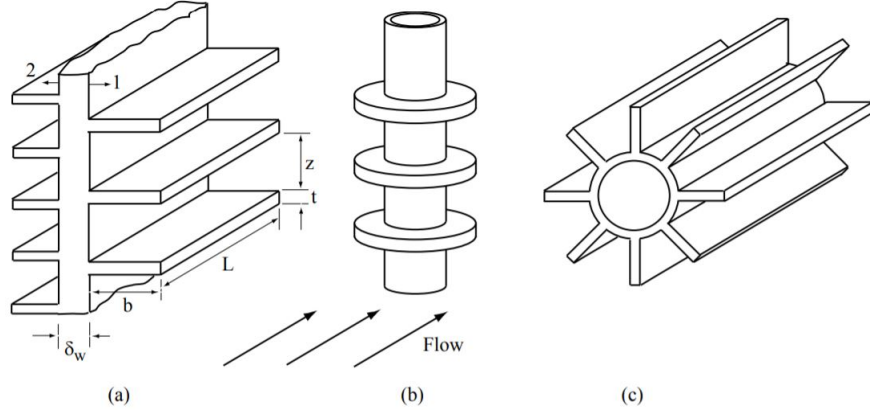


Figure 32: Extended fins types, plate-fin (rectangular fin) (a), circular finned-tube (b), and longitudinal finned-tube (c) [3]

$$\eta_f = \frac{\tanh(mb)}{mb} \quad (15)$$

where; b is the profile length and m can be expressed as,

$$m = \sqrt{\frac{hp}{kA_c}} = \sqrt{\frac{2h}{kt}} \quad (16)$$

with the thermal conductivity k of fin material, h is the convection heat transfer coefficient, P is the fin perimeter and  $A_c$  is the fin cross sectional area.

The single fin area  $A_f$  with adiabatic tip can be expressed as,

$$A_f = 2(L + t)b \quad (17)$$

The total heat transfer area  $A_t$  is the sum of the fin area and the primary area

$$A_t = n(2(L + t)b + Lz) \quad (18)$$

where; n is the number of fins and z is the fin spacing.

The overall surface efficiency can be expressed as,

$$\eta_o = 1 - n \frac{A_f}{A_t} (1 - \eta_f) \quad (19)$$

and the combined thermal resistance of the fin and primary surface area can be expressed as,

$$R_{to} = \frac{1}{\eta_o h A_t} \quad (20)$$

Considering the fin arrangement in Figure 32 (a), the overall heat transfer coefficient based on the area  $A_{t1}$  can be expressed as,

$$U_{t1} = \frac{1/A_{t1}}{\frac{1}{\eta_{o1} h_1 A_{t1}} + R_w + \frac{1}{\eta_{o2} h_2 A_{t2}}} \quad (21)$$

This is the more simple approach to calculate the heat transfer improvement of a heat exchanger arrangement with included fins to increase the heat transfer area. But in the actual cases as shown in Figure 31, the calculations are much more complicated and it will be more efficient to use a numerical analysis using CFD for evaluate the thermal efficiency of the heat exchanger.

---

### 3.3 Thermal Simulation for the Waste Heat Recovery Performance Analysis

The main part of the WHRS which is focused in this study is EGE unit. This unit is working according to the principles of heat exchanger. EGE unit provides an effective heat transfer between the two working fluids which are the water and the exhaust gas in this study. It is complex to analyze the performance of heat exchangers due to its geometry and the physical phenomena of the heat exchange between the two fluids. Basically, the first and second laws of thermodynamics are used to study both analytical and experimental studies [32]. It is required to conduct a numerical study using CFD simulations for the EGE unit to assess the performance using available software for this research study. This will allow to do the optimizations and new concept designs to evaluate efficiencies based on the simulation data which is faster and cost effective than prototype testing of the units for implementations and new concepts.

#### 3.3.1 Conjugate Heat Transfer - CHT

Heat transfer process involving an interaction of conduction within a solid body and the convection from the solid surface to fluid moving over the solid surface is described from the CHT. Hence, a realistic analysis of CHT problems requires the coupling of the conduction in the solid and the convection in the fluid [42]. Satisfying the conditions of continuity in temperature and heat flux at the fluid–solid interface is used to fulfill this requirement for the CHT problems. Heat transfer analysis becomes important in heat exchangers in which the conduction in the tube wall is greatly influenced by the convection in the surrounding fluid. CHT problem can be found in heat transfer applications with extended fins applications such as heat sinks and compact heat exchanger devices. The conduction within the fin and convection in the fluid surrounding need to be analyzed simultaneously to acquire the performance details of the device.

#### 3.3.2 CFD Modeling of Heat Exchanger

For a conjugate heat transfer analysis, the energy equation is solved throughout the fluid and the solid solution domain with an efficient implicit thermal coupling at the fluid/solid interface. All other conservation equations are solved within the fluid only. The numerical model for the heat exchanger consists with three dimensional steady-state turbulent flow system. To evaluate efficiency of the system it is important to obtain the output temperatures of the system according to the given input parameter if the exhaust flow. STAR-CCM+ is a commercial CFD software from Siemens which is currently using is various flow simulation applications for design and development purpose. This software is capable to simulate conjugate heat transfer problems which is important in this research study.

All the physics represented in CFD stem from a core set of fundamental laws. These fundamental laws are presented here in differential form, for an infinitesimal control volume. Continuum mechanics studies the behavior of continua in response to mechanical forces. The fundamental laws that govern the mechanics of fluids and solids are the conservation of mass, momentum, and energy. Navier-stokes equations which consists with the momentum and continuity equations are used to solve the flow simulations and these equations are coupled with the heat transfer principles to simulate the thermal flow problems. The mathematical notation of these equations are in differential form which are introduced here to understand the basic principles used in CFD to solve thermal flow cases with convection heat transfer [20].

#### Conservation of Mass

The mass conservation through a control volume is expressed by the continuity equation,

$$\frac{\partial \rho}{\partial t} + \nabla \cdot (\rho \mathbf{v}) = 0 \quad (22)$$

---

where;  $\rho$  is the density, which is the mass per unit volume and  $\mathbf{v}$  is the continuum velocity.

### Conservation of Momentum

The momentum conservation is expressed as the time rate of change of linear momentum is equal to the resultant force acting on the continuum,

$$\frac{\partial(\rho\mathbf{v})}{\partial t} + \nabla \cdot (\rho\mathbf{v} \otimes \mathbf{v}) = -\nabla \cdot (p\mathbf{I}) + \nabla \cdot \mathbf{T} + \mathbf{f}_b \quad (23)$$

where  $\mathbf{f}_b$  is the resultant of the body forces (such as gravity and centrifugal forces) per unit volume acting on the continuum,  $p$  is the pressure and  $\mathbf{T}$  is the viscous stress tensor and identity matrix defined by  $\mathbf{I}$  [20].

### Conservation of Energy

When the first law of thermodynamics is applied to the control volume, the conservation of energy can be written as,

$$\frac{\partial(\rho E)}{\partial t} + \nabla \cdot (\rho E\mathbf{v}) = \mathbf{f}_b \cdot \mathbf{v} + \nabla \cdot (\mathbf{v} \cdot \boldsymbol{\sigma}) - \nabla \cdot \mathbf{q} + S_E \quad (24)$$

where  $E$  is the total energy per unit mass,  $\mathbf{q}$  is the heat flux, and  $S_E$  is an energy source per unit volume.  $\boldsymbol{\sigma}$  is the stress tensor and it defined as sum of normal stress and shear stress for fluids  $\boldsymbol{\sigma} = -p\mathbf{I} + \mathbf{T}$  [20].

### Reynolds-Averaged Navier-Stokes (RANS) Turbulence Models

Reynolds number is a non-dimensional quantity which is commonly used in the turbulence modeling. This number defines the ratio of inertial over viscous forces. The following definitions for the Reynolds number are used in turbulence modeling problems.

Wall-distance Reynolds number,

$$Re_d = \frac{\sqrt{k}d}{\nu} \quad (25)$$

where;  $k$  is the turbulent kinetic energy,  $d$  is the distance to the wall and  $\nu$  is the kinematic viscosity.

Turbulent Reynolds number,

$$Re_t = \frac{k^2}{\nu\varepsilon} \quad (26)$$

or,

$$Re_t = \frac{k}{\nu\omega} \quad (27)$$

where;  $\varepsilon$  the turbulent dissipation rate and  $\omega$  is the specific dissipation rate.

RANS turbulence models govern the transport of the mean flow quantities. The RANS are developed by decomposing each solution variable  $\phi$  in Navier-Stokes equations into two parts as its mean, or averaged, value  $\bar{\phi}$  and its fluctuating component  $\phi'$ . Where the  $\phi$  can be the velocity, pressure or energy component.

$$\phi = \bar{\phi} + \phi' \quad (28)$$

---

Using these average values, mass and momentum equations can be expressed as,

$$\frac{\partial \rho}{\partial t} + \nabla \cdot (\rho \bar{\mathbf{v}}) = 0 \quad (29)$$

$$\frac{\partial(\rho \mathbf{v})}{\partial t} + \nabla \cdot (\rho \bar{\mathbf{v}} \otimes \bar{\mathbf{v}}) = -\nabla \cdot \bar{p} \mathbf{I} + \nabla \cdot (\mathbf{T} + \mathbf{T}_t) + \mathbf{f}_b \quad (30)$$

where:  $\rho$  is the density,  $\bar{\mathbf{v}}$  and  $\bar{p}$  are the mean velocity and pressure respectively,  $\mathbf{I}$  is the identity tensor,  $\mathbf{T}$  is the viscous stress tensor and  $\mathbf{f}_b$  is the resultant of the body forces (such as gravity and centrifugal forces).

$\mathbf{T}_t$  is known as Reynolds stress tensor which is an additional tensor quantity in the stress term in the momentum equation. Hence, these two new equations are identical to the Navier-Stokes equations and approximations for solving equations with mean flow quantities is used according to this method.

### Heat Transfer Modeling

Heat transfer is the exchange of thermal energy between media at different temperatures. Heat transfers from locations of high temperature to locations of low temperature in order to reach an equilibrium state. The three main mechanisms of heat transfer are: conduction, convection, and radiation. In CFD, heat transfer can be calculated within a fluid (single or multi-phase), between different fluid streams, between a fluid and a solid, and within a solid. The coupled heat transfer within a fluid and an adjoining solid is called conjugate heat transfer. For a conjugate heat transfer analysis, the energy equation is solved throughout the fluid and the solid solution domain with an efficient implicit thermal coupling at the fluid/solid interface. All other conservation equations are solved within the fluid only.

CFD implements the energy equation in the following integral form using FVM,

$$\frac{\partial}{\partial t} \int_V \rho E dV + \oint_A \rho H \mathbf{v} \cdot d\mathbf{a} = - \oint_A \dot{\mathbf{q}}'' \cdot d\mathbf{a} + \oint_A \mathbf{T} \cdot \mathbf{v} d\mathbf{a}_V + \int_V \mathbf{f}_b \cdot \mathbf{v} dV + \int_V S_u dV \quad (31)$$

where;  $E$  is the total energy,  $H$  is the total enthalpy,  $\dot{\mathbf{q}}''$  is the heat flux vector,  $\mathbf{T}$  is the viscous stress tensor,  $\mathbf{v}$  is the velocity vector,  $\mathbf{f}_b$  is the body force vector representing the combined body forces of rotation, gravity,  $S_u$  contributes energy source terms, such as radiation sources, interphase energy sources, or energy sources due to chemical reactions. User-defined volumetric sources also enter through this term [20].

It is more important to consider the convection heat transfer and conduction heat transfer for a heat exchanger model analysis using CFD. Convective heat transfer is the transfer of thermal energy by the combined effects of random molecular motion (diffusion) within the fluid, and the overall movement of the fluid from one place to another. It is used to provide specific temperature changes. Convection heat transfer between a fluid in motion and a bounding surface is of particular interest. Near the surface, where fluid velocity is zero, heat transfer occurs by diffusion only. Moving away from the surface, heat is transported downstream by the fluid motion and passes into the bulk fluid flow. Convection is usually described as being either natural, where natural buoyancy forces drive the bulk fluid motion, or forced, where an external driving force moves the fluid.

Convective heat transfer at a surface is governed by Newton's law of cooling,

$$q_s = h (T_s - T_{ref}) \quad (32)$$

where:  $q_s$  is the local surface heat flux (that is, power per unit area),  $h$  is the local convective heat transfer coefficient,  $T_s$  is the surface temperature,  $T_{ref}$  is a characteristic temperature of the fluid moving over the surface.

---

$q_s$ ,  $T_s$  and  $T_{ref}$  are fundamental in nature, while the heat transfer coefficient is a constant of proportionality that relates the three fundamental parameters. While  $q_s$  and  $T_s$  are unambiguous, there is some latitude in the choice of the fluid temperature  $T_{ref}$ . Depending upon the choice of  $T_{ref}$ , the heat transfer coefficient is different in order to satisfy equation (28). Therefore, heat transfer coefficients can not be defined without also defining a reference temperature: there is an infinite number of heat transfer coefficient and reference temperature combinations that give the same surface heat flux [20].

Consider the expression for the local surface heat flux,

$$q_s = \frac{\rho_f(y_c) C_{p,f}(y_c) u_\tau}{T^+(y^+(y_c))} (T_s - T_c) \quad (33)$$

where;  $\rho_f$  is the fluid density,  $C_{p,f}$  is the fluid-specific heat capacity,  $u_\tau$  is a velocity scale that is based on the wall shear stress,  $T^+$  is the dimensionless temperature,  $y^+ = (u_\tau y_c) / \nu_f$  is a Reynolds number,  $y_c$  and  $T_c$  are the normal distance and temperature of the near-wall cell, respectively

In STAR-CCM+, standard wall functions are used to model the flow physics in the boundary layer (near wall region) of the fluid flow which are semi-empirical functions. They give relationships for  $T^+$  and  $u_\tau$  in terms of the laminar and turbulent Prandtl numbers, the dimensionless near-wall flow velocity, and the turbulent kinetic energy [20].



---

## 4 Case Studies

### 4.1 Proposed Cases

In this research study, several case studies are proposed to build up the methodology which has discussed in the previous section and the final results will support to deliver the out put of the research. This is discussed in the results and discussion section. The case studies are mainly focused on the setting up the CFD model to evaluate and compare the performance data of the existing EGE unit and conduct the optimizations accordingly to increase the performance of the unit. Also, the new design concept for EGE units are developed to increase the efficiency using CFD simulations. These studies help to identify the important aspects of the performance improvement of the EGE unit. The EAT unit development is also included in this case study with concept development of the unit individually which is then combined to the EGE unit for the purpose of retrofitting. The case studies are defined as,

Case 1 - CFD Model Setup

Case 2 - Economizer Optimization to Increase the Efficiency

Case 3 - New Economizer Design Concepts

### 4.2 Case 1 - CFD Model Setup

There is a wide range of EGE units available for WHRS depending on the engine size and the exhaust pipe diameter. Here it is used the CFD simulations for the flow and thermal analysis to compare the available measurement data of specific EGE unit which is DN500. This unit is designed to fit into the engine exhaust line which has a standard inner diameter of 500mm exhaust pipe connected to the engine.

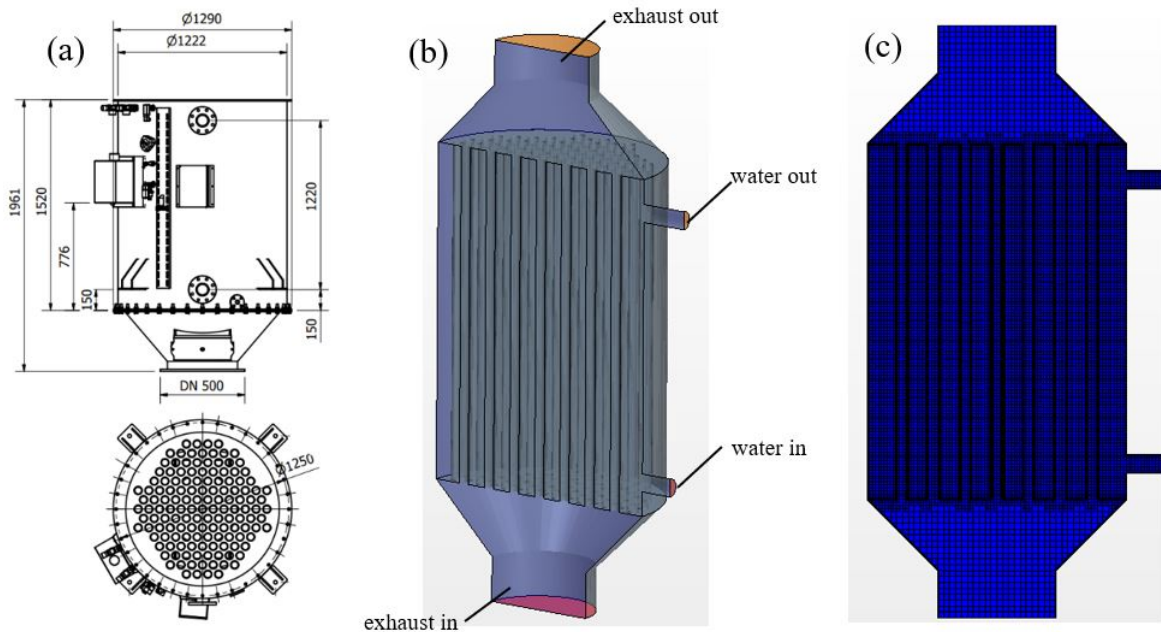


Figure 33: DN500 EGE unit, main dimensions (a), simplified model for CFD analysis (b), finite volume mesh for the CFD simulations (c)

The DN500 EGE unit has the geometrical dimensions according to the Figure 33 (a) and the

design 3D model is simplified for the CFD simulations as shown in Figure 33 (b). The EGE unit has a pipe bundle with 150 units of steel pipes which has an inner diameter of 49mm and 4mm thickness. The water flows around the pipes and the water inlet and outlet have 80mm diameter each. The exhaust gas enter through the 500mm diameter inlet, flows through the pipe bundle and exists through the 500mm diameter outlet. The unit can supply water up to 115°C by changing the supply flow rate of the water and the pressure inside the water region is maintained up to 6 bars to keep the water in liquid phase in a higher temperature values above 100°C.

### 1. Physical Properties of the Water and Exhaust

To compare the measurement data with the CFD simulation data, there are 3 exhaust flow conditions used according to the engine power. The data sheet has provided the exhaust inlet flow rate and it is required to calculate the exhaust inlet flow velocity for the CFD model development. For this calculations, it is required to use the exhaust density according to the exhaust temperature. The exhaust gas properties are shown in Table 3.

Consider the exhaust gas flow for the 350°C condition,

Temperature (°C)	Velocity (m/s)	Flow rate (kg/s)	Density (kg/m <sup>3</sup> )
350	37.2	4.17	0.570
365	34.8	3.78	0.553
395	29	3.0	0.527

Table 3: Exhaust gas inlet conditions for the DN500 with different exhaust temperatures

$$Q = AV \quad (34)$$

where;  $Q$  is the Volume flow rate,  $A$  is the Cross section area of inlet and  $V$  is the flow velocity.

$$\dot{m} = AV\rho$$

where;  $\dot{m}$  is the mass flow rate and  $\rho$  is the density of the fluid.

In this calculation,  $\rho = 0.57\text{kg/m}^3$   $\dot{m} = 4.17 \text{ kg/s}$  and  $A = 0.196 \text{ m}^2$

$$V = \frac{4.17}{0.196 \cdot 0.57} = 37.2\text{m/s}$$

For the water, inlet velocity is 1.5m/s and the inlet temperature is 75°C and the flow rate is calculated using  $Q = AV$ .

Diameter (mm)	Velocity (m/s)	Flow rate (kg/s)	Temperature (°C)	Density (kg/m <sup>3</sup> )	Specific heat (J/kg·K)
80	1.5	7.52	75	997.5	4181.7

Table 4: Water flow inlet properties for DN500

Exhaust gas properties are significantly changed with the temperature value. In each case the, following values in the Table 5 is used for the CFD model gas properties.

Temperature (°C)	Density (kg/m <sup>3</sup> )	Dynamic viscosity (Pas)	Specific heat (J/kg·K)	Thermal conductivity (W/m·K)
350	0.57	$3.06 \times 10^{-5}$	1051	0.0466
365	0.553	$3.14 \times 10^{-5}$	1060	0.0482
395	0.527	$3.23 \times 10^{-5}$	1067	0.0499

Table 5: Exhaust gas properties for different flow temperatures

---

## 2. Thermal Resistances due to Fouling and Pipe Thickness

According to the equation (09) the thermal Resistance build up in the pipes due the pipe wall thickness  $R_{wall}$  can be calculated as,

$$R_{wall} = \frac{t_p}{k_p}$$

with;  $t_p$  is the pipe thickness(4mm) and  $k_p$  is the pipe thermal conductivity.

Assume that the pipe material is carbon steel and the thermal conductivity is  $45W/K.m$ ,

$$R_{wall} = \frac{4 \cdot 10^{-3}}{45} = 0.000088m^2K/W$$

The fouling resistance due to exhaust gas is available in Appendix B and the inner fouling layer of the tubes has a fouling Resistance of  $R_{f,a}$  due to the exhaust.

$$R_{f,a} = 0.00176m^2K/W$$

The pipe outer fouling layer has a fouling resistance of  $R_{f,w}$  due to water.(for clean water temperature over  $50^\circ C$  and velocity over  $1m/s$ )

$$R_{f,w} = 0.00035m^2K/W$$

The total thermal resistance  $R_{total}$  of the fouling is the summation of these three resistance values. Thermal resistance of the pipe material is relatively low value when it compared with the fouling resistance. The dominating resistance for in this unit is the fouling resistance and the total resistance is almost similar to the total fouling resistances.

$$R_{total} \approx 0.00211m^2K/W$$

## 3. Assumptions for the CFD Analysis

It is assumed that the flow is reached to steady state and heat transfer CFD simulation is modeled with considering both exhaust and water turbulent flow characteristic. Also, both flows has constant density without considering the temperature variations in the flow field. The heat dissipation to the surrounding through the outer surface is neglected with assuming perfect thermal insulation of the outer surfaces of the EGE unit. Radiation heat transfer is also neglected for these study cases and it is not included for CFD simulations. It is assumed that there is no phase change in the water region due to the local boiling which can occur due to the flow disturbances. The same CFD model is used for 3 different exhaust flow conditions with different flow rates and temperatures. The out put data of the CFD simulations for temperature and pressure values are taken as an average value of the out let surface.

## 4. Mesh Generation

The finite volume mesh is refined near the inlet and out let regions of the EGE unit and geometric symmetry is used to reduce the number of finite volume cells in the model. For the CFD models which are discussed in this study has a cell size of 50mm and 50% mesh refinement in the inlet and out of the exhaust flow region. There are two prism layers in the fluid interfaces in both exhaust and water region. The detailed image of the generated mesh trough the symmetry plane of DN500 is shown in Figure 34 with aligned mesh for both exhaust and water regions. This mesh size is selected with considering the available computational power for the CFD simulations. Smaller mesh size which is more than this selected value is required higher computational power and simulation run time. This model consists 2.5 million cells for DN500 with mesh refinements for the symmetry condition.

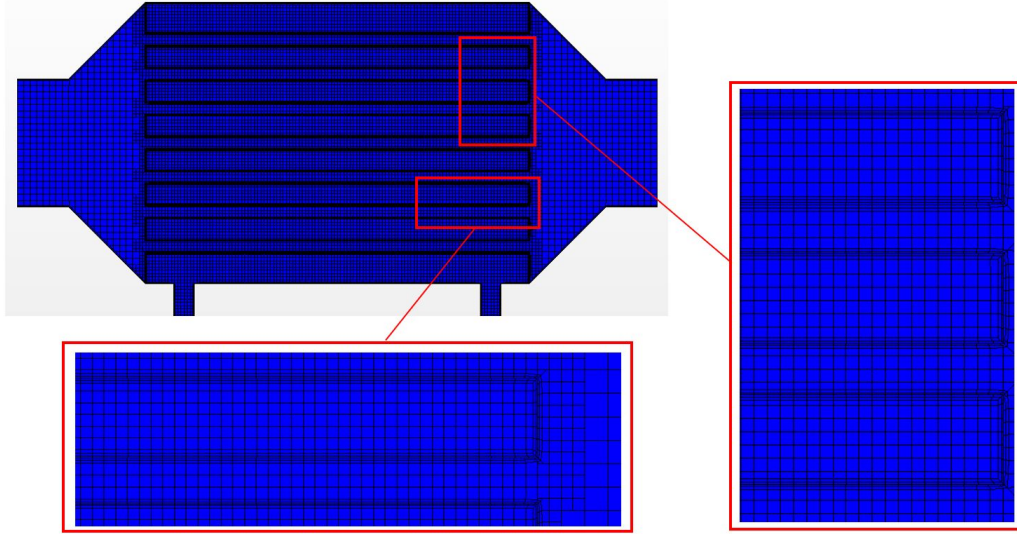


Figure 34: DN500, Detailed view of the generated finite volume cells for CFD simulation

## 5. Boundary Conditions

The boundary conditions are needed to define properly to get the accurate output data from the CFD simulation with reducing the complexity. For this case, the EGE model is exported to the simulation environment using the geometric symmetry of the model which is a half section through the symmetry plane with reducing the half of the cell amount of the mesh. This helps to reduce the simulation time and this can be used only for model which has a geometric symmetry plane through flow inlets and outlet. The inlet and outlet properties of both flows are defined according to the 3 exhaust gas temperature conditions. Water and exhaust region is only contained in this model without the solid region of steel pipes. Hence, the contact interface of water and exhaust region is modeled as boundary interface which is available as an option in STAR-CCM+ with thermal resistance of the fouling. Total thermal resistance is defined as the interface resistance between water and exhaust regions.

## 6. Physics Models for CFD Analysis

Physics models are assigned for both water and air regions (exhaust gas) according to the available physics model set up in the CFD software. The main physics characteristics for the flow simulation is implemented to simulate the flow behavior with the thermal effects for both water and exhaust regions in the EGE unit. It is considered as the both flows have a turbulent behavior, and the Reynolds Average Navier-Stokes's equations are used to model the flow which is selected the K-Epsilon turbulence for these simulations. The flows are considered as incompressible which has a constant density for specified temperature values. These simulations are carried out for single phase flows with the adiabatic heat transfer between two fluids regions. The heat transfer interface is created as boundary interface with the thermal resistance modeled as a the interface resistance using the available options in CFD tool.

### 4.2.1 Performance Analysis of DN500 Economizer

#### 350°C Exhaust Temperature

The first simulation is conducted using the development method mentioned above and the exhaust condition of 350°C is used the same flow properties as mentioned in the performance data sheet in Appendix A for DN500. The temperature distribution of the water region on the symmetry plane and the sections close to water inlet and outlet is shown in Figure 35 from the simulation results.

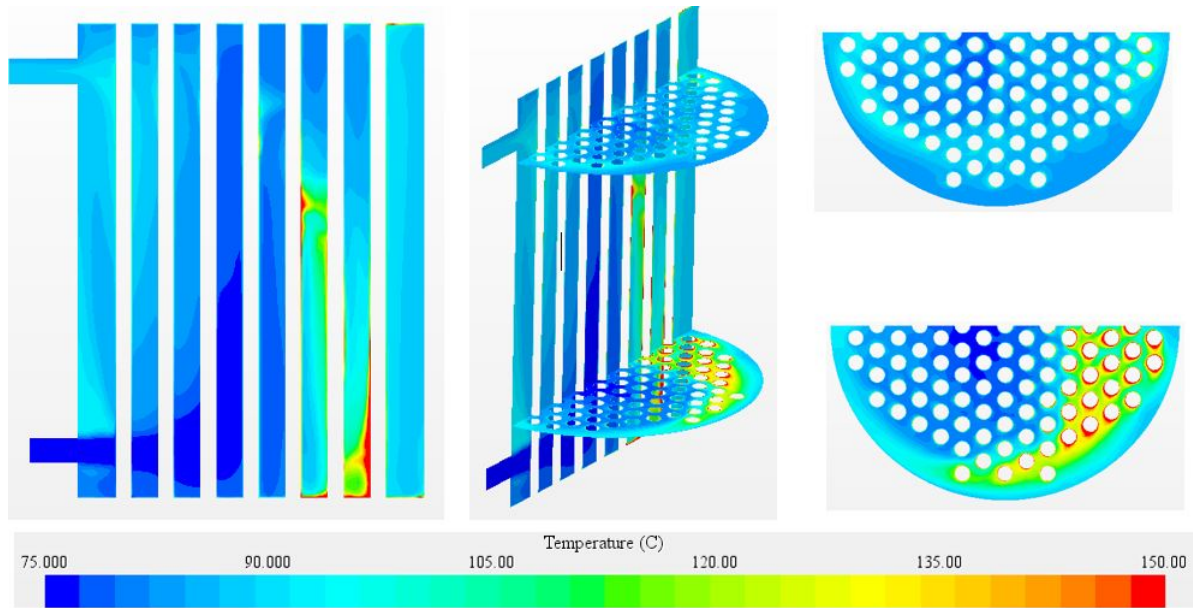


Figure 35: Water region temperature distribution plot of DN500 for 350°C exhaust flow

The water and exhaust temperatures of the out let is plotted for the steady state flow behaviour which is shown in Figure 36. The pressure which is build up in the flow inlets and outlets is also plotted and it is shown in Figure 37. This plot is used for the pressure drop calculation across the inlet and outlet of the exhaust. The surface average value of the temperature and pressures is used for these plots. The steady state occurs when the state variables of temperature, pressure, flow velocity and the heat transfer rate reach to constant value over the time. The plots are not dependent on the time and the iterations are conducted till the convergence of the simulations as shown in the plots. These plots shows the steady value for the state variables after number of iterations which is considered as the steady state flow characteristics required for the performance analysis of the EGE unit.

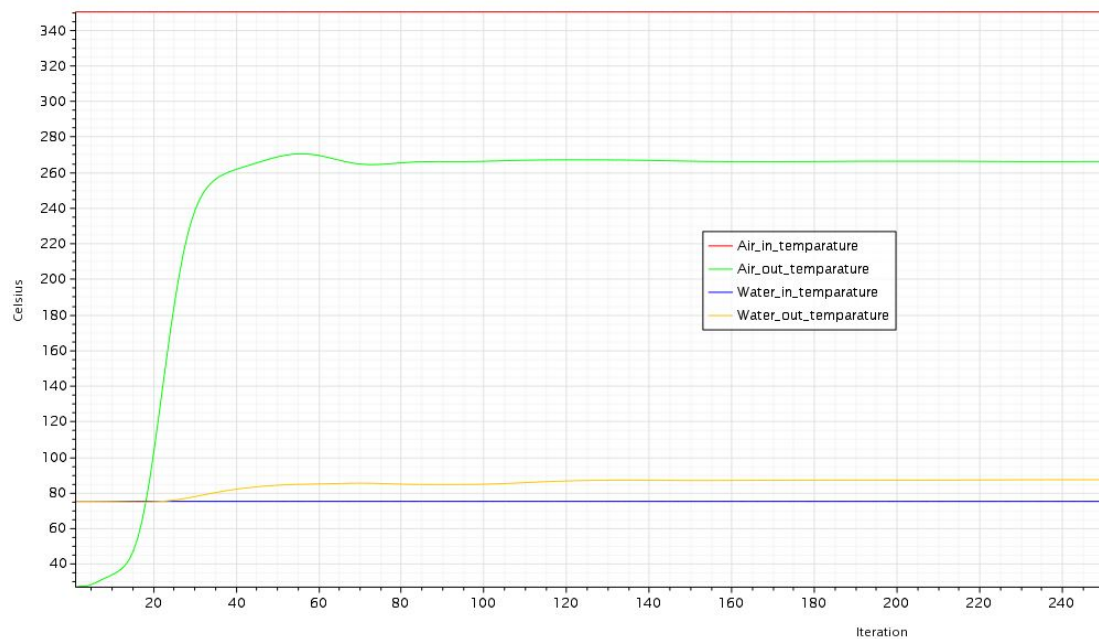


Figure 36: Water and exhaust flow temperature convergence plot from the CFD simulation

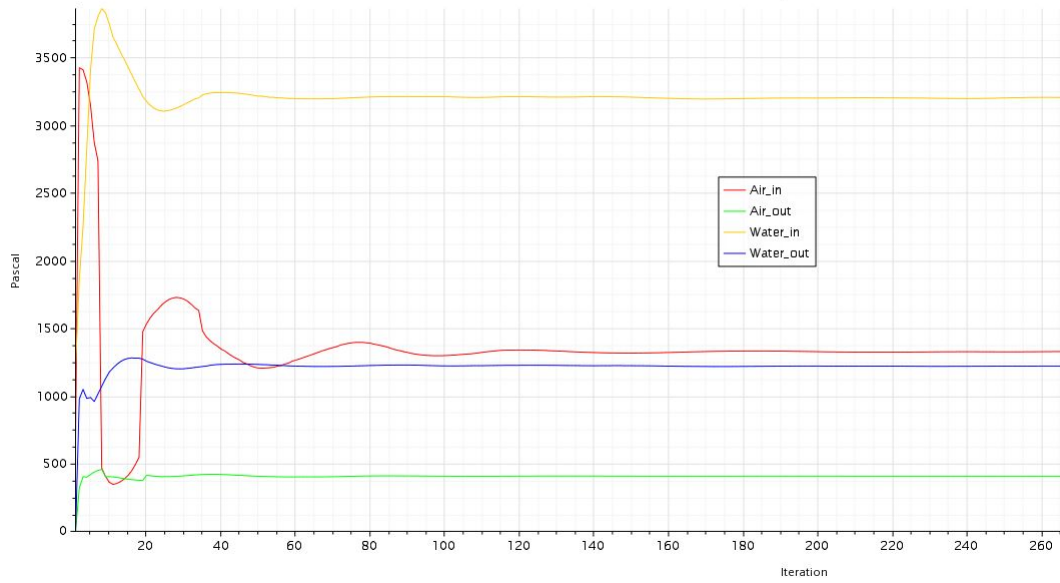


Figure 37: Water and exhaust flow pressure convergence plot from the CFD simulation

The heat transfer rate between the water and air interface is plotted in the graph shown in figure 38 for the steady state and this shows the two graphs for heat supplied by the air and the heat absorbed by the water. The small deviation between this two plots are caused by the interface mesh alignment errors which is almost negligible in this case.

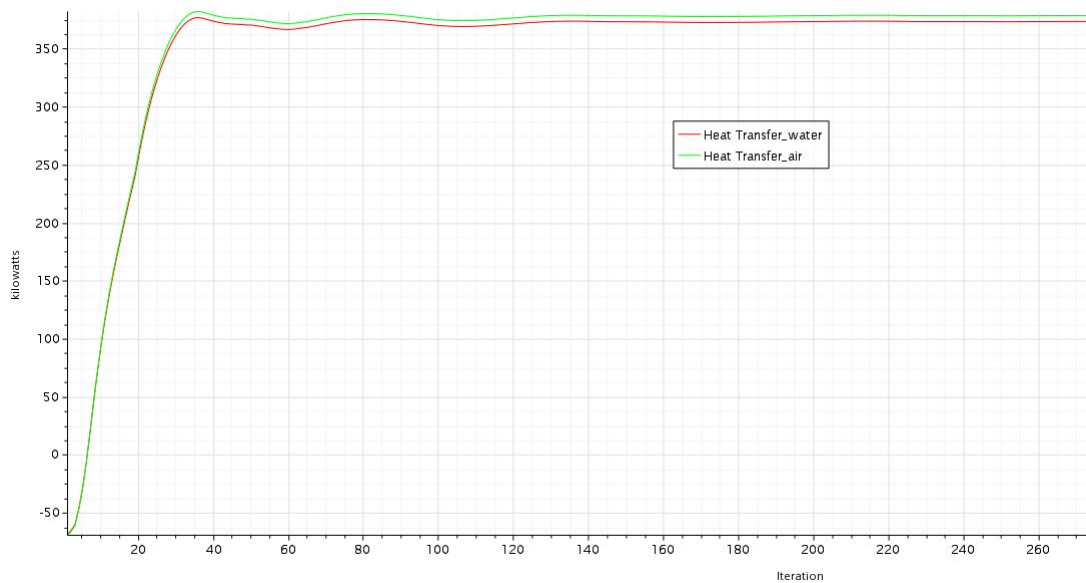


Figure 38: Water and exhaust region heat transfer rate convergence plot from the CFD simulation

The data which is gathered from the CFD simulations and the measured performance data for 350°C are arranged in the Table 6.

The heat transfer rate to the water by the exhaust gas can be calculated using equation (03) referring to the CFD results of temperature increase in water region,



	Exhaust in (°C)	Exhaust flow(kg/s)	Water in (°C)	Water flow(kg/s)	Exhaust out(°C)	Water out(°C)	Heat out(kW)	Pressure drop(Pa)
Measured data	350	4.17	75	7.52	263	N/A	389	774
CFD results	350	4.17	75	7.52	266	87.1	378.8	813

Table 6: CFD simulation results and the measured data for DN500 with 350°C exhaust inflow

$$\dot{q} = \dot{m}c_p\Delta T$$

where;  $\dot{m}$  = water mass flow rate (7.52 kg/s)  $c_p$  = specific heat of water (4181.7 J/kg.K)

$$\dot{q} = 7.52 \cdot 4181.7 \cdot (87.1 - 75) = 380kW \approx 378.8kW$$

The CFD result for the heat transfer has almost similar value for the calculated value of heat transfer from the water temperature increase.

The same procedure is followed for both 365°C and 395°C exhaust temperatures and the data is gathered in Table 7 and 8 with the temperature distributions of the water region is shown in Figure 39 and 40.

### 365°C Exhaust Temperature

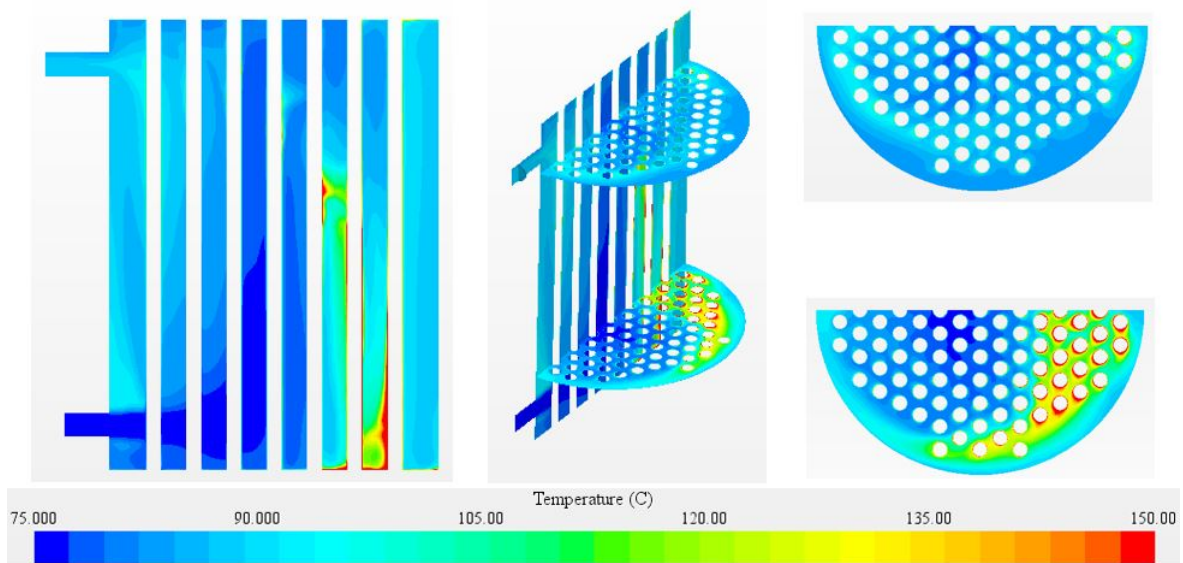


Figure 39: Water region temperature distribution plot of DN500 for 365°C exhaust flow

	Exhaust in (°C)	Exhaust flow(kg/s)	Water in (°C)	Water flow(kg/s)	Exhaust out(°C)	Water out(°C)	Heat out(kW)	Pressure drop(Pa)
Measured data	365	3.78	75	7.52	270	N/A	385	657
CFD results	365	3.78	75	7.52	272.6	87.0	374.6	788

Table 7: CFD simulation results and the measured data for DN500 with 365°C exhaust inflow

### 395°C Exhaust Temperature

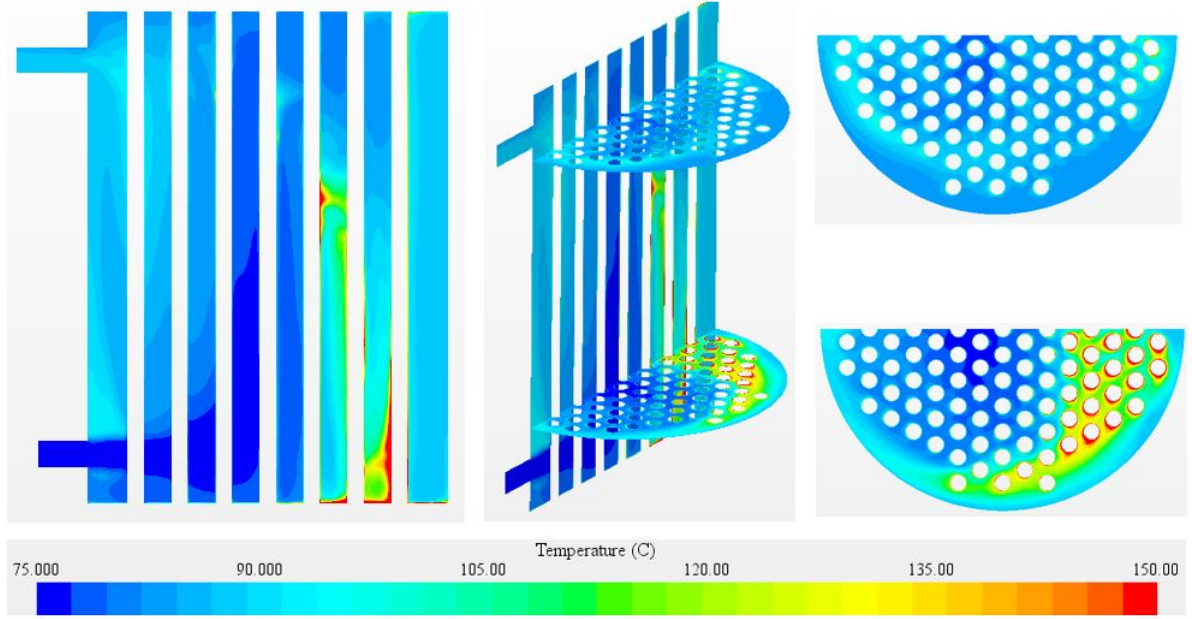


Figure 40: Water region temperature distribution plot of DN500 for 395°C exhaust flow

	Exhaust in (°C)	Exhaust flow(kg/s)	Water in (°C)	Water flow(kg/s)	Exhaust out(°C)	Water out(°C)	Heat out(kW)	Pressure drop(Pa)
Measured data	395	3.00	75	7.52	283	N/A	364	431
CFD results	395	3.00	75	7.52	282.2	86.7	367.8	535

Table 8: CFD simulation results and the measured data for DN500 with 395°C exhaust inflow

#### CFD Simulation without Fouling Resistance from the Exhaust

The fouling resistance from the exhaust is mainly caused by the soot development inside the pipes as described in earlier sections. This is mainly caused by the unburnt hydrocarbon of the exhaust flow. Introducing the DOC and DPF to the EAT unit referring to the section 2.2, will help to reduce the soot development by the exhaust which will reduce the fouling resistance from the exhaust. Assume that, there is no exhaust fouling inside the pipes of the unit after implementing DOC and DPF unit to the exhaust system, the thermal resistance will be only generated by the water fouling resistance and the thermal resistance of the pipe material. Hence,  $R_{total}$  the new total thermal resistance for the CFD model contact interface of water and air

$$R_{total} = R_{wall} + R_{f,w} = 0.000088m^2K/W + 0.00035m^2K/W = 0.000438m^2K/W$$

where;  $R_{wall}$  is the thermal resistance of the pipe material and  $R_{f,w}$  is the fouling resistance of the water referring to the section 3.2.3.

CFD analysis for the 3 exhaust temperature cases with the new thermal resistance value, without including the thermal resistance due to the fouling in the exhaust side is conducted with the same simulation set up as the DN500. The results which are taken from the simulations are shown in the Table 9.



Exhaust temperature (°C)	Heat transfer rate with exhaust fouling (kW)	Heat transfer rate without exhaust fouling (kW)	Improvement
350	378.8	410.1	8.2%
365	374.6	409.2	9.2%
395	367.8	392.5	6.7%

Table 9: CFD simulation results for the DN500 without exhaust fouling

### 4.3 Case 2 - Economizer Optimization to Increase the Efficiency

According to the CFD analysis of the DN500, the temperature distribution of the water region shows uneven heat distribution with the water flow which leads to develop uneven thermal stresses in the water region. Hence, the CFD analysis of DN700 mainly focus on the optimization of the EGE unit to increase the performance of the unit with new implementations in both fluid and air regions and reduce the soot development due to fouling inside the tubes from exhaust air.

#### 4.3.1 Performance Analysis of DN700 Economizer

DN700 is a expanded version of DN500 which has the dimensions shown in Figure 41. The unit has 280 number of pipes with 49mm inner diameter and 4mm thickness. The water inlet and out let pipes have a diameter of 100mm. This unit is designed to fit into the engine exhaust line which has the standard diameter of 700mm. This unit ic combined with a 4MW Wartsila diesel engine which is mentioned in section 2.4 and the exhaust flow properties of this engine is used for the CFD simulations.

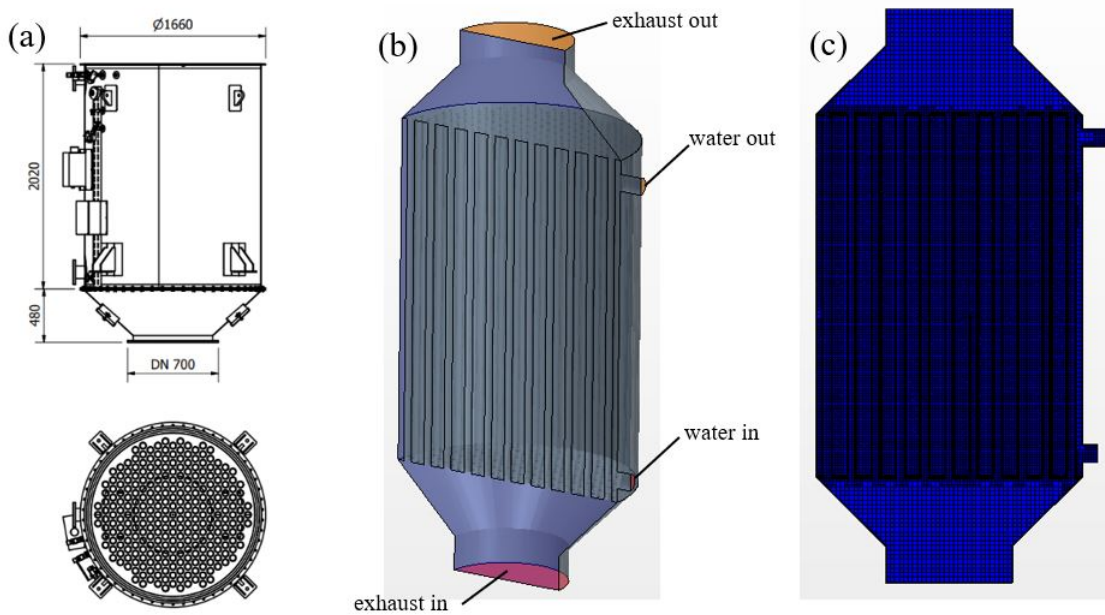


Figure 41: DN700 EGE unit, main dimensions (a), simplified model for CFD analysis (b), generated mesh for the CFD simulations (c)

The CFD model is implemented with using the development procedure which has used in the Case 1. The thermal resistance between water and air region is not accounted for this model. Because

the main purpose of developing DN700 is to study the efficiency improvement of the existing model and all the development has the same physics conditions. The inlet flow properties for the study are mentioned in Table 10.

	Speed (m/s)	Temperature (°C)	Flow rate (kg/s)
Exhaust gas	35	350	7.63
Water	2.5	75	19.58

Table 10: DN700 water and exhaust gas inlet conditions

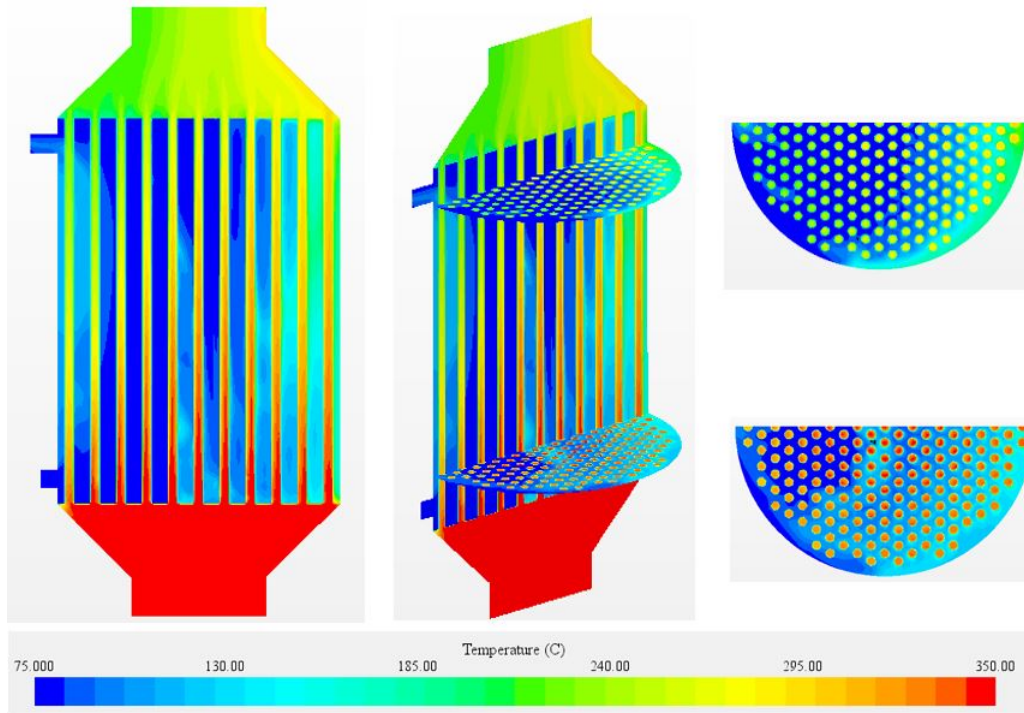


Figure 42: Temperature distribution of the water and exhaust region of DN700

Temperature distribution in the water and air regions at steady state from the CFD simulations is shown in Figure 42. The surface average values of outlet temperatures of both regions and the calculate pressure drop between the inlet and outlet of the exhaust are mentioned in the table 11.

Water outlet temperature (°C)	Air out let temperature (°C)	Heat output (kW)	Pressure drop (Pa)
85	242	877	893

Table 11: CFD simulation result of DN700

#### 4.3.2 Using Baffles

The temperature distribution in the water region at steady state for DN700 shows the same behavior as DN500. Some local areas in the water region have very slow movement which enables the overheating in those areas. Hence, the uneven thermal stresses are developed inside the unit. The areas which have the temperature above this value can be create local boiling in the water region in the existing EGE unit. The water flow velocity distribution for the existing unit in Figure 45

(a) and the temperature distribution in the water region for actual unit in Figure 46 (a) illustrates the significant relationship between the velocity and temperature distribution. The areas which has almost zero velocity in the water region starts to overheat and the higher amount of the water flow take the closest path to reach the out let, without flowing evenly inside the unit. It can be clearly seen from the Figure 44 (a) which is the flow streamlines of the actual unit. The water inlet and out let positioned in the same side of the unit for the assembly purpose of the EGE unit.

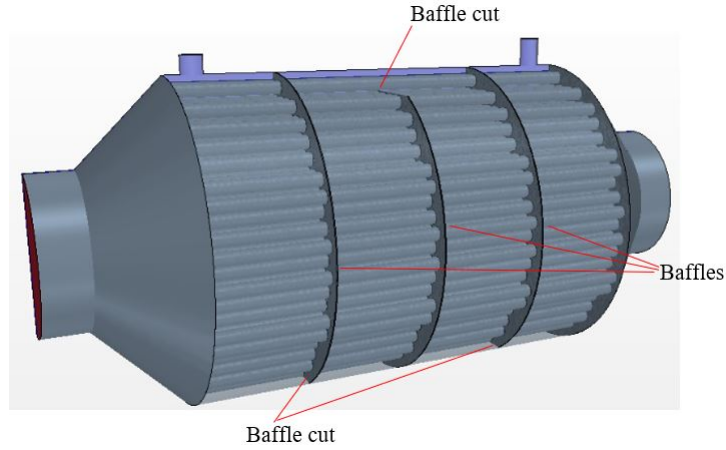


Figure 43: DN700 EGE unit 3D model with 3 baffles

Using baffles can distribute the water flow by disturbing the water flow path to avoid the closest path to reach the outlet. This study case mainly focused on the optimization using baffles for the overall efficiency and the performance of the EGE unit.

**Effect of Number of Baffles**

The 3D model consisting of 3 baffles for DN700 is shown in Figure 43 and the number of baffles is used as 1,3 and 5 which are the odd numbers due to the inlet and outlet position of the water region.

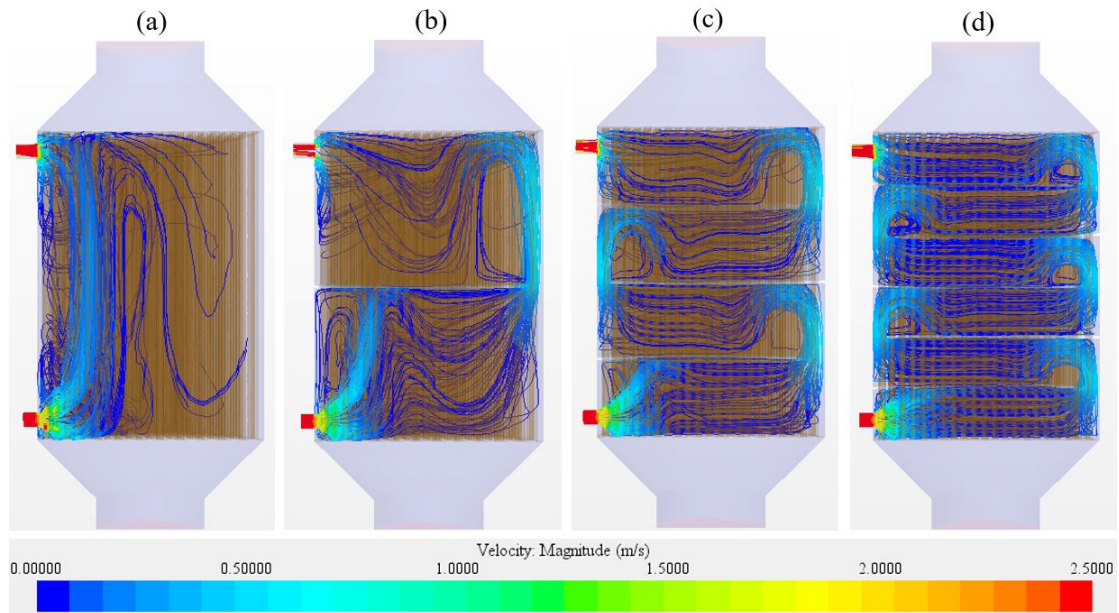


Figure 44: Water flow streamlines of DN700, without baffles (a), 1 baffle (b), 3 baffles (c) and 5 baffles (d)

The flow streamlines plotted from the CFD simulations results are shown in Figure 44 for each case. The velocity distribution and the temperature distribution of the water region is shown in Figure 45 and Figure 46 through the symmetry plane of the model.

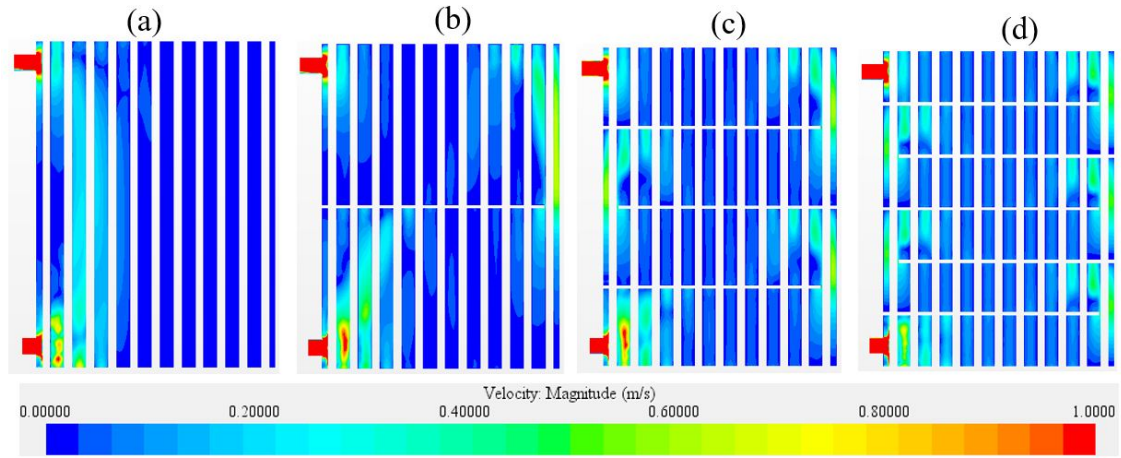


Figure 45: Water flow velocity distribution through the vertical mid section of DN700, without baffles (a), 1 baffle (b), 3 baffles (c) and 5 baffles (d)

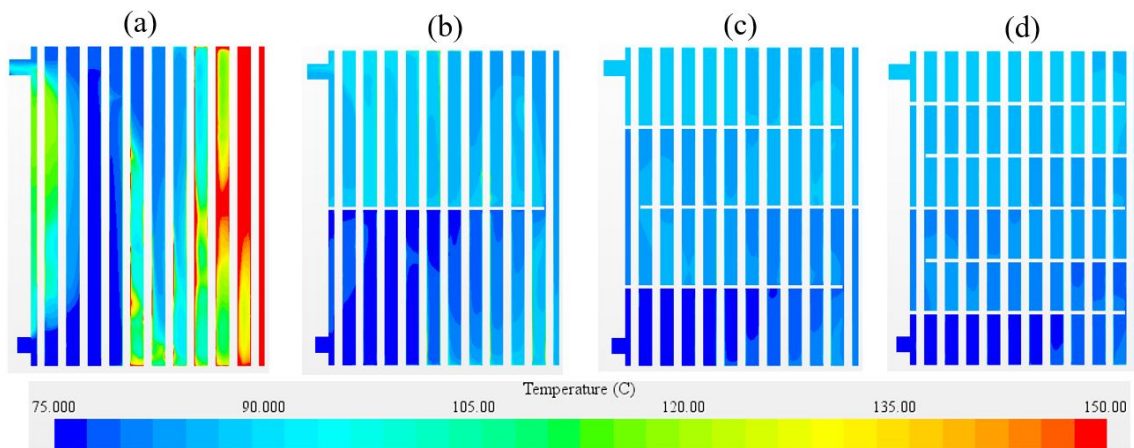


Figure 46: Water flow temperature distribution through the vertical mid section of DN700, without baffles (a), 1 baffle (b), 3 baffles (c) and 5 baffles (d)

The outlet flow condition and heat transfer in each simulation is illustrated in Table 12 and the heat output increase which illustrates the increase of the efficiency due to using the baffles is also mentioned in the table.

No of Baffles	Exhaust out temperature (°C)	Water out temperature (°C)	Water flow pressure drop(Pa)	Heat output kW	Heat output increase with baffles
0	242	85	6000	877	N/A
1	224	87.5	6345	1019	16.2%
3	221	88	6800	1039	18.5%
5	220	88.2	7400	1056	20.4%

Table 12: CFD simulation results comparison for the increased number of baffles for DN700



---

### Effect of The Baffle Cut Percentage

The baffle cut percentage has a significant effect to the heat transfer rate in shell and tube heat exchangers, according to the section 3.2.4. In this section of the study, it is focused on the baffle cut percentage effect to the heat transfer rate with using 3 baffle arrangement which has already shown a significant improvement in the heat transfer rate with compared to the other arrangements. The baffle cut percentage defined according to the percentage from the diameter of the exhaust chamber and it is changed from 50% to 10% from the size of the diameter. In some models, the baffle cut has changed slightly to match with the tubes without creating complex contact areas in the CFD model. The same CFD model for DN700 with the inlet conditions in the previous section is used to conduct this study with changing the baffle cut percentage by 10% in each simulation.

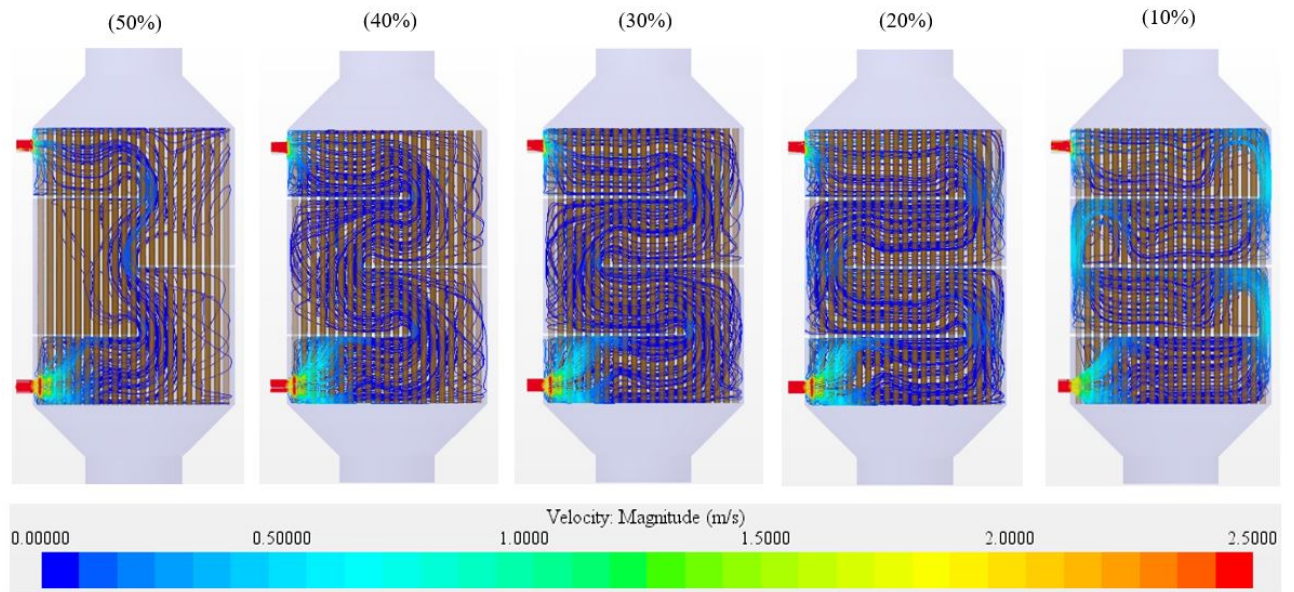


Figure 47: Water flow streamlines of DN700 with reducing the baffle cut by 10% for the 3 baffle arrangement

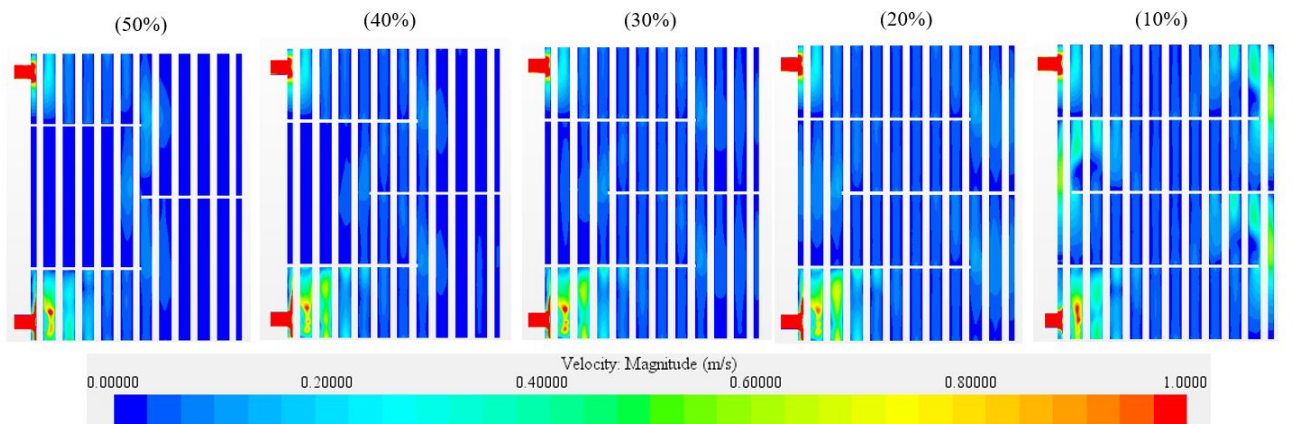


Figure 48: Water flow velocity distribution through the vertical mid section of DN700 with reducing the baffle cut percentage by 10% for the 3 baffle arrangement

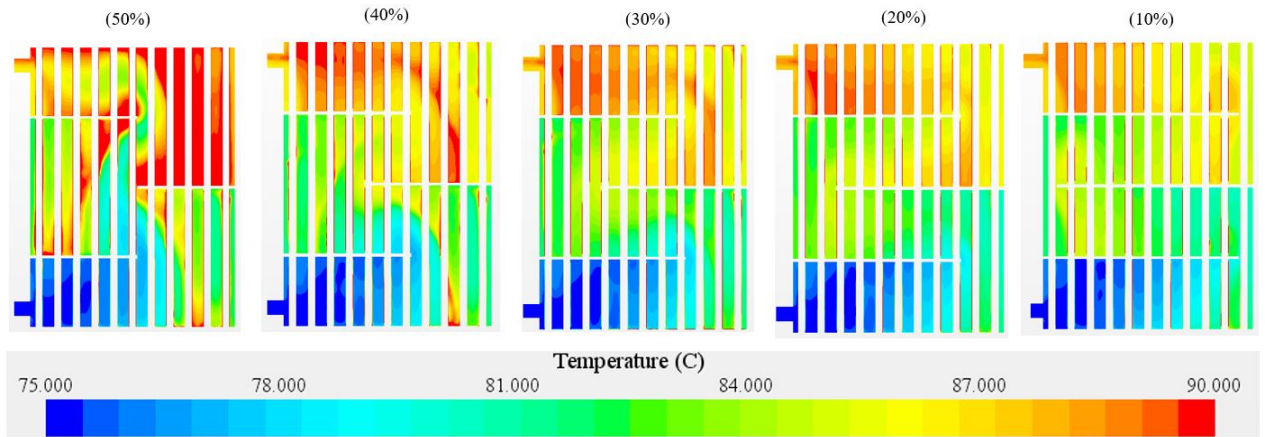


Figure 49: Water flow temperature distribution through the vertical mid section of DN700 with reducing the baffle cut percentage by 10% for the 3 baffle arrangement

The results from the CFD simulations of each simulation with reducing the baffle cut percentage is shown in the table 13 with the calculated values for heat transfer rate increment due to the size of the baffle cut. This comparison is done with DN700 EGE unit which does not have the baffles in the water region

Baffle cut	Exhaust outlet temperature (°C)	Water outlet temperature (°C)	Water flow pressure drop(Pa)	Heat output kW	Heat output increase with baffles
No baffle	242	85	6000	877	N/A
50%	226	87.4	6239	997	13.7%
40%	224	87.7	6586	1026	17.0%
30%	223	87.8	6602	1033	17.8%
20%	221	88	6705	1039	18.5%
10%	221	88	6800	1039	18.5%

Table 13: CFD simulation results comparison for the reducing the size of the baffle cut for DN700

#### 4.3.3 Using Exhaust Inlet Flow Directional Controlling

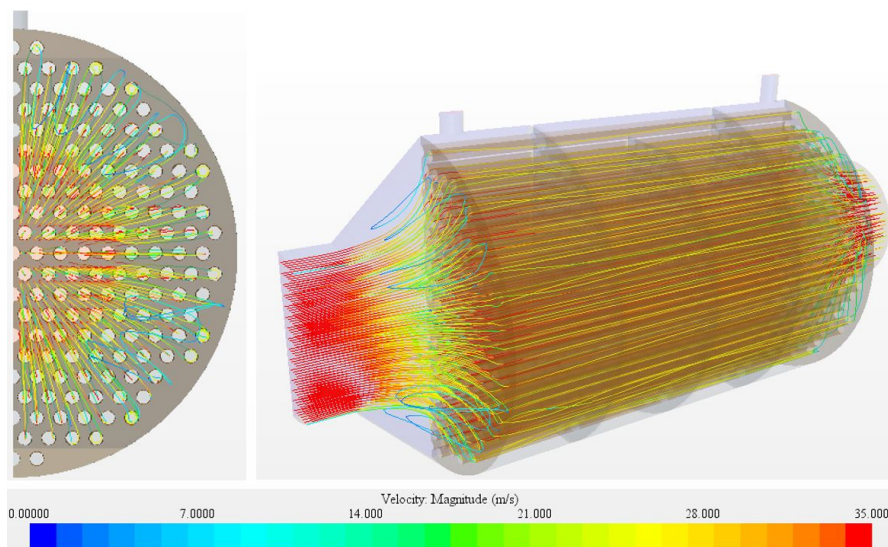


Figure 50: Exhaust flow velocity streamlines of the DN700

---

The flow velocity distribution of the exhaust gas inside the tubes shows an uneven flow distribution as shown in the Figure 50 which creates a high velocity in the center areas of the pipe bundle and a low velocity distribution close to the outer boundary of the pipe bundle. The exhaust flow distribution method is analyzed in this section with evaluating performance effect without changing the length of inlet cone shape of the EGE unit, which has  $45^\circ$  angle to the vertical centerline.

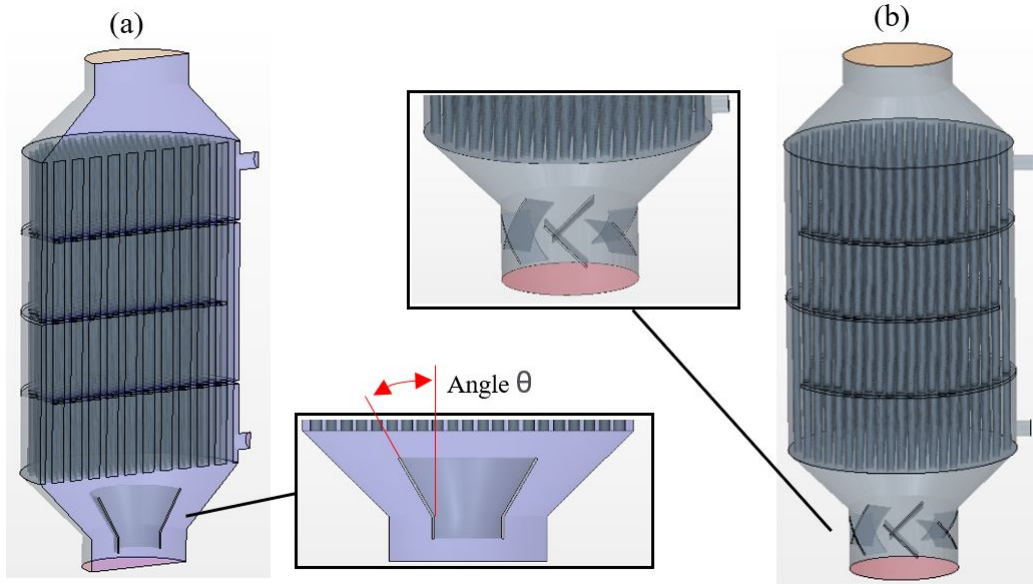


Figure 51: Exhaust flow direction control of DN700 using, cone shape (a) and angular blades (b) 3D models for CFD analysis

The main analysis consists with two approaches with flow guiding through a conical shape mounted inside the exhaust inlet and creating a higher flow disturbance to the exhaust flow by using angled blades mounted in the EGE gas inlet. For all the analysis in this section. It is used EGE with 3 baffles inserted for the water region to create a even temperature distribution in the water region to independently evaluate the exhaust flow behavior change with the implementations.

The inlet flow directional controlling cone shape is analyzed with the change of the angle by  $10^\circ$  to the vertical centerline of the cylinder and the performance data from the CFD simulations are collected. The symmetry of the unit is used for cone shape flow controller and the full geometry is used for the swirl flow analysis. The swirl flow is analyzed after evaluating the results from the direction controlling by using the cone shape flow controller.



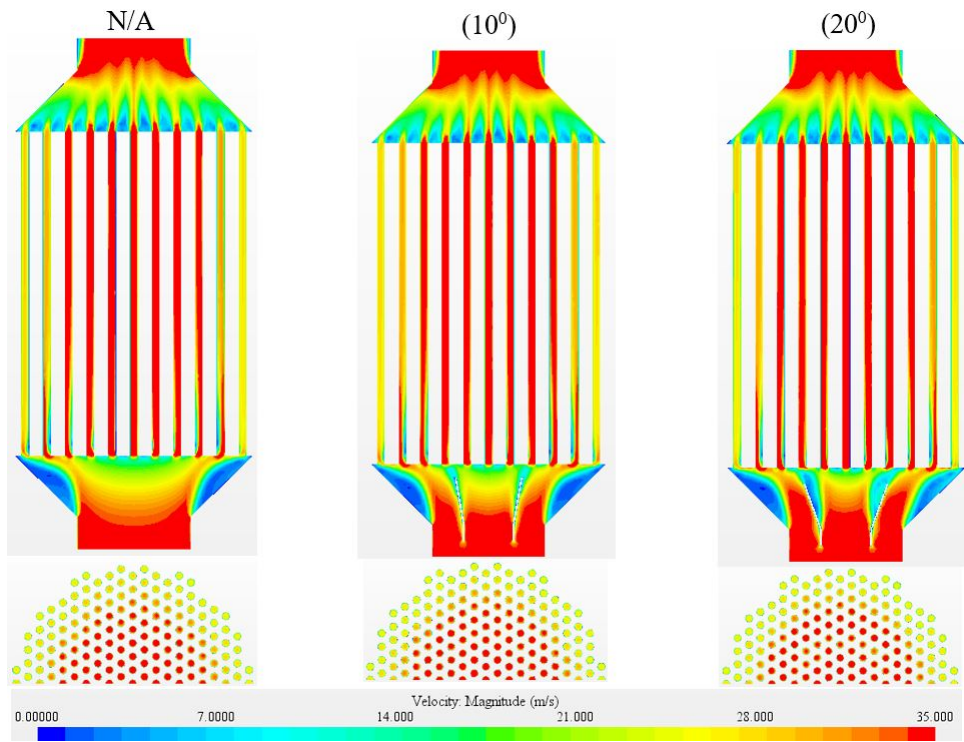


Figure 52: Exhaust flow velocity distribution through the vertical mid section of DN700 with exhaust flow direction controlling (without flow controlling and increasing cone shape angle)

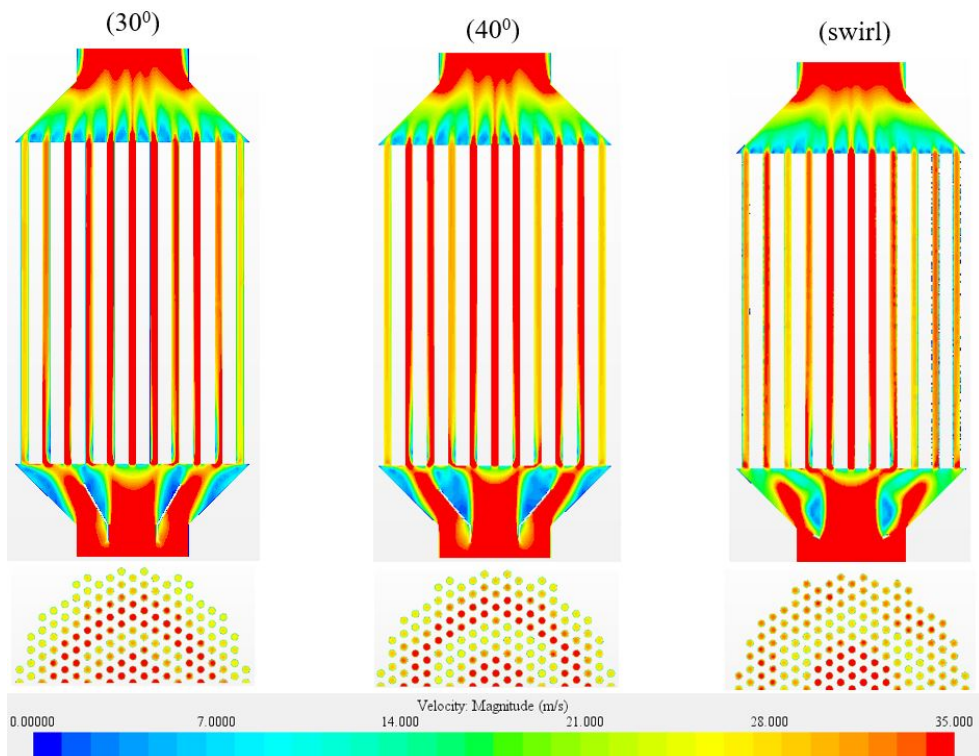


Figure 53: Exhaust flow velocity distribution through the vertical mid section of DN700 with exhaust flow direction controlling (increasing cone shape angle and swirl flow using angular blades)



The results of the CFD simulations are shown in the Figure 52 and 53 for the flow behavior inside the tubes trough the vertical symmetry plane of the tube bundle and the mid horizontal section of the tube bundle.

The heat transfer rate and the pressure drop of the exhaust chamber are the main performance indicators required to analyze using simulations and these values are mentioned in the Table 14 according to the flow modification of directed flow and the swirl flow.

	Water outlet temperature (°C)	Exhaust out let temperature (°C)	Heat output (kW)	Exhaust pressure drop (Pa)
Without	88	221	1039	893
10°	88	221	1039	931
20°	88	221	1040	949
30°	88	221	1040	1004
40°	88.1	220	1046	1097
Swirl flow	88.3	217	1064	1269

Table 14: CFD simulation results comparison for the exhaust flow direction control for DN700 with 3 baffles

#### 4.4 Case 3 -New Economizer Design Concepts

In Case 1 and 2, it has discussed the existing EGE unit and the modifications of the water flow and the exhaust flow. Case study 3 is mainly focused on the new design concepts for the heat transfer efficiency improvement of the EGE unit. In the existing unit, it has the same heat transfer area for both water and air regions without considering the thickness of the pipes. The overall heat transfer coefficient, U which is governed the heat transfer rate of the unit referred to the equation (06). For the equal contact surface area, the heat transfer rate for parallel flow heat exchanger is defined in the equation (13) as,

$$\dot{q} = UA\Delta T_{lm}$$

where; U can be defined as,

$$U = \frac{1}{\frac{1}{h_w} + \frac{1}{h_a}}$$

with;  $h_w$  is the convective heat transfer coefficient of water and  $h_a$  is the convective heat transfer coefficient of air

The  $h_a$  has a very low value than the  $h_w$  referring to the convective heat transfer coefficients values mentioned in the Table 2. Hence, the  $h_a$  is the dominant factor of controlling the overall heat transfer coefficient U in water/air heat exchangers. According to the equation (21), a heat exchanger with different surface areas for the two working fluids, the overall heat transfer coefficient need to increase to improve the heat transfer rate. This can be done by increasing the contact surface area of the fluid region which has the low convective heat transfer coefficient. In this study, it is the exhaust region contact surface area.

Contact area of water (m <sup>2</sup> )	Contact area of exhaust (m <sup>2</sup> )
86.2	86.2

Table 15: Water and exhaust contact surface area of DN700 without considering pipe thickness

It is not feasible to increase the surface area of the air region (exhaust) in the existing EGE unit due to the compact design of many pipes inside the cylinder and it is not possible to increase the

---

surface area inside the steel pipes. Hence, the possible design alternative is using the pipes for water flow instead of air and directing the exhaust flow around the water pipeline inside the EGE unit as shown in Figure 54 (c). All the new design concepts are based on this base concept and the arrangement of the pipes are different according to the gradual performances improvements with changing fluid contact area.

Also, the outer dimensions and the inlet flow properties from the DN700 case study is used to develop the new design in this case study which are analyzed through this section. (also the inlet and out let pipe diameter of the water line is 100mm) The air contact surface area is increased by using the plate fins. Specific thickness for the plate fins is used for every design due to reduce the complexity of the modeling and CFD simulation process. The fins has a efficiency factor when it is used in a heat transfer applications as described in equation (19). The increase surface area using fins affects to the heat transfer rate is more reliable to analyse using CFD simulations which is conducted for each new design in this section. This case study of the new design concept development is mainly focused on the heat transfer rate improvement between air and water region with considering the effect of developed pressure drop in exhaust chamber, between the inlet and outlet of the EGE unit.

#### 4.4.1 Design 1 - Spiral Water Pipe with Fins

In Design 1, water flow inside a spiral tubes and it is connected to plate fins around the spiral while the exhaust is flowing around the tube and fins as shown in Figure 54 (c). The water tube has a inner diameter of 100mm same as the DN700 and 50 plate fins with a thickness of 5mm are arranged in a circular array around 360° inside the exhaust chamber with connecting to the water coil.

These new design CFD models with fins to increase the heat transfer is modeled as three regions instead of two regions which has discussed in earlier cases. These models have water, air, and solid region in the CFD models due to the complexity of modeling a common interface for the conjugate heat transfer. Hence, it is modeled as two contact interfaces with the solid region of pipes and fin assembly as shown in Figure 54 (a) and (b).

Contact area of water (m <sup>2</sup> )	Contact area of exhaust (m <sup>2</sup> )
10.1	112.2

Table 16: Water and exhaust contact surface area of Design 1

The material of the solid region is assigned as carbon steel and used the material properties accordingly. The heat transfer is assumed as adiabatic through the solid region and exhaust gas properties and water flow properties of DN700 is used for this simulation. The contact surface area for the water and air regions are mentioned in the Table 16 for the Design 1. The approximation of the fin efficiency of this type of design is complex and the CFD simulation data provides a better understanding about the heat transfer rate change due to the increase of contact surface area of the exhaust region.

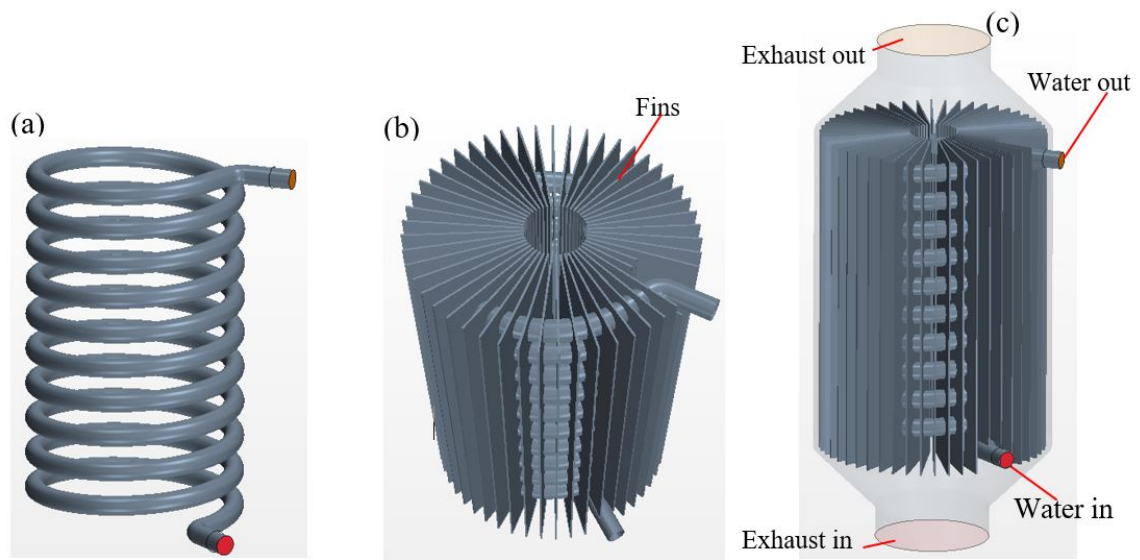


Figure 54: Design 1; water volume (a), pipe and fin arrangement (b) and model for the CFD simulation (c)

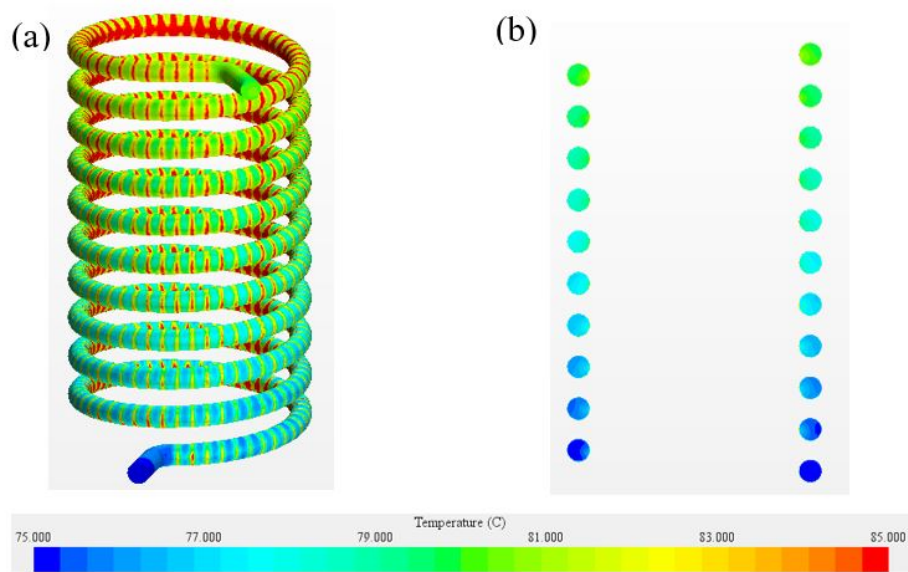


Figure 55: Design 1; water flow temperature distribution of outer surface of the volume (a) and through the vertical cross section (b)

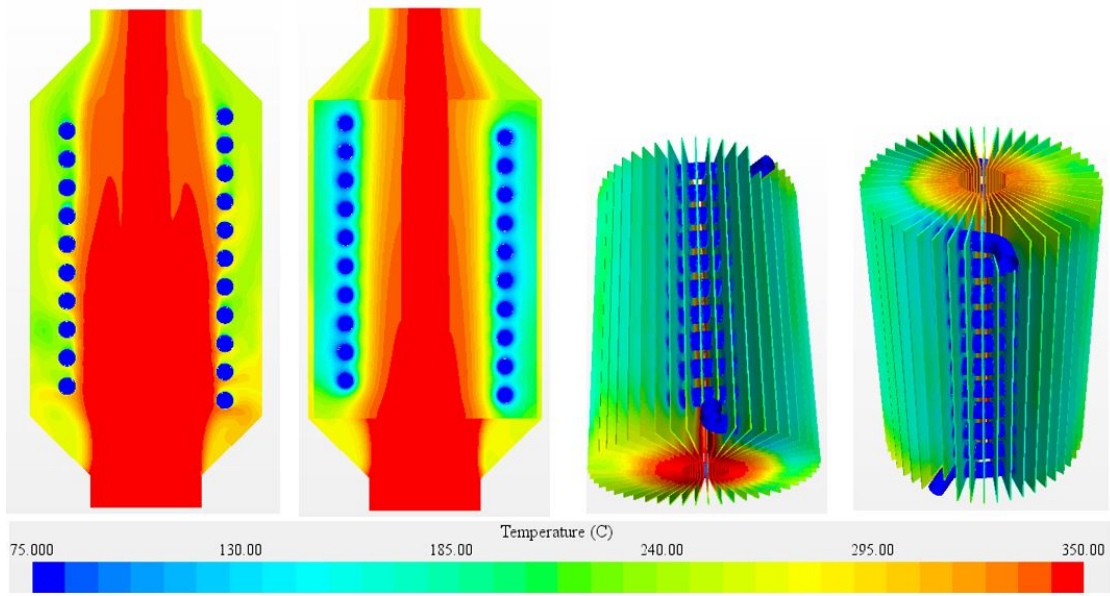


Figure 56: Temperature distribution through the vertical section of the EGE unit (left) and temperature distribution of the outer surface of the fins and pipe assembly (right) of Design 1

Exhaust out temperature( $^{\circ}\text{C}$ )	Water out temperature( $^{\circ}\text{C}$ )	Heat transfer rate (kW)	Exhaust pressure drop(Pa)
295.5	80.2	416	341

Table 17: CFD simulation results of Design 1

#### 4.4.2 Design 2 - Rectangular Water Pipe with Fins

The Design 2 has more surface area for the exhaust contact than the Design 1 with changing the water flow pattern from spiral shape to rectangular shape as shown in Figure 57 (a). The water region contact area has almost similar size as the Design 1 and the water flow shape has changed to increase the number of fins to increase the exhaust contact surface area. This design also has the 5mm thick plate fins with a 30mm gap between two fins which are arranged equally space in the horizontal direction. The fins has different length as shown in Figure 57 (b) due to the cylindrical shape of the exhaust chamber.

Contact area of water ( $\text{m}^2$ )	Contact area of exhaust ( $\text{m}^2$ )
10	132

Table 18: Water and exhaust contact surface area of Design 2

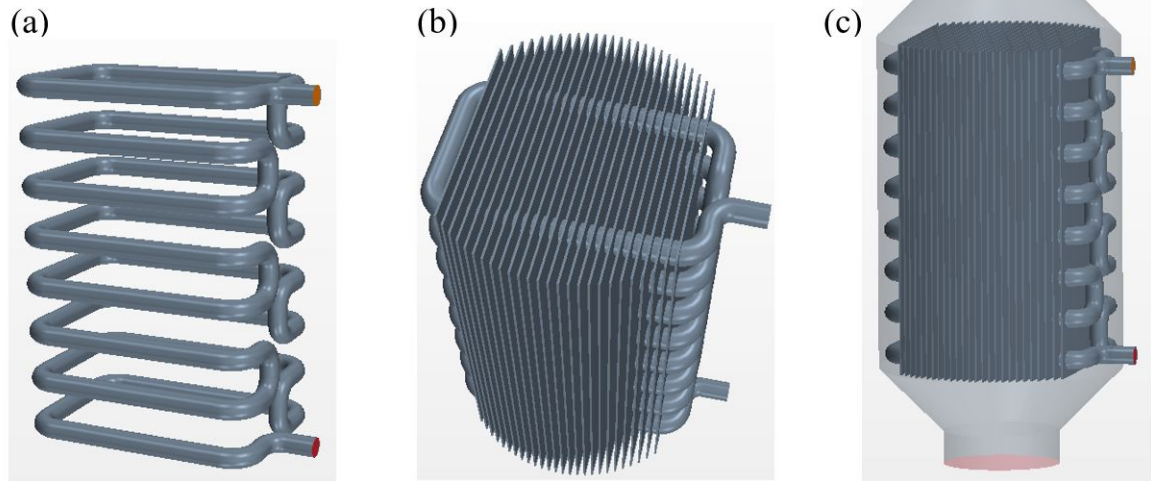


Figure 57: Design 2; water volume (a), pipe and fin arrangement (b) and model for the CFD simulation (c)

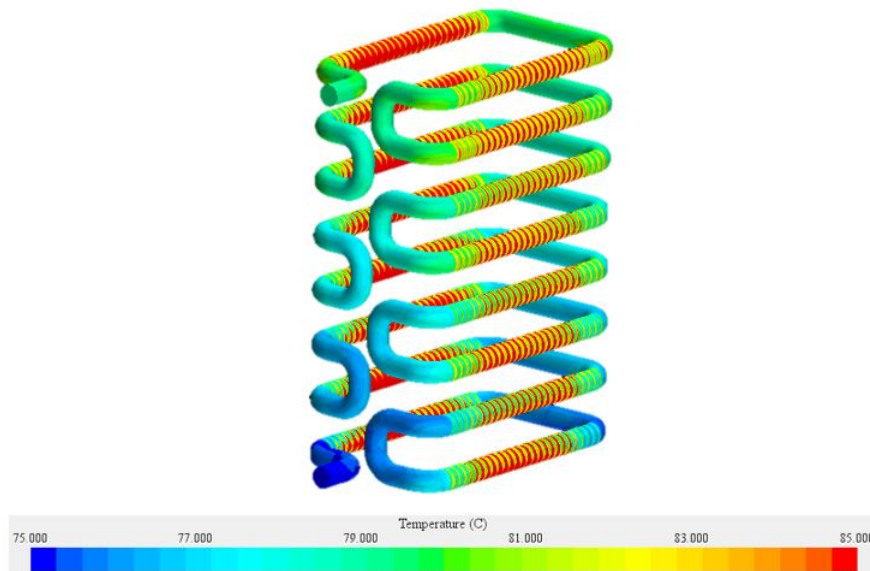


Figure 58: Design 2; water flow temperature distribution of outer surface of the volume

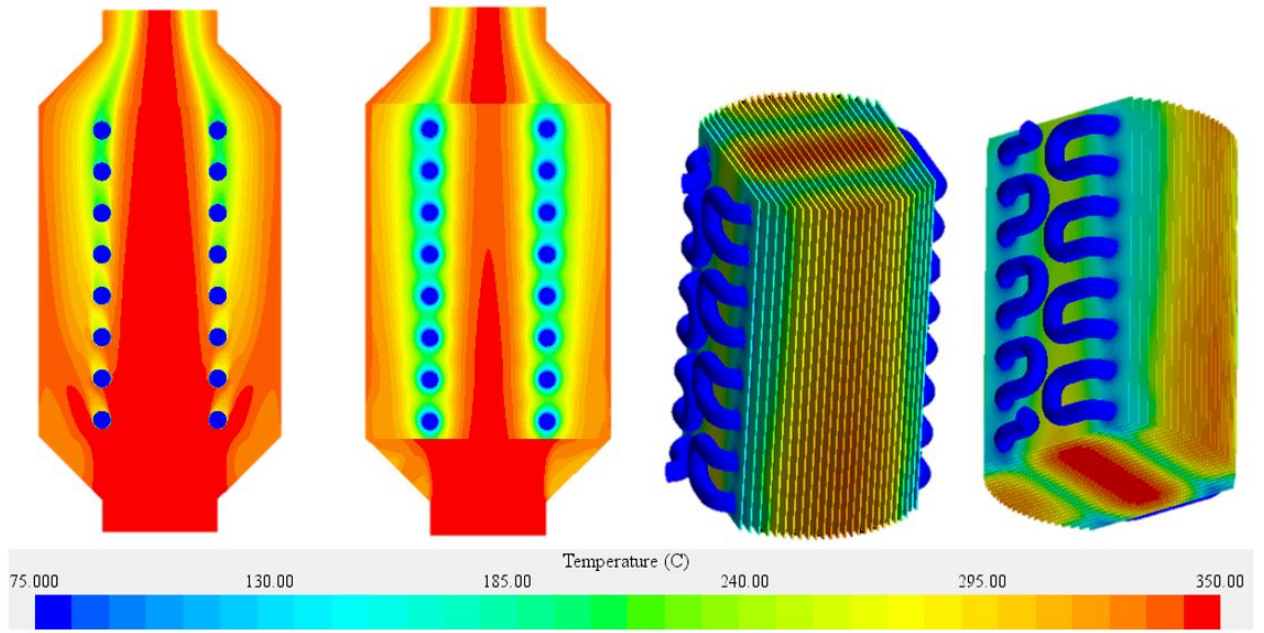


Figure 59: Temperature distribution through the vertical section of the EGE unit (left) and temperature distribution of the outer surface of the fins and pipe assembly (right) of Design 2

Exhaust out temperature( $^{\circ}\text{C}$ )	Water out temperature( $^{\circ}\text{C}$ )	Heat transfer rate (kW)	Exhaust pressure drop(Pa)
308	79.2	346	376

Table 19: CFD simulation results of Design 2

#### 4.4.3 Design 3 - Cuboid Water Pipe Bundle with Fins

The Design 3 is modeled with additional water contact surface area than Design 1 and 2 with increasing the exhaust contact surface area as mentioned in the Table 20. Instead of using single pipe for the water flow. Pipe bundle with inner diameter of 54mm to a main pipe of 100mm diameter for inlet and outlet is used for this design. The pipe bundle has a cuboid shape as shown in Figure 60 (a) and the geometrical symmetry of the model is used to conduct the CFD simulation model. The plate fins have thickness of 5mm and 25mm gap between two fins. The unit is fixed in the middle of the chamber to expose in to the high velocity exhaust flow.

Contact area of water ( $\text{m}^2$ )	Contact area of exhaust ( $\text{m}^2$ )
31.6	141.2

Table 20: Water and exhaust contact surface area of Design 3

CFD simulation results for the Design 3 is shown in Figure 61 and 62 for the temperature distribution of the water region and the exhaust region. The simulation is conducted for the half section of the unit and the results plots of the temperature distribution is created with vertical and horizontal cross-sectional planes. The results from the CFD simulation results are presented in the Table 21.



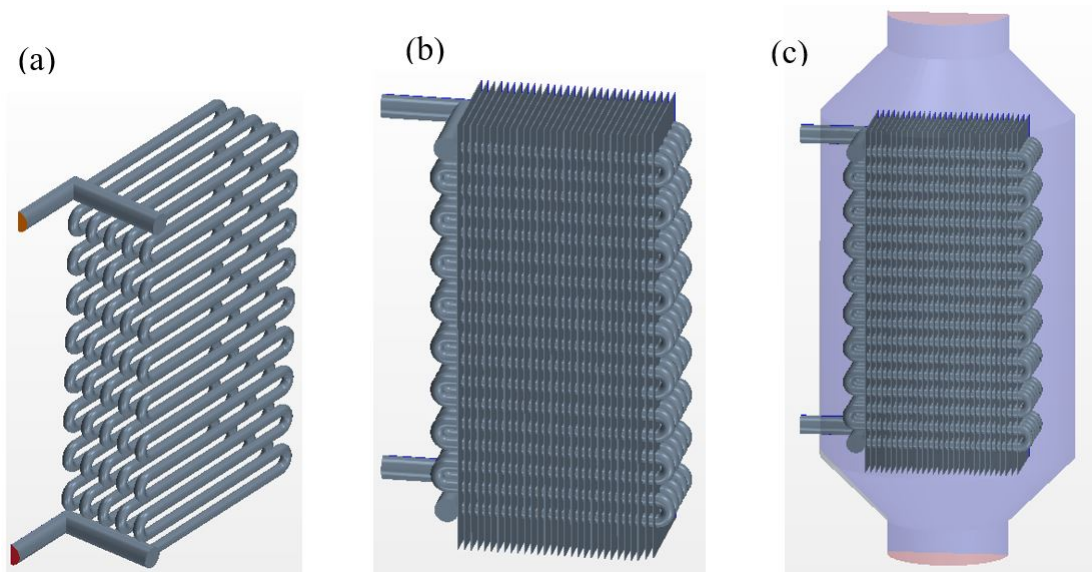


Figure 60: Design 3; water volume (a), pipe and fin arrangement (b) and model for the CFD simulation (c)

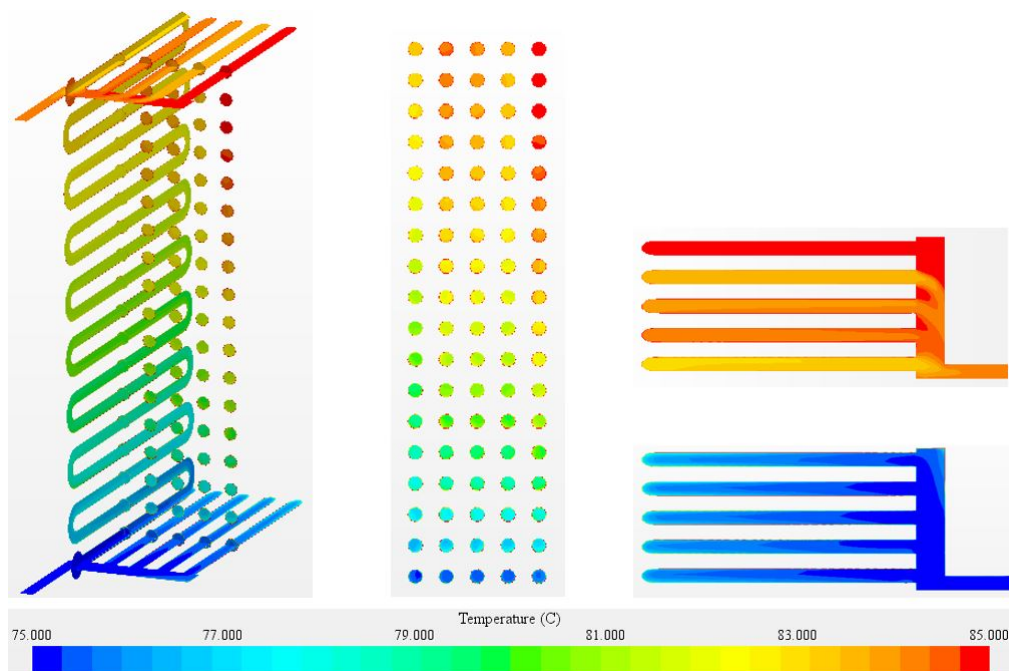


Figure 61: Design 3; water flow temperature distribution through the sections of the water volume

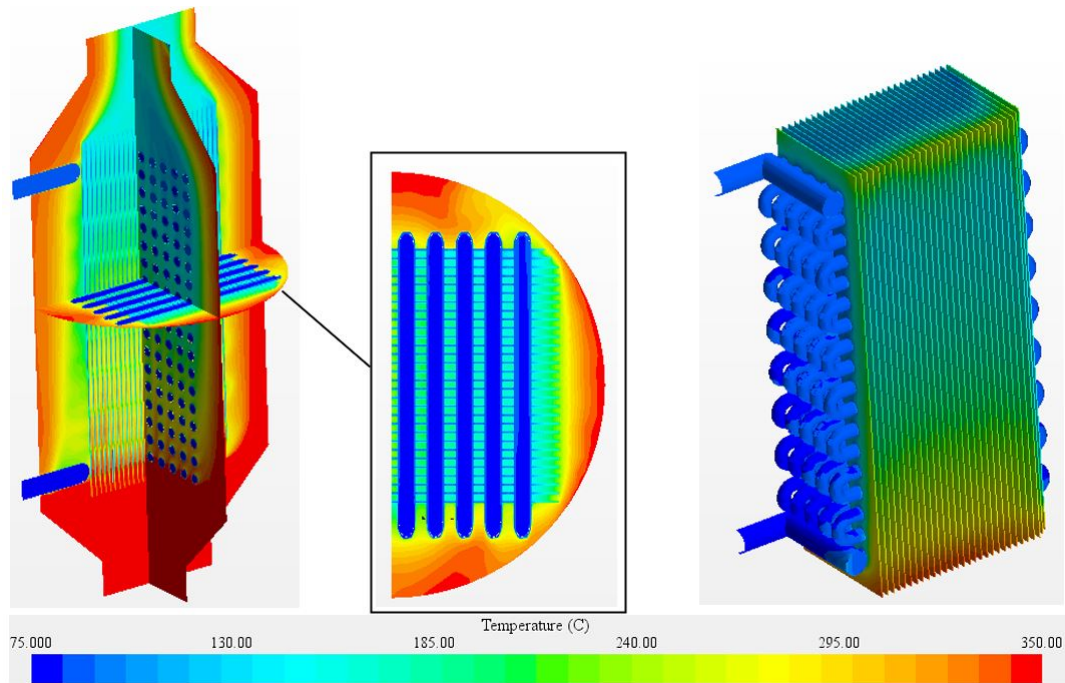


Figure 62: Temperature distribution of the vertical section of the EGE unit (left) and temperature distribution of the outer surface of the fins and pipe assembly (right) of Design 3

Exhaust out temperature(°C)	Water out temperature(°C)	Heat transfer rate (kW)	Exhaust pressure drop(Pa)
257	84	742	480

Table 21: CFD simulation results data of Design 3

#### 4.4.4 Design 4 - Cylindrical Water Pipe Bundle with Fins

Referring to the CFD results of the Design 3, certain amount of the exhaust air escapes from the outer region of the water tube bundle due to the square shape cross section of the tube bundle which is shown in Figure 62. The Design 4 is modified to create a shape of tube bundle with connected the fins in to a cylindrical shape as shown in Figure 63. This has 54mm inner diameter pipe bundle connected to 100mm inlet and outlet pipe. Contact surface area of the water and air is increased through this compact design concept as mentioned in the Table 22. However, the water contact surface area of this design is still lower than the DN700 design. The plate fins have a thickness of 5mm and 25mm gap between adjacent fins surfaces. Geometrical symmetry of the unit is used for the CFD simulation as shown in Figure 63 (b).

Contact area of water (m <sup>2</sup> )	Contact area of exhaust (m <sup>2</sup> )
70.1	185.9

Table 22: Water and exhaust contact surface area of Design 4



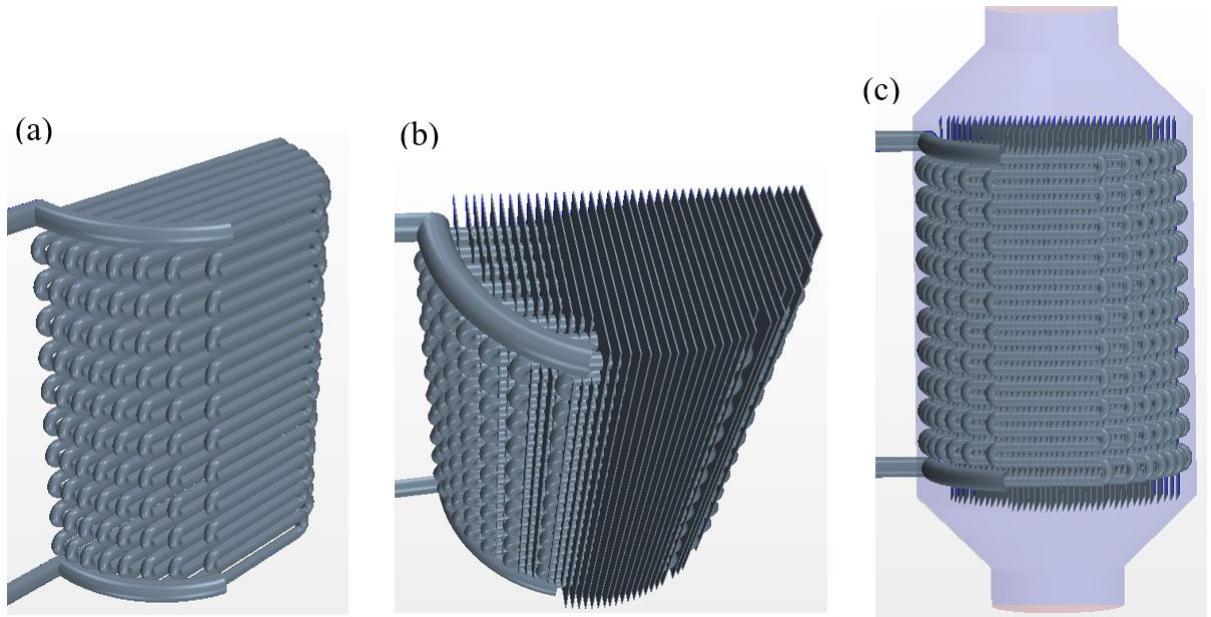


Figure 63: Design 4; water volume (a), pipe and fin arrangement (b) and model for the CFD simulation (c)

CFD simulation results for the Design 4 is shown in Figure 64 and 65 for the temperature distribution of the water region and the exhaust region. The simulation is conducted for the half section of the unit in this case and the results plots of the temperature distribution is created with vertical and horizontal cross-sectional planes. The results from the CFD simulation results are presented in the Table 23.

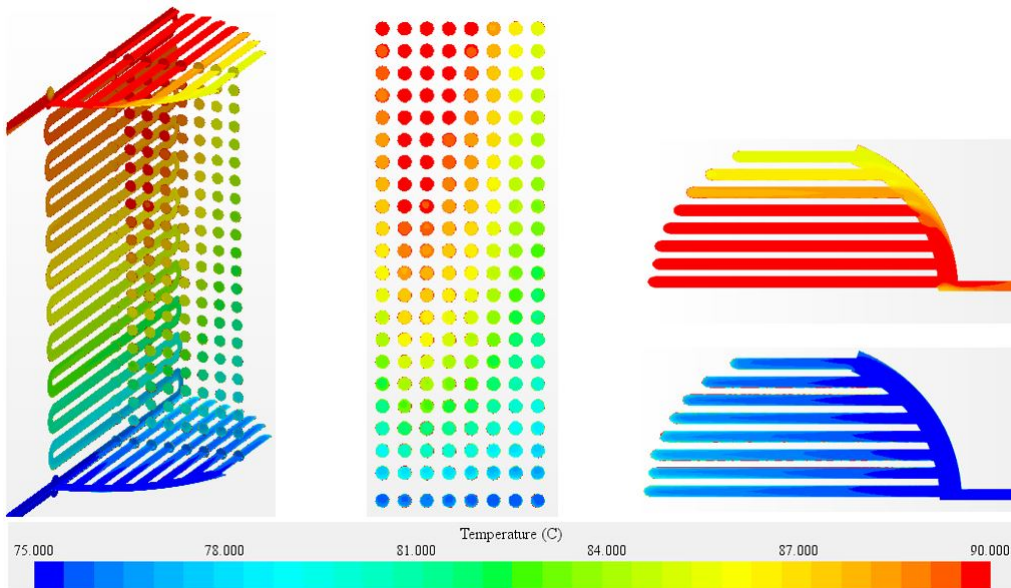


Figure 64: Design 4; water flow temperature distribution through the sections of the water volume

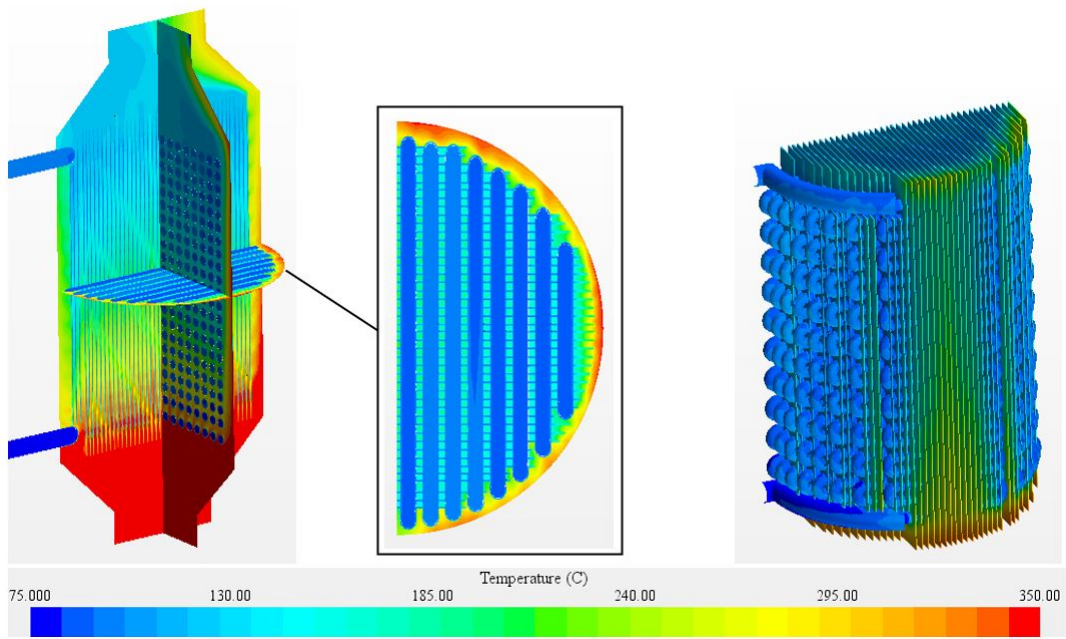


Figure 65: Temperature distribution of the vertical section of the EGE unit (left) and temperature distribution of the outer surface of the fins and pipe assembly (right) of Design 4

Exhaust out temperature(C)	Water out temperature(C)	Heat transfer rate (kw)	Exhaust pressure drop(Pa)
204	89.4	1150	1350

Table 23: CFD simulation results of Design 4

---

## 5 Results and Discussion

### 5.1 Comparison of Measured Data with the CFD Results

According to the CFD simulation result data for the DN500 with 3 different exhaust flow conditions refer to the Tables 6, 7 and 8 are plotted with considering the exhaust temperature values which is illustrated in Figure 66 plot (a) and (b). The heat transfer rate and the exhaust pressure drop from the CFD results and the measured values are presented by plot (a) and (b) in this figure.

The heat transfer rate from the CFD results and the measured values has a slight variance referring to the plot (a). The CFD results have a lower value than the measured data for the heat transfer rate in 350°C and 365°C while 395°C exhaust flow has vice versa. The pressure and temperature measurements has taken from the sensors which are positioned as shown in the Figure 67. The exhaust pressure drop is calculated using the sensor reading and the supply pressure. This pressure sensor is positioned in the mid-section of the EGE unit. The water temperature is also measure using a temperature sensor positioned close to the water outlet of the EGE unit. The exhaust temperatures are also measured using temperature sensors posited close to the center-line of the unit. But the CFD results are taken from the average values from the exits and inlets for both water and exhaust regions. According to the sensor positions, these measured values can have a higher error percentage than the simulation results. Because the sensor takes the values from the point other than an average value. Adding more sensors to take average value can be more accurate for these measurements for an experimental set up.

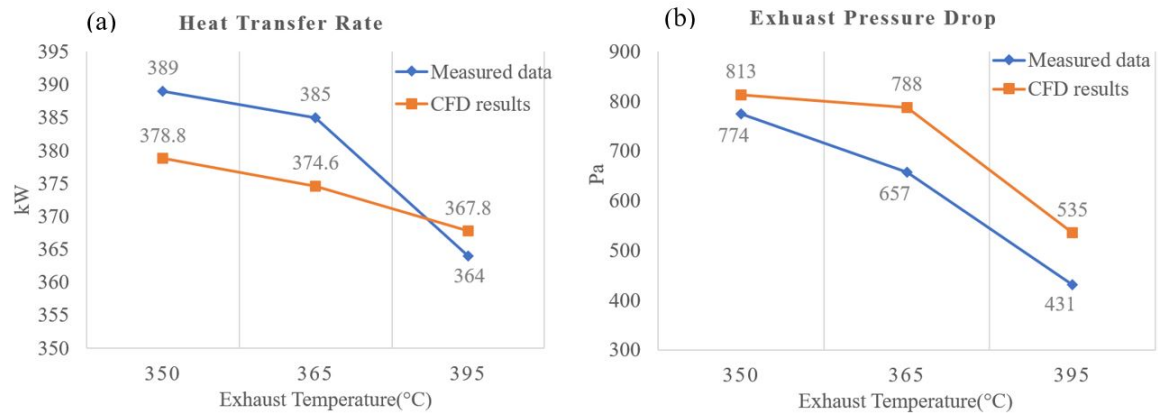


Figure 66: DN500 measured data and CFD simulation results comparison graphs for, heat transfer rate (a) and exhaust gas pressure drop (b)

The pressure drop between the inlet and outlet of the exhaust flow of the EGE unit is plotted in Figure 66 graph (b). As mentioned in the section 4.2.1, pressure of the inlets and outlets has taken as a average value of the surface perpendicular to the flow. The difference of the two values from the measurements and the CFD results are expanding when the temperature of the exhaust flow increases. According to the exhaust flow data, the exhaust flow rate is decreasing when the temperature increases. As similar to the heat transfer rate, measured value can vary according to the type of measurement and it is not a surface average value as the CFD results. Also, the density of the exhaust gas which is used for the CFD simulation is constant value for the individual temperature values and the actual case can be different due to the local density changes with high temperature and low flow rate exhaust gas as 395°C exhaust flow. But for the high flow rate and lower temperature exhaust flow, the CFD results and measured data have closer values. This effect

illustrates from the heat transfer rate plot, which has a slight increment in the CFD results for the 395°C flow.

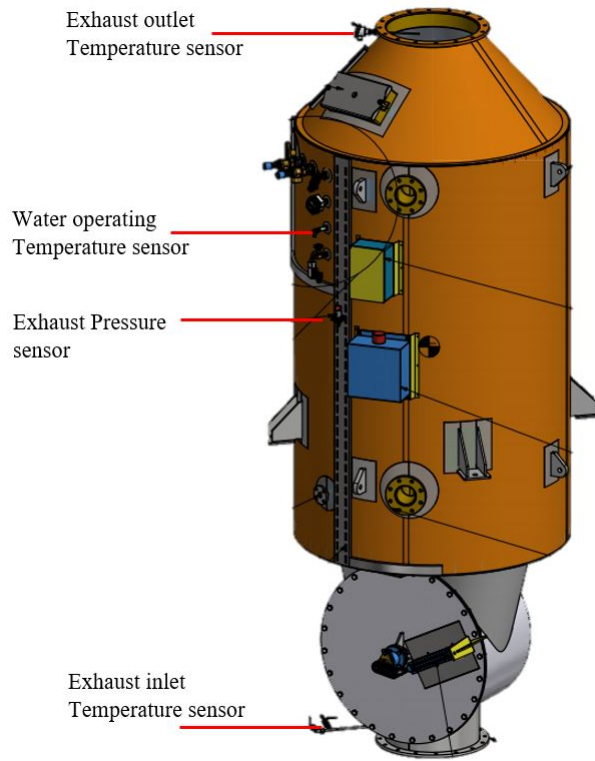


Figure 67: DN500 temperature and pressure sensors positions

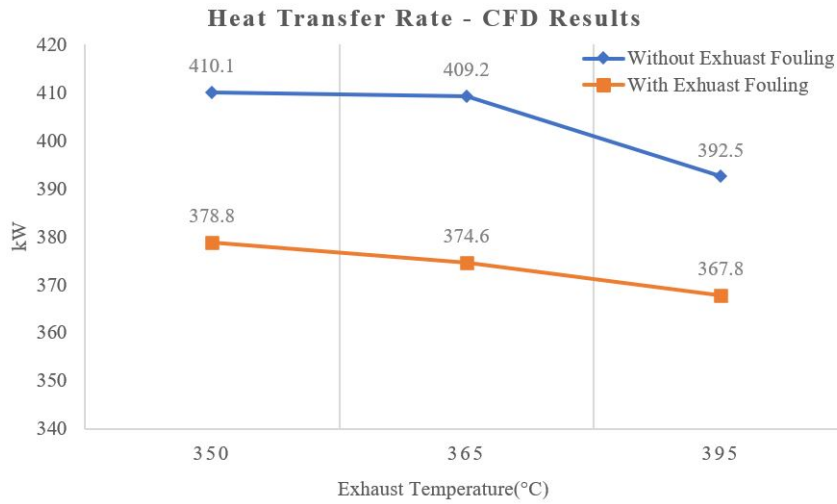


Figure 68: DN500 CFD simulation results comparison graphs of heat transfer rate with and without exhaust fouling resistance

With referring to the CFD result data in Table 9 in section 4.2.1 for DN500, the graph in Figure 68 is plotted to identify the heat transfer efficiency change with and without the exhaust fouling in the exhaust side of the EGE unit. It is clear that, the reducing the thermal resistance between two

fluid regions cause a significant improvement in the heat transfer which is nearly between 7% -9% according to the exhaust flow rate and temperature levels. This can be achieved by introducing DPF-DOC unit into the exhaust system to avoid the soot build up in the unit. However, it will be not possible to avoid 100% soot build up in the unit with these filters. But it will be more than 90% according to the performance levels of the DOC-DPF units. Avoiding fouling can also be effective in the exhaust flow performance which can reduce the peruse drop of the exhaust side. This CFD analysis does not reflect the pressure variation by soot generation due the complexity of geometrical representation of the soot builds up inside the tubes.

## 5.2 Effects of Using Baffles

### 5.2.1 Number of Baffles

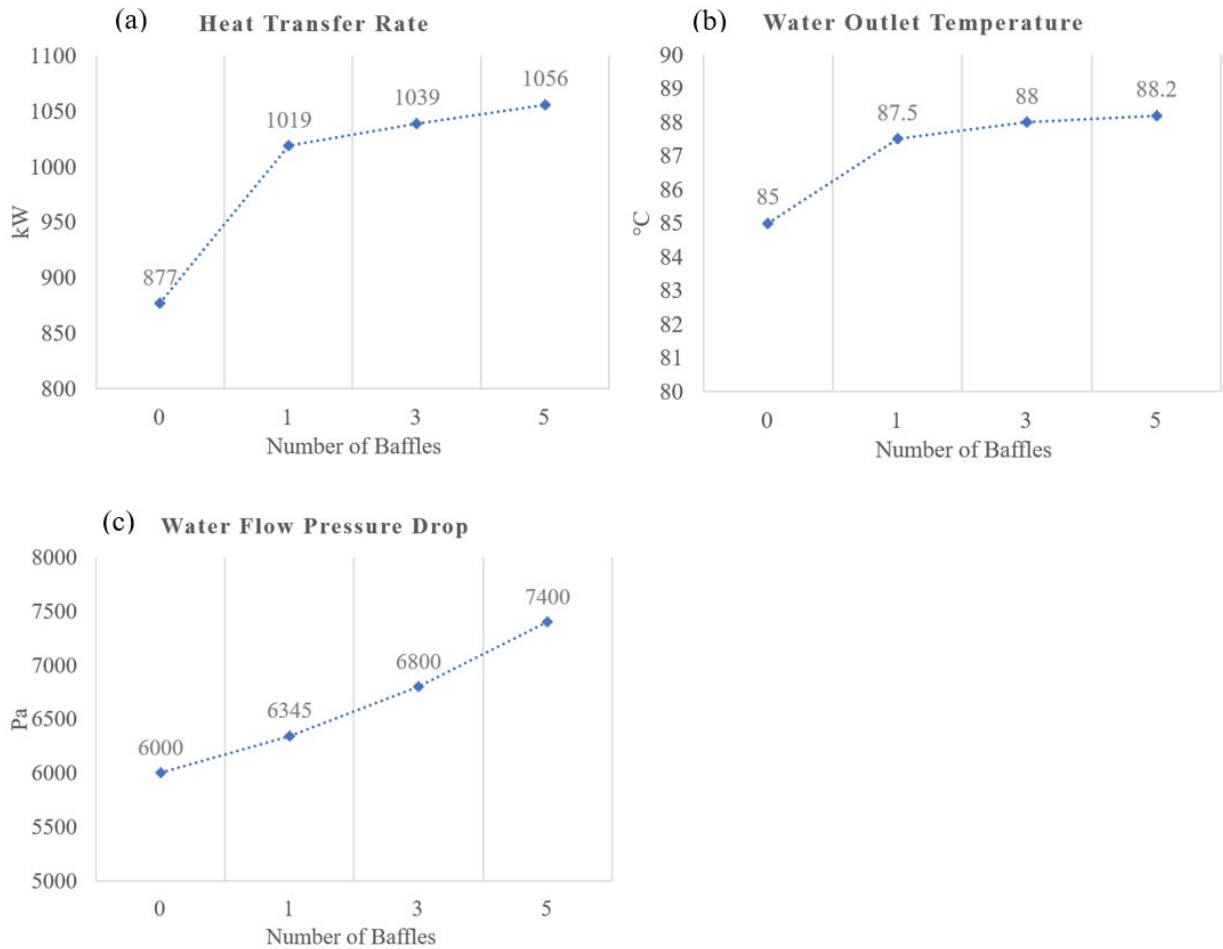


Figure 69: DN700 CFD simulation results for increasing number of baffles, heat transfer rate (a), water outlet temperature (b) and water flow pressure drop (c)

Based on the CFD simulations results of the implementing baffles on the water side of the DN700 EGE, the heat transfer rate and the average water outlet temperature plotted with increased number of baffles in Figure 69. The original model without baffles is illustrated from the 0 baffles in the graph and the number of baffles increased as 1, 3 and 5 depending on the water exit and outlet positions in the original design of DN700.

According to plot (a), the heat transfer rate rapidly increases by including a single baffle in to the unit. Increasing number of baffles, gradually increase the outlet flow temperature with increasing

the heat transfer rate. Also, the water flow pressure drop is increasing with the number baffles in the system. Increasing baffles from 1 to 5 is not creating a significant change in the water outlet temperature. But referring to the temperature distribution plots with number of baffles in Figure 46 in section 4.3.2, it is clearer that the increasing baffles up to 3 and 5 has more even temperature distribution in the water region with distributed thermal stress development rather than the higher thermal stress fluctuations.

Using 3 baffles for this purpose is more feasible than using 5 baffles with considering the amount of heat transfer increase from 3 baffle to 5 baffles which is not significant change in the heat transfer. The water flow pressure drop increasing will not be an issue due to the high pressure in the water region which is used to keep the water in liquid state above 100°C. The cost will be higher when it comes to higher number of baffles used in the EGE unit. This study has conducted only up to 5 baffles to keep the sufficient distance between two baffles and the higher number of baffles will not give significant increment in the heat transfer rate according to the above results.

### 5.2.2 Baffle Cut Percentage

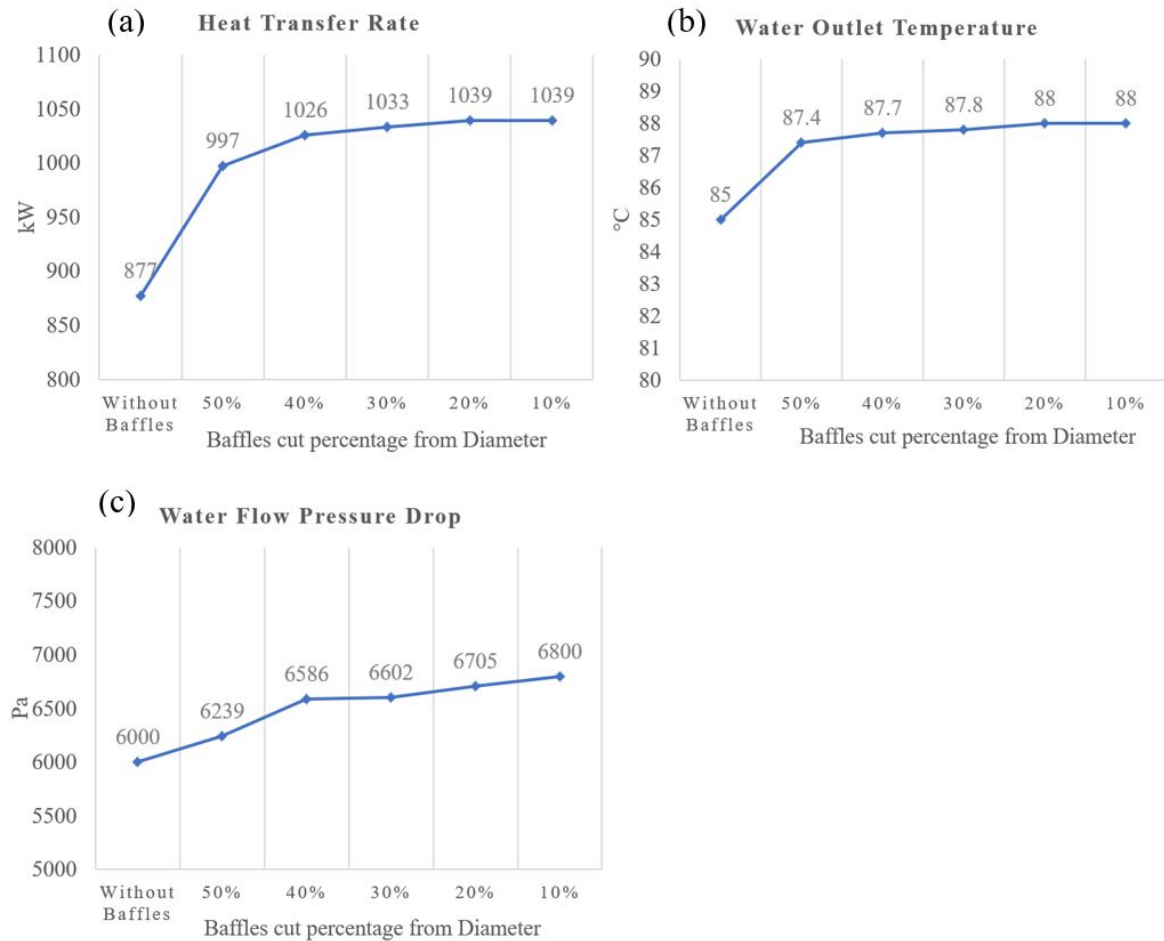


Figure 70: DN700 CFD simulation results for reducing baffle cut size, heat transfer rate (a), water outlet temperature (b) and water flow pressure drop (c)

The heat transfer rate, water outlet temperature and the pressure drop of the water flow from the CFD simulation results are plotted in the graphs shown in Figure 70. As described in the section 4.3.2 for the changing of the baffle cut length percentage from the diameter is compared with the EGE unit without any baffles. According to the graph (a) and (b), the efficiency has a influence from the baffle cut percentage. Between 20-10% of the baffle cut has similar performance data in



the heat transfer rate which is effective to use in the EGE unit. Also, the water flow pressure drop increase with baffle cut percentage decrease. With considering these data values, the baffle cut percentage of 20% has a significant improvement in the heat transfer rate with a lower water flow pressure for below 20% of baffle cut percentage. With considering the results from the number of baffles and the baffle cut percentage CFD simulation results, using 3 baffles with a baffle cut of 20% of exhaust chamber diameter is more effective for the EGE unit.

### 5.3 Effects of Using Inlet Flow Directional Controlling

The results from the CFD simulation with the exhaust flow directional controlling method which has described in the section 4.3.3 is plotted for the heat transfer rate, water outlet temperature and the exhaust pressure drop as shown in the Figure 71. The first simulation is the DN700 with 3 baffle EGE unit without having the flow controlling funnel near the exhaust inlet. The results with increasing the angle by 10° up to 40° of angle and the swirl flow simulations are shown in the plots in Figure 71. The main purpose of this section is to analyze how the flow disturbance of the exhaust flow affects to the performance of the EGE unit.

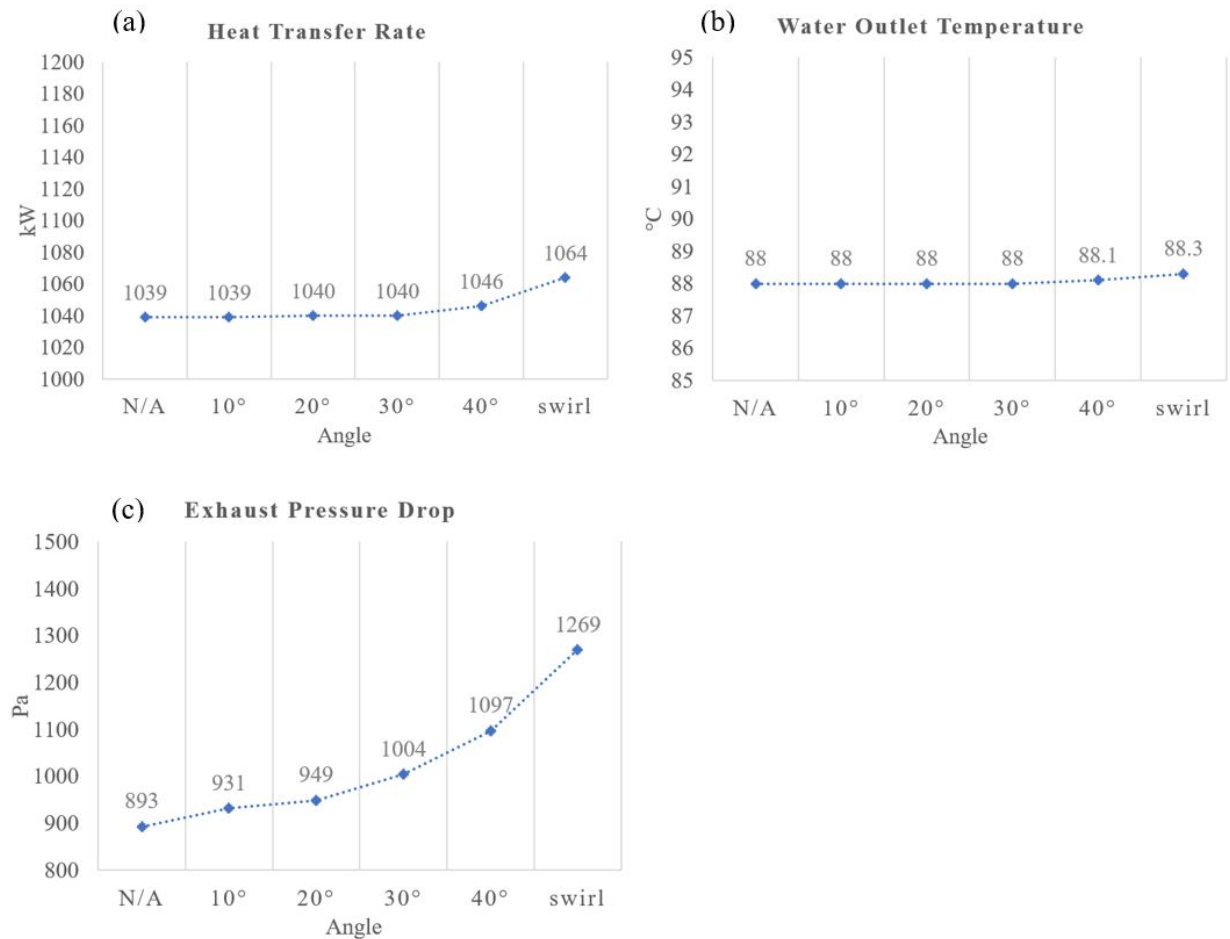


Figure 71: DN700 CFD simulation results for exhaust flow direction control, heat transfer rate (a), water outlet temperature (b) and exhaust pressure drop (c)

According to the heat transfer rate and the water outlet temperature, there is no significant improvement from the exhaust flow direction control using the funnel shape. But the swirl flow creates a slight increase in the heat transfer of the unit. However, all these methods create a disturbance of the exhaust flow and it leads to a higher pressure drop in the exhaust flow which is much higher in the swirl flow. The exhaust flow has more even flow distribution in the swirl

flow according to the flow distribution plots shown in Figure 53 which will lead to create even soot generation inside the pipes than the original case. However, it cannot be predicted exactly due to the slow speed flows can create more soot than the high speed flows.

## 5.4 Performance of the New Economizer Design Concepts

Plot (a) and (b) in Figure 72 illustrate the heat transfer rate and the water outlet temperatures from the CFD simulation results. The new design concepts which are noted as D1, D2, D3 and D4. Performance data is compared in this section with the original design of DN700 and the DN700 with added 3 baffles. The heat transfer rate has a significant improvement with the 3 baffles and the new concept Design 4.

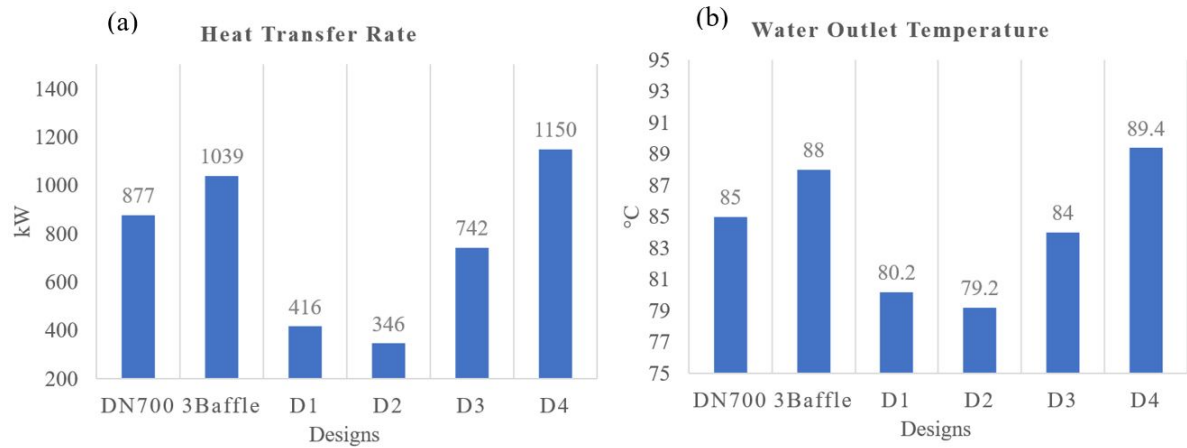


Figure 72: DN700 existing design, DN700 with 3 baffles and new designs CFD simulation result for, heat transfer rate (a) and water outlet temperature (b)

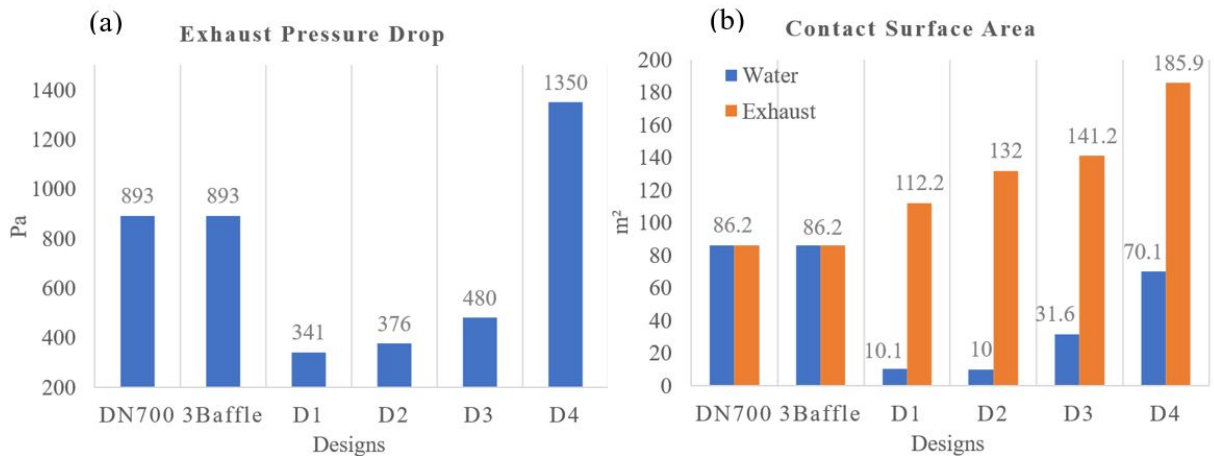


Figure 73: DN700 existing design, DN700 with 3 baffles and new designs CFD simulation result for exhaust pressure drop (a) and comparison of water and exhaust contact surface area (b)

In new designs concepts, the main focus is to study the effects of increasing heat transfer area of water and exhaust flow towards the EGE unit performance improvement. As discussed in the section 4.4 for the Case 3, the amount of heat transfer areas of each design for both water and exhaust region are plotted in the bar chart (b) in Figure 73. The original design DN700 and with 3 baffles has equal heat transfer area for both water and exhaust regions. The added plate fins in all new designs increase the effective heat transfer area of the exhaust side. Water contact area of



---

the new designs are lower than the original design and it is gradually increased with the designs to evaluate the performance.

Referring to the equation (21) in section 3.2.4, the overall heat transfer coefficient for the new designs with plate fins can be expressed as,

$$U = \frac{1/A_a}{\frac{1}{\eta_a h_a A_a} + \frac{1}{h_w A_w}}$$

where;  $A_w$  is the water contact surface area,  $A_a$  is the exhaust gas contact area,  $h_w$  is the convective heat transfer coefficient of water,  $h_a$  is the convective heat transfer coefficient of exhaust and  $\eta_a$  is the plate fin efficiency. Assume that there is zero thermal resistance between the two surfaces,

According to this expression of the overall heat transfer coefficient of the system which govern the heat transfer rate, the fin efficiency and the contact surface area of both fluids are important factors. The contact surface area of the air is more important due to the low convective heat transfer coefficient compared to the water, specially for a heat ex-changer device with working fluids of exhaust gas and water like this EGE unit.

It is more complex to achieve the efficiency of the fins in a complex design arrangement like the new design concepts discussed in this study. Hence, using CFD simulations to evaluate the heat transfer rate of the designs is a more reliable approach for the efficiency improvements. Even increasing large amount of contact surface area using fins is not so effective without increasing the water contact area according to the bar graph details of the contact surface area in Figure 73 (b). This is mostly optimizing the EGE unit using CFD simulations which is not possible to do using conventional design approach. The pressure drop of the new designs are increased when it increases the number of fins which creates a compact design arrangement as in Design 4. The exhaust gas has a very narrow path to flow trough the fins in these new designs to extract more heat from the gas. However, further design changes can be used to reduce this pressure drop value while increasing the heat transfer. Increasing the water contact surface area of the design close to the original design with increased exhaust gas contact surface area will provide a higher heat transfer rate with referring to the CFD simulation results.

The Design 4 is more complex than the other designs, because it has designed according to the cylindrical shape of the exhaust chamber to avoid flow escaping around the outer region of the tube bundle as in Design 3. Using a cuboid shape for the exhaust chamber instead of the cylindrical shape can be reduced the complexity of the design with lower pressure drop. Also, it will help to reduce the complexity of the manufacturing of the unit.

## 5.5 Combined System of Exhaust Gas Economizer and Exhaust After Treatment unit

The EAT system need to be consists with DOC, DPF and SCR unit to clean the CO, NO<sub>x</sub>, HC and PM from the exhaust gas, according to the section 2.2. The existing EAT unit considered in this study consists with a SCR unit in the exhaust system to remove the NO<sub>x</sub> from the exhaust. Combining EGE unit with EAT unit need to proceed with considering several important factors which will affect the performance of the total system and the retrofitting needs. The key factors are the pressure drop building across each unit which affects the exhaust back pressure and the exhaust temperature coming out from each sub unit.

According to the operational conditions of the DOC, converting NO to NO<sub>2</sub> takes place in temperatures higher than 350°C at an efficiency rate of 60%. Also, the oxidation of HC and CO inside this creates additional heat into the exhaust which is effective for the passive regeneration for the DPF. The DPF is absorbs the particle matter into the filters from the exhaust and this soot will block the filters after some time. The Active regeneration is used to burn off the soot from the filter as described in the section 2.2.2. Hence it is important to keep both DOC and DPF unit in a high temperature exhaust flow stream. The SCR unit need to be maintained 200-400°C to activate

the catalyst for the reaction process of breaking down NO<sub>x</sub> in to N<sub>2</sub> and H<sub>2</sub>O. According to the required temperatures for the EAT modules the main configurations can be organized as shown in the Figure 74 for a combined unit of EAT and EGE for a diesel exhaust system. The EGE unit is placed after the EAT modules which required higher temperature ranges for the reactions which cannot be fulfilled after the waste heat recovery due to the lower exhaust gas temperatures after the EGE unit.

These two configurations are mainly used in ground vehicles, specially in trucks. Configuration (a) as shown in the Figure 74 is consisted with combined DOC and DPF unit connected to the SCR unit for the exhaust cleaning process. According to *G Tan Weiwei* [45], the generated back pressure in DOC-DPF integrated unit for marine diesel engines is lower than the separate units. The pressure drop across these units are typically high due to the filtering units and it is more beneficial to reduce the pressure drop using an integrated unit of DOC-DPF which reduce the impact for the engine performance.

The Configuration (b) without the EGE unit is also used in ground vehicle applications where the required fuel amount of the active regeneration is comparatively lower than the Configuration (b). However the main factor need to be considered in the combined unit of EGE and EAT is the exhaust backpressure created by the total system. In that point, the Configuration (a) is beneficial to keep the backpressure lower than arrangement in Configuration (b).

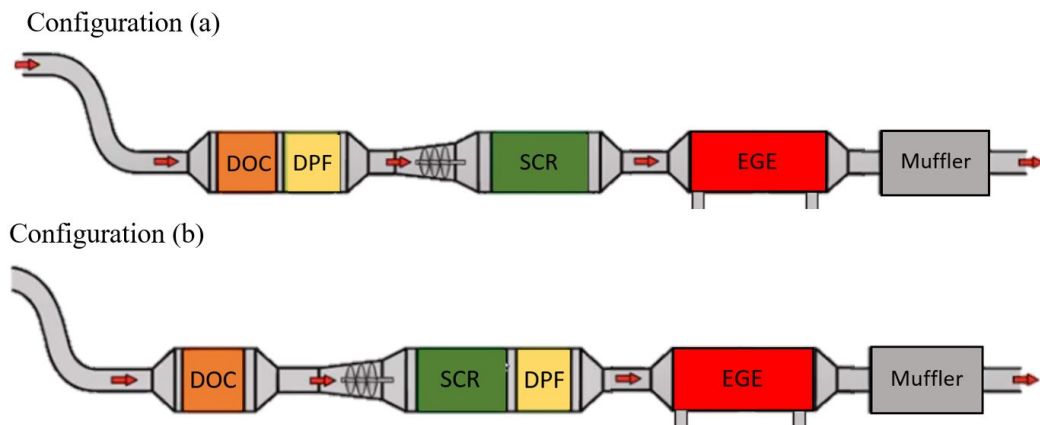


Figure 74: Main configurations of EAT system arrangement used for diesel engines combined with the EGE unit for waste heat recovery

### 5.5.1 System Arrangement

As discussed in the previous section, the Configuration (a) is proposed for the combined unit arrangement with considering the back pressure and the temperature requirements of the each sub units included as shown in the Figure 75 for the retrofitting in the vessel. The CRT unit consist with the integrated DOC-DPF unit and the SCR unit consist with the SCR catalysts and ammonia slip catalyst referring to the section 2.2.3. The EGE unit for the waste heat recovery is connected

---

after the SCR unit and the muffler is connected at the end of the exhaust line to control the noise.

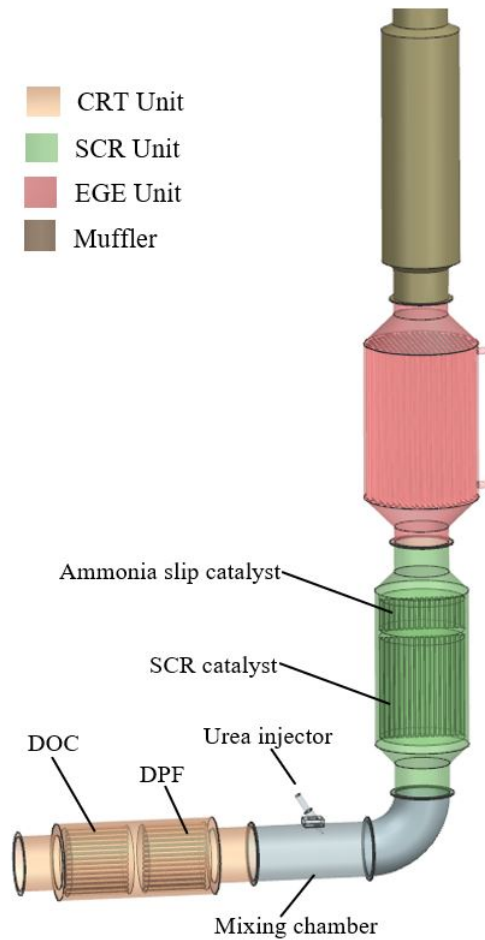


Figure 75: 3D conceptual design of complete assembly of WHR and EAT unit for exhaust system

### 5.5.2 Combined System for Retrofitting

The existing exhaust system arrangement of which has discussed in the section 2.4 is shown in Figure 76 (a). This system consists with four diesel engines with two capacity ranges of 4MW and 3MW which required two sizes of EGE units to waste heat recovery. The proposed exhaust system arrangement for the four engines with combining EAT unit and EGE is shown in Figure 76 (b). The available space in the exhaust pipe system need to use for the system retrofitting which can be a challenging task due the complexity of the arrangement of the pipelines and other equipment on-board. This is only an illustration of the required arrangement for the combined unit which can be further modified with considering total system arrangement inside the exhaust chamber. Furthermore, the silencing effects due to the filters in the EAT system and the pipe arrangements of the EGE unit can be caused to reduce the noise in the exhaust system which can be used to remove the muffler from the system. This will further reduce the backpressure of the total system and the space required for the retrofitting. However, it will be required to investigate using the acoustic models of the sub-units of the system to identify the noise reduction capabilities of the total system arrangement.

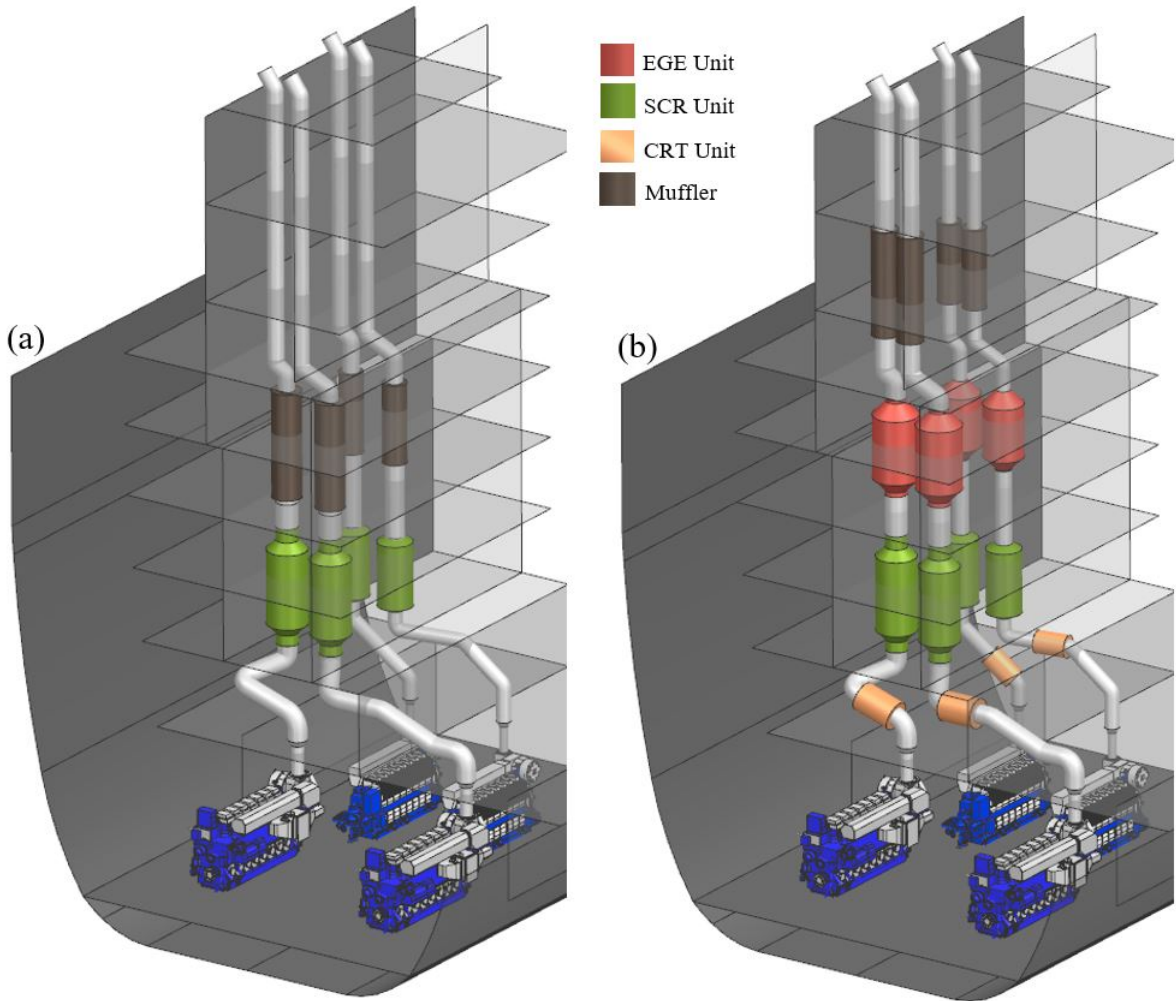


Figure 76: Existing exhaust system arrangement (a) and proposed combined system with EAT and EGE (b)

---

## 6 Conclusions

Performance evaluation of heat exchanger units with complex flow behaviour is difficult to perform using conventional methods when it comes to evaluate different design arrangements such as the cases discussed in this report. CFD thermal analysis gives more flexibility to design evaluation through performance data of the heat exchanger units. STAR-CCM+ is an effective CFD tool applicable for these thermal analysis in EGE units referring to the simulation results discussed in this research study. Also, the software can be used to evaluate different design arrangements with varying the resistance values between the fluid interfaces to optimize the designs with different flow arrangements. Due to the complexity of the design arrangements, the required computational power can be high and a proper design simplification method can reduce this complexity in specific cases.

The EGE units which are used for this study do not consist with the baffles in the water side. This causes water flow to take the shortest path to exit from the chamber which creates a higher temperature variations in the water region. This illustrates from the CFD simulations for both flow and temperature distributions as discussed previously. Implementing even a single baffle to the system can increase the efficiency of the unit by 16% and further increasing the number of baffles can reach up to 18-20% efficiency. Single baffle is more effective than 3 or 5 baffles with considering the manufacturing costs. Using 3 baffle is more reliable than using a single baffle with considering both thermal stresses and cost of manufacturing. The baffle cut percentage needs to be kept close to 20% from the diameter of the chamber according to the CFD simulation results to get the desired efficiency. These are the optimization for DN700 and it can be used to implement for the other sizes of EGE units to create as a design parameter through CFD analysis. A proper validation of the CFD simulation results can be done with a data from an experimental set up of the EGE unit.

The exhaust flow direction controlling does not have a significant improvement towards the efficiency increment according to the CFD simulation results. The higher turbulence of the exhaust flow with the swirl effect has a small improvement. However, it results a higher pressure drop across the EGE unit. However, the exhaust flow can be distributed in the tube bundle with the aid of flow direction controlling method to equally distributed soot generation inside the tube bundle. This modification for the existing unit is not an effective solution as a performance optimization referring to the simulation results from the CFD analysis.

The existing EGE unit design has a limited contact surface area for the exhaust which is a limiting factor to improve the efficiency. This limitation is changed in the new design concepts by alternating the water and exhaust regions. Due to the large difference between convective heat transfer coefficients of the water and exhaust gas, it is important to increase the exhaust contact area to reach higher efficiencies for the selected range of EGE unit. In this study, the CFD analysis are carried out to identify the changing of the contact surface area affect to the heat transfer rate with keeping the outer geometry of the EGE unit same as the existing EGE unit DN700. Referring to the result of the simulation for 4 different new design concepts, it is clear that the increasing the exhaust contact area has a significant improvement towards the efficiency of the unit. Also, it requires to keep the water contact area close to the existing design. This is always a trade off between the two contact surface area. Especially for a heat exchanger unit which has working fluids of fluid and air. A proper design arrangement can be further developed to increase the efficiency and reduce the pressure drop with referring to the new design case study in this research. The outer geometry of the unit can also be changed to improve performance and it will add another variable to the design implementation process which is not included in this study. Using a cuboid shape chamber instead of cylindrical shape can be effective from the manufacturing perspectives and it will help to avoid the complex tube and fin arrangement of the unit. The cylindrical shape of the unit is more important for the existing unit due to the high pressure maintaining inside the water region. Hence, the new design with alternating the fluid regions does not need to be cylindrical due to high pressure in the water region acts inside the pipes.

The key factors need to be considered for a combined system design with WHR and EAT unit are the pressure drop across each sub-unit which creates the total back pressure of the system and the required temperature levels for each unit operation. These temperature levels are mainly

---

important for the EAT unit due to the catalytic reactions. The system components need to be arranged according to the available space of the vessel which is highly important for retrofitting these units into the existing system. The EAT unit mainly requires higher temperatures around 250 -350°C for the chemical reactions and activate the catalysts in sub-units which needs to fit in to the exhaust system before the EGE unit. Otherwise, EGE unit will absorb the heat from the exhaust and will drop the temperature of the exhaust below these temperature ranges according to the CFD results shown in this study. These EAT units are caused for higher back pressure in the system due to the inner arrangements and it will negatively impact for the performance of the engine. However, it is important to control the emission to protect the environment with using these technologies. This is a tradeoff between emission controlling and engine performance and it needs to be considered in a broader scope to protect the environment. DPF-DOC units can be helpful to avoid the soot build up in the EGE unit as well as controlling the emissions. Based on the CFD study result data, this can be increased the efficiency of the units by 7-9% of efficiency of the WHRS. This will add a higher cost for the system and will result increase of the back pressure as mentioned earlier. For marine diesel engines, recent regulations on emissions have been designed to control sulfur concentrations in fuel instead of PM emissions. However, regulations are expected to be more stringent in the future. DPFs for marine diesel engines are being developed to avoid the pollution of shipping products by PM emissions.

Combine systems are more important to develop for the retrofitting purpose which is highly important for the existing vessels. Because these vessels will be in service for several decades in the future. This research approach of combine system concept of EGE and EAT with optimizations for marine vessels will be a reliable concept for energy wastage and emission control for the sustainability of the marine environment.

---

## 7 Future Work

This research study mainly focused on the implementing new design concept through CFD simulations for the EAT and EGE combined system with increasing efficiency using existing EGE unit optimization. It is required to implement an experiment set up for validation of CFD results based on the simulation of the existing unit in the future state of this research study. Data comparison of the DN500 measurements from and CFD results is used in this study, and it can be future evaluated using a proper experimental set up which is not possible to conduct in this study due to the limited time period of the research. Also, the effects of fins using in the air and fluid heat exchanger can be conduct separately in the future state to evaluate effects of different fin arrangements and the relationship between the water contact area and the exhaust contact area towards the heat transfer rate. Experimental set up for this purpose can be evaluated trough CFD simulations as it is discussed in this research. This research study mainly focused on the steady state heat transfer of the EGE unit and this will not reflect the time dependant behaviour of the heat distributions. Time dependant study can be implemented using dynamic system simulation tools such as 20-SIM in the future state. It is required to evaluate importance of conducting a transient thermal simulation using CFD for this case due to the higher computation power demand which is required to conduct transient flow simulations.

The proposed combined system for this research consists with a muffler unit to reduce the noise level of the exhaust system. However, the combined EAT system and EGE unit can be more effective with the noise reduction capabilities due to the filter arrangements and the pipe bundles contacting the exhaust flow. With a proper acoustic study for these units can be useful to evaluate the noise reduction performance of the combined unit with using proper system simulation tools. If the system has proper noise levels without the muffler unit, it can be removed from the system which will help to reduce the back pressure of the exhaust system.

The flow behavior inside the EAT unit also need to be studied using CFD simulations to evaluate the pressure drop through the EAT unit in the future state. It is important to study the existing EAT unit components of the DPF, DOC and the SCR units in details to conduct a CFD simulations for these units. The study will be more complex due to the chemical reactions take place inside these units which varies the flow characteristics and temperature. However, proper assumption can reduce the complexity of the simulations. This is important to find out the total back pressure of the system. Also, new design concepts can be developed with combining these EGE and EAT units integrating into single unit with recovering heat from the chemical reactions and the exhaust gas.

In the future state of this research, these developments can be implemented as a product family for the combined system with selecting categories according to the engine capacities which will be useful when it comes to the retrofitting needs. The DOC-DPF units are not considered in the present for the marine diesel exhaust cleaning systems. However, it is more important to consider in the environmental protection perspectives which will be added into the emission control regulations in the future and this is already focused on the current research and developments in worldwide. The manufacturing feasibility of the new design concepts of the EGE units need to be evaluated in the future state with expanding the scope of the geometrical model of the unit to make it into reality. The complexity of the new concepts can be reduced with this type of approach with analyzing the performance trough CFD simulations for better approximations for the future concepts.

---

## Bibliography

- [1] Bergen 32 engine. [https://www.rolls-royce.com/~media/Files/R/Rolls-Royce/documents/marine-product-finder/Project%20Guide%20B32\\_40P.pdf/](https://www.rolls-royce.com/~media/Files/R/Rolls-Royce/documents/marine-product-finder/Project%20Guide%20B32_40P.pdf/). Accessed: 2021-01-25.
- [2] Blogs Siemens. <https://blogs.sw.siemens.com/simcenter/thermalstressin-heatexchangers/>. Accessed: 2021-01-20.
- [3] Compact Heat Exchangers - West Michigan University. Available at <http://homepages.wmich.edu/~leehs/ME539/Chapter%205%20HSL.pdf>. Accessed: 2021-03-10.
- [4] CUMMINS. <https://www.cummins.com/components/aftertreatment>. Accessed: 2021-03-22.
- [5] Dieselnet-IMO. <https://dieselnet.com/standards/inter/imo.php>. Accessed: 2021-05-17.
- [6] Exhaust Back Pressure - Dieselnet. [https://dieselnet.com/tech/diesel\\_exh\\_pres.php/](https://dieselnet.com/tech/diesel_exh_pres.php/). Accessed: 2021-04-30.
- [7] Exhaust Properties - Dieselnet. [https://dieselnet.com/tech/diesel\\_exh.php/](https://dieselnet.com/tech/diesel_exh.php/). Accessed: 2021-04-10.
- [8] GESAB. <https://www.gesab.net/catamiser>. Accessed: 2020-11-10.
- [9] International Maritime Organization (IMO). [https://www.imo.org/en/OurWork/Environment/Pages/Nitrogen-oxides-\(NOx\)](https://www.imo.org/en/OurWork/Environment/Pages/Nitrogen-oxides-(NOx)). Accessed: 2021-05-17.
- [10] Lauterbach Verfahrenstechnik GmbH. <https://www.lv-soft.de/modulehelp/en/coil/index.html#!WordDocuments/typicalfoulingresistances.htm/>. Accessed: 2021-02-20.
- [11] MAHLE. <https://www.mahle.com/en/about-mahle/story/there-s-more-than-one-way-to-achieve-your-goal>. Accessed: 2020-11-10.
- [12] MAN Engines. <https://www.engines.man.eu/global/en/fascination-and-technology/scr-system/SCR-System.html>. Accessed: 2021-02-22.
- [13] Maritime Executive. <https://www.maritime-executive.com/article/emissions-projected-to-rise-50-percent-by-2050-in-imo-fourth-ghg-study>. Accessed: 2021.01.05.
- [14] Maritimt Magasine. <https://maritimt.com/nb/batomtaler/island-wellserver-032008/>. Accessed: 2021-01-16.
- [15] Nowaste.eu. <http://nowasteproject.eu/>. Accessed: 2020-11-15.
- [16] ORCAN. <https://www.orcan-energy.com/en/#solutions>. Accessed: 2020-11-10.
- [17] Process Engineers Tool. [https://powderprocess.net/Tools\\_html/Data\\_Diagrams/Heat\\_Exchanger\\_Fouling\\_Factor.html/](https://powderprocess.net/Tools_html/Data_Diagrams/Heat_Exchanger_Fouling_Factor.html/). Accessed: 2021-02-20.
- [18] Pyro WHRS. <https://www.pyro.no/pyro-waste-energy-recovery-system/>. Accessed: 2021-01-14.
- [19] Smith twp et al. third imo ghg study 2014. london, united kingdom: International maritime organization (imo); 2014.
- [20] STAR-CCM+ Product Guide. <https://CD-adapco/12.04.011/STAR-CCM+12.04.011/doc/en/>. Accessed: 2021-03-11.
- [21] VOLVO PENTA. <https://nordicblog.volvopenta.com/exhaust-aftertreatment-system-cleaning-process-exhausts/>. Accessed: 2020-11-12.



- 
- [22] Wartsil 32 Engine. Available at <https://www.wartsila.com/marine/build/engines-and-generating-sets/diesel-engines/wartsila-32/>. Accessed: 2021-01-25.
- [23] *Thermo efficiency system for reduction of fuel consumption and CO<sub>2</sub>*. MAN Diesel and Turbo, 2014.
- [24] C. Abeykoon. Compact heat exchangers – Design and optimization with CFD. *International Journal of Heat and Mass Transfer*, Volume 146, 2020.
- [25] B. Apicella, E. Mancaruso, C. Russo, A. Tregrossi, M. M. Oliano, A. Ciajolo, and B. M. Vaglieco. Effect of after-treatment systems on particulate matter emissions in diesel engine exhaust. 2020.
- [26] S. Bari and S. N. Hossain. Waste heat recovery from a diesel engine using shell and tube heat exchanger. 16:355–363, 2013.
- [27] F. Bettoja, A. Perosino, V. Lemort, L. Guillaume, T. Reiche, and T. Wagner. No waste: Waste heat re-use for greener truck. Volume 14:2734–2743, 2016.
- [28] K. Hanamoto, K. Goi, and H. Tanimoto. *SCR system complied with IMO NO<sub>x</sub> tier III*. J. Jpn. Inst. Mar. Eng, 2016.
- [29] D. Henriksson and R. N. Vierto. Exhaust gas economizer on auxiliary engines. *Department of Shipping and marine technology*, CHALMERS UNIVERSITY OF TECHNOLOGY, Gothenburg, Sweden, 2016.
- [30] G. Koltsakis and A. Stamatelos. *Catalytic automotive exhaust after treatment*, volume Sci. 23. Prog. Energy Combust, 1997.
- [31] F. Kreith and W. Z. Black. *Basic Heat Transfer*, chapter 1-7. Harper Row, 1980.
- [32] A. Kushwah, K. D. Pandey, A. Gupta, and G. Saxena. Thermal modeling of heat exchanger: A review. *International Journal of Advance Research in Engineering, Science Technology*, Volume 04, 2017.
- [33] T. Lao, J. Akroyda, N. Eavesa, A. Smith, N. Morgan, D. Nurkowski, A. Bhave, and M. Kraft. Investigation of the impact of the configuration of exhaust after-treatment system for diesel engines. Volume 267, 2020.
- [34] D. Mikielwicz, J. Mikielwicz, and P. Doerffer. Heat transfer intensification in heat exchangers of air source heat pumps. Available at <http://www.heatexdesign.com/technical-information/white-papers/white-paper-on-renewx-heat-exchangers/>.
- [35] R. Mukherjee. Effectively design hell-and-tube heat exchangers. *Chemical Engineering Progress*, Volume 94:21–37, 1998.
- [36] M. Nonokawa, T. Furui, and S. Noshiro. *PM reduction technology using the Cerallec system ceramic filter for marine diesel engines*. J. Jpn. Inst. Mar. Eng, 2013.
- [37] M. OKUBO and T. KUWAHARA. *New Technologies for Emission Control in Marine Diesel Engines*. Butterworth-Heinemann is an imprint of Elsevier, 2020.
- [38] R. Perry. *Perry’s Chemical Engineers’ Handbook*, chapter 6th edition. McGraw-Hill, 1984.
- [39] D. P. Nolan. *Fire Pump Arrangements at Industrial Facilities*, volume Third Edition. 2017.
- [40] A. Russell and W. Epling. Diesel oxidation catalysts. Rev. 53 (4):337–423, 2011.
- [41] D. V. Singh and E. Pedersen. A review of waste heat recovery technologies for maritime applications. 111(6223):315–328, 2016.
- [42] S. Jahangeer, M. K. Ramis, and G. Jilan. Conjugate heat transfer analysis of a heat generating vertical plate. *International Journal of Heat and Mass Transfer*, Volume 50, 2007.
-

- 
- [43] C. Sprouse and C. Depcik. Combining a diesel particulate filter and heat exchanger for waste heat recovery and particulate matter reduction. 2014.
- [44] L. Ulrik, S. Oskar, and F. Haglind. A comparison of advanced heat recovery power cycles in a combined cycle for large ships. 2014.
- [45] T. Weiwei, C. Aiguo, Z. Fengyang, and Z. Jinxi. Application of the doc-dpf integrated exhaust particle treatment device for new marine diesel engines. *IOP Conf. Series: Earth and Environmental Science*, 358, 2019.
- [46] C. Wik and Wärtsilä. Reducing medium-speed engine emissions. Volume 9, 2010.
- [47] L. Ying. Marine diesel engine energy saving and emission reduction technology. *IOP Conference Series: Earth and Environmental Science*, 4th International Conference, 2019.

# Appendix

## A DN500 Economizer Performance Data Sheet

# PYRO

### EKSOSKJELBEREGNING

Island Offshore - Retrofit - A300kjel

Beregningnr

3651

Beregnetdato

11.02.2021

Island Crusader - Gass motor

Artikkelnr	E1952
Kjeltype	A300
Diameter ytterkappe [mm]	1 110
Diameter tilslutning [mm]	508
Antall rør	150
Rørlengde [mm]	1 500
Rørdiameter innv [mm]	49
Rørtykkelse [mm]	4
Fouling tillegg mmVS	1 000
Vanntemperatur inn [°C]	95
Vanntemperatur ut [°C]	115

Motor	RRM
Motortype	C26:33L9AG
Innlesingsform	Røygass
Motorytelse [kW]	2 430
Røygassutnyttelse i %	100

Motor belastning	Eksos temp Inn °C	Eksos temp Ut °C	Eksos mengde kg/time	VO Tall W/m <sup>2</sup> °C	Kjelytelse kW	Kjelytelse kcal	Trykkfall kropp mmVS	Trykkfall total mmVS
0,25	450	300	3 790	19,1	171	147 000	5	6
0,50	425	289	7 205	35,1	294	253 000	17	21
0,75	400	284	10 245	45,2	356	306 000	33	40
0,80	395	283	10 809	46,9	364	313 000	37	44
1,00	365	270	13 608	54,8	385	332 000	56	67
1,10	350	263	15 022	58,4	389	335 000	66	79

---

## B Fouling Factors of Gases and Water

Fouling factors of gases according to the reference [17]

### Fouling factors : gases and vapors

Fluid		Fouling resistance in h.ft <sup>2</sup> .F/Btu	Fouling resistance in m <sup>2</sup> .K/W
Acid gas	Fouling factor of Acid gas	0.002	0.0003526
Ammonia vapor	Fouling factor of Ammonia vapor	0.001	0.0001763
Chlorinated hydrocarbons vapors	Fouling factor of Chlorinated hydrocarbons vapors	0.001	0.0001763
Chlorine Vapor	Fouling factor of Chlorine Vapor	0.002	0.0003526
CO2 vapor	Fouling factor of CO2 vapor	0.001	0.0001763
Coal flue gas	Fouling factor of Coal flue gas	0.01	0.001763
Compressed Air	Fouling factor of Compressed Air	0.001	0.0001763
Engine exhaust gas	Fouling factor of Engine exhaust gas	0.01	0.001763
Hydrogen	Fouling factor of Hydrogen	0.0005	8.815E-05
Hydrogen (saturated with water)	Fouling factor of Hydrogen (saturated with water)	0.002	0.0003526

Fouling factors of water according to the reference [10]

**Fouling resistances for water in shell and tube heat exchangers (m<sup>2</sup>K/W)**

Temperature of heating medium	Up to 120°C		120–200°C	
Temperature of water	50°C		Over 50°C	
	Flow velocity		Flow velocity	
Cooling water	≤ 1 m/s	> 1 m/s	≤ 1 m/s	> 1 m/s
Seawater	0.00009	0.00009	0.00018	0.00018
Brackish water	0.00035	0.00018	0.00053	0.00035
Cooling tower and artificial spray pond:				
Treated make up	0.00018	0.00018	0.00035	0.00035
Untreated	0.00053	0.00053	0.00090	0.00075
City or well water	0.00018	0.00018	0.00035	0.00035
River water:				
Clean	0.00035	0.00018	0.00053	0.00035
Normal	0.00053	0.00035	0.00070	0.00053
Sewer	0.00141	0.00090	0.00175	0.00141
Muddy or silty water	0.00053	0.00035	0.00075	0.00053
Hard (over 250 ppm)	0.00053	0.00053	0.00090	0.00090
Engine jacket	0.00018	0.00018	0.00018	0.00018
Distilled or closed circle	0.00009	0.00009	0.00009	0.00009
Treated boiler feedwater	0.00018	0.00009	0.00018	0.00018
Boiler blowdown	0.00035	0.00035	0.00035	0.00035